To Explode or to Implode: How Cells Decide Between Apoptosis and Necroptosis
Following Viral or Chemical Stress

by

Brian Patrick Johnson

A Dissertation Presented in Partial Fulfillment
of the Requirements for the Degree
Doctor of Philosophy

Approved June 2018 by the
Graduate Supervisory Committee:

Bertram Jacobs, Chair
Joseph Blattman
Jeffrey Langland
Valerie Stout

ARIZONA STATE UNIVERSITY

August 2018

ABSTRACT

Cell death is a powerful tool through which organisms can inhibit the spread of viruses by preventing their replication. In this work, I used viral and chemical stressors to elucidate the mechanisms by which one anti-viral system might be activated over another, focusing on the programmable death pathway necroptosis and Protein Kinase R (PKR). PKR can detect viral dsRNA and trigger antiviral effects such as cessation of translation and induction of programmed death. Necroptosis is a rapid cellular death that can be induced via sensors such as DNA-dependent activator of IFN-regulatory factors (DAI), also known as Z-DNA-binding protein 1 (ZBP1). DAI contains a Z-form nucleic acid (ZNA) binding domain. E3, the primary vaccinia virus (VACV) interferon resistance protein, contains a similar domain in its amino terminus. We have previously reported this domain to be necessary for the inhibition of both PKR activation and DAI/ZBP1-mediated necroptosis.

Monkeypox virus is a reemerging human pathogen. Despite a partial amino-terminal deletion in its E3 homolog, it does not activate PKR. In chapter 2, I show that MPXV produces less dsRNA than VACV, which could explain how the virus avoids activating PKR.

The amino-terminus of vaccinia is associated with ZNA binding, inhibition of PKR, and inhibition of necroptosis. To determine the roles of PKR inhibition and ZNA binding in necroptosis inhibition, I characterized the VACV mutants Za(ADAR1)-E3, which binds ZNA but does not inhibit PKR, and E3:Y48A, which cannot bind ZNA. I found that while Za(ADAR1)-E3 fails to induce necroptosis, E3:Y48A does not activate PKR but does induce necroptosis. This suggests that Z-form nucleic

acid binding is not necessary for vaccinia E3-mediated inhibition of PKR, nor is the inhibition of PKR sufficient for the inhibition of necroptosis.

Finally, all known ZNA-binding proteins have immune functions and home to stress granules. I asked if stress granule formation alone could lead to necroptosis. I found that in L929 cells sodium arsenite, a known inducer of stress granules, could trigger DAI-dependent necroptosis. This suggests that DAI/ZBP1 is not necessarily a sensor of viral ligands but perhaps is a sensor of stress signals brought about by infection.

DEDICATION

To my teachers past, present, and future.

A teacher affects eternity; he can never tell where his influence stops.

-Henry Adams

ACKNOWLEDGEMENTS

TABLE OF CONTENTS

LIST OF FIGURES

Chapter 1

INTRODUCTION

Viral infection is a persistent threat. Upon entering a cell, a virus is able to hijack the cells biochemical reactions in order to synthesize new virions, which can go on to infect other cells and other hosts. Organisms utilize a number of techniques in order to mitigate this risk. One of the most potent of these is the programmed death of infected cells. By rapidly destroying themselves, infected cells can effectively prevent the replication of intracellular organisms such as viruses, thereby inhibiting their spread [1]. To be successful in this environment, some viruses have evolved mechanisms to evade, suppress, or co-opt the systems that can cause an abortive infection due to premature death.

Vaccinia virus makes dsRNA, a potent pathogen-associated-molecular-pattern. Vaccinia virus (VACV) is the prototypical member of the Orthopoxvirus genus, whose members include variola virus, the causative agent of smallpox, and the human pathogen monkeypox virus. VACV has a large dsDNA genome, encoding approximately 200 proteins, many of which are involved in immune evasion [2]. The members of Poxviridae are unique among DNA viruses in that their entire life cycle is cytosolic. This necessitates the production of their own polymerases as they do not have access to those in the nucleus. The vaccinia virion contains the components necessary for transcription and is responsible for the expression of genes immediately after entry. These so-called Early genes encode potent inhibitors of the antiviral response, such as E3, the factors necessary for DNA replication, and transcription

factors for post-replicative gene expression. Following DNA replication, the virus enters the Intermediate stage of its life cycle. Genes associated with this phase include the transcription factors for the final, Late phase [3].

A curious aspect of the Intermediate and Late phases of VACV infection is that transcription termination becomes unregulated. Early genes have specific termination signals that are recognized by the viral RNA polymerase. These sequences are absent in Intermediate and Late genes, so RNA polymerase does not disassociate upon reaching the end of the open reading frame. This results in transcripts that can be considerably longer than the actual genes they encode [4]. This is significant because throughout the poxvirus genome there are instances of genes on opposite strands that face one another. The resulting long transcripts can overlap and hybridize into double-stranded (ds)RNA [5, 6]. Figure 1 illustrates this process. Although some dsRNA is produced naturally by the host, in general long dsRNA segments are aberrant and an indication of pathology. Therefore, numerous cellular sensors exist to detect dsRNA. The activation of these sensors can result in the induction of type I interferons [7].

Type I interferons signaling puts the cell into an antiviral state. It was observed in the 1930s that exposing tissue to a virus would protect it from subsequent exposure [8]. It was not until 1957 that interferon (IFN) was first described as a distinct factor released from chick chorioallantoic membrane after exposure to heat-inactivated influenza [9]. Since then, a great deal has been learned about the pathways leading to the production of interferons and the mechanisms by which they inhibit viral replication [10].

The known interferons are grouped into three families. Type I interferons consist

of IFNβ and the many subtypes of IFNα. IFNγ the only known Type II interferon. The type III family contains IFNλ1, λ2, and λ3 [11]. Although type II and III interferons have important functions in immunity, the type I system is the most relevant to the work described in this manuscript.

Consistent with their potent roll in antiviral immunity, virtually all cells are capable of expressing type I interferons. The key transcription factors regulating Type I IFN expression are IRF3 and IRF7 [12]. These factors are also upregulated by the interferon they produce, leading to a positive feedback loop that amplifies the IFN signal [13]. Multiple pathways exist in the cell to activate them in response to diverse pathogen associated molecular patterns.

The adapter protein TIR-domain-containing adapter-inducing interferon-β (TRIF) is recruited by Toll Like Receptor (TLR) 3, which recognizes endosomal dsRNA, and TLR 4, which binds to extracellular LPS. TRIF mediates the signal cascade that results in the phosphorylation of IRF3, leading to it translocating to the nucleus where it initiates the initial expression of IFNα and IFNβ[14, 15, 16]. dsRNA can also be sensed in the cytosol by the RNA helicases retinoic acid-inducible gene I (RIG-I) and melanoma differentiation-associated gene 5 (MDA5) [17]. RIG-I and MDA5 signaling leads to the phosphorylation and activation of inhibitor of NF-κB kinase ε (IKK ε) and TANK-binding kinase (TBK-1). TBK-1 and IKKε phosphorylate and activate IRF-3, IRF-7. This also activates the transcription factor NF-κB, which has roles in inflammation and may contribute to IFN induction as well [18].

Type I interferons are then expressed and secreted by the cell, where they bind to the receptors that recognize them, IFNAR1 and IFNAR2. These receptors are expressed in virtually all cells. Secreted interferon can act upon neighboring cells as

3

well as the expressing cell itself. IFN signaling induces the expression of over 100 genes [11]. These interferon stimulated genes include sensors and effectors that greatly enhance the cell's ability to identify and respond to a viral infection. Three such ISG are DNA-dependent Activator of IFN-regulatory factors (DAI), Protein Kinase R (PRK), and members of the 2'-5' linked oligoadenylate synthetase (OAS) family.

OAS activates the nucleic acid enzyme RNaseL. Active RNaseL cleaves ssRNA, agnostic to whether it is viral or cellular in origin. Besides inhibiting total protein synthesis, this also creates RNA fragments that can be detected my MDA5, leading to additional IFN induction [19]. PKR is able to bind to dsRNA; dimerized PKR auto-phosphorylates and activates, while DAI is activated by dimerization following dsDNA binding. Both proteins have been shown to stimulate type I interferon expression to further enhance the interferon response, and both are associated with programmed cell death [20, 21, 22, 23].

Apoptosis is an anti-inflammatory and implosive cell death pathway. In 1962, it was reported that serum isolated from mice treated with endotoxin and a bacterial polysaccharide had anti-tumor properties when injected into non-treated mice [24]. It was later shown that this was not due to the persistence of the bacterial components in the serum but instead by a factor induced by them, dubbed Tumor Necrosis Factor [25]. In the mid 80's, two such factors were isolated and characterized: TNFα[26] and Lymphotoxin [27] (later renamed TNFβ due to sequence similarity between the two). Through DNA sequence analysis, 17 additional members of the TNF superfamily have been identified [28]. Fas Ligand (FasL) is a membrane bound protein that can be cleaved and released or secreted by CD8+ T-cells and interacts with the Fas receptor [29]. Tumor necrosis factor-Related Apoptosis-Inducing Ligand

(TRAIL) is broadly expressed, but appears to primarily effect tumor cells while having little effect on normal cells [30].

In addition to their anti-tumor properties, these death receptor ligands has also been identified as inhibitors of a broad range of viruses, including encephalomyocarditis virus, vesicular stomatitis virus, adenovirus-2, and herpes simplex virus II [31, 32, 33]. This restriction of viruses is associated with the induction of apoptosis [34, 35]. VACV expresses proteins that inhibit TNFα-mediated apoptosis, and VACV engineered to express TNFα has been found to be attenuated in mice [36, 37].

Apoptosis is a programmed cell death in which cells disassemble in an ordered fashion. Hallmarks of apoptosis are membrane blebbing, nuclear condensation, and chromosomal fragmentation. A key aspect of apoptosis is that the plasma membrane remains intact; this prevents the release of the majority of intracellular components and facilitates clearance of the remaining apoptotic bodies by phagocytes [38]. For this reason, apoptosis is generally considered to be anti-inflammatory [39]. Two main signal pathways lead to apoptosis. The first, extrinsic apoptosis, is initiated by external stimuli binding to cell membrane receptors. Intrinsic apoptosis is initiated by intracellular signals [40]. The major proteins associated with apoptosis and their signaling pathways are shown in Figures 3 and 4.

The binding of TNFα to TNF receptor 1 (TNFR1) leads to the recruitment of the adapter protein Tumor necrosis factor Receptor type 1-Associated DEATH Domain protein (TRADD), which associates with TNFR1 due to their shared DEATH domain. This same domain allows TRADD to recruit Receptor-Interacting Protein Kinase (RIP or RIPK) 1. This assembly of proteins is referred to as Complex 1. The ultimate fate of the cell depends upon the regulation of this complex.

5

The proteins TNF receptor-associated factor 2 (TRAF2) and the inhibitors of apoptosis (cIAP) 1 and 2 have been implicated in the ubiquitination of RIP1. If RIP1 is ubiquitinated, Complex I will initiate a signal cascade that results in dissociation of IκB from the transcription factor NF-κB [41]. NF-κB is expressed constitutively in the cytosol; upon release from IκB, it translocates to the nucleus and initiates transcription [42, 43, 44].

Like type I IFN, there is a broad diversity in the genes induced by NF-κB. Generally, they are considered to be pro-inflammatory and pro-survival [45, 46]. Examples of pro-survival proteins are IAPs, cellular FLICE-Inhibitory Proteins (cFLIPs), and some members of the B cell lymphoma/leukemia type 2 (Bcl-2) protein family. The Bcl-2 protein Bfl-1/A1 inhibits the mitochondrial release of cytochrome C, thereby restricting intrinsic apoptosis [47]. cIAP1 and cIAP2 induce the ubiquitination of RIP, inhibiting extrinsic apoptosis. Finally, x-IAP binds to and inhibits caspases 3 and 7 and the long isoform of cFLIP can competitively binds caspase 8, thereby inhibiting both apoptosis pathways [48, 49, 50, 51, 52].

If RIP1 is not ubiquitinated or has its ubiquitin removed, it will recruit additional proteins and form into Complex II [53]. TRADD will recruit Fas-Associated protein with Death Domain (FADD), which in addition to a Death Domain has a Death Effector Domain. This allows it to recruit procaspase 8 [54]. Caspases (cysteine-aspartic proteases) are a family of proteolytic enzymes with important signaling and effector functions. Caspase-mediated cleavage can either activate or inactivate a given target; in this manner they can act as inhibitors and activators of various cell signaling pathways [55]. The aggregation of procaspase 8 with Complex II allows it to self-cleave. This activates it, allowing it to cleave and activate caspases 3 and

6

7, the effector caspases [56]. These enzymes initiate apoptosis by modulating the activities of proteins such as Caspase Activated Dnase (CAD). CAD is released by caspase-mediated cleavage of its inhibitor, allowing it to translocate to the nucleus and cleave genomic DNA [57, 58].

Intrinsic apoptosis is an alternate pathway to death receptor-mediated death that is initiated by intracellular messengers. Intrinsic apoptosis is associated with the release of signals from the mitochondria, and can be caspase independent or dependent. Caspase independent apoptosis is associated with the release of Apoptosis Inducing Factor (AIF), which causes chromatin condensation and DNA fragmentation [59]. Alternatively, stresses such as the activation of RnaseL have been found to lead to the release of cytochrome C from the mitochondria [60]. This release leads to the formation of a complex, the apoptosome, that activates caspase 9. Like caspase 8, caspase 9 is able to cleave and activate caspases 3 and 7, leading to apoptosis [61]. An additional caspase-dependent intrinsic pathway is initiated by the interferon-stimulated gene PKR. Active PKR can directly interact with and activate caspase 8; PKR in turn is able to be cleaved by caspase 8 into a constitutively active form [62, 63, 64].

The promiscuity of the enzymes associated with apoptosis allows for connections between seemingly separate pathways. Although caspase 9 is associated with caspase-dependent intrinsic apoptosis, it is known that caspase 8 is able to cleave and activate it [65]. Caspase 8 can also cleave and inactivate RIP1, thereby preventing its initiation of the signal cascade that activates NF-ϰB [66]. However, other activating pathways exist. In addition to activating caspase 8, PKR has been shown to have the seemingly-contradictory ability to activate NF-ϰB [67, 68]. Interestingly, kinase activity does not appear to be necessary for this function [69].

Necroptosis is an inflammatory and explosive cell death pathway. An alternate death pathway to apoptosis is programmed necrosis, also known as necroptosis. In necroptosis, the plasma membrane ruptures, releasing the contents of the cell [70]. In contrast to the anti-inflammatory death of apoptosis, necroptosis is considered to be pro-inflammatory. This is because the rupturing of the plasma membrane releases numerous damage associated molecular patterns that can serve as a "danger" signal to surrounding cells [71]. Necroptosis and apoptosis also differ morphologically. Cells undergoing necroptosis tend to round and then burst, leaving a faint "halo" around the dead cells, while apoptotic cells involute and bleb. This can be seen in Figure 2, in which L929 cells were treated to induce either apoptosis or necroptosis as described in [72].

The major proteins associated with necroptosis and their signaling pathways are shown in Figures 5 and 6. Unlike necrosis, which is considered to be a disordered process, necroptosis follows an ordered signal cascade program in a similar manner to apoptosis. Also like apoptosis, multiple signal pathways can lead to the induction of necroptosis [70]. All known pathways share the need for the proteins RIP3 and Mixed Lineage Kinase domain Like pseudokinase (MLKL). Activated RIP3 is able to phosphorylate and activate MLKL [73, 74]. While unphosphorylated MLKL is involved in endosomal trafficking [75], activated MLKL is considered to be the effector of necroptosis. Upon phosphorylation, MLKL trimerizes and homes to the cell surface, where it triggers the influx of calcium ions into the cell. This influx is dependent on the cation channel TRPM7 [76]. Death can be delayed by the activity of the plasma membrane-repairing Endosomal Sorting Complex Required for Transport III (ESCRT-III) machinery [77].

One of the best characterized necroptosis pathways is RIP1-dependent necroptosis. This path is an alternate outcome of the formation of Complex II. If caspase 8 is able to be activated by this complex the cell will shift towards an apoptotic death as previously described. However, if the activation of caspase 8 is inhibited, RIP1 is able to dissociate from Complex II and autophosphorylate [78, 79, 80]. This allows it to interact with RIP3 via their shared RIP Homotypic Interaction Motif (RHIM) domains, forming Complex IIb (also known as a necrosome) [81, 82]. The aggregation of RIP3 allows it to auto-phosphorylate and activate, leading to MLKL phosphorylation, activation and death. Death receptor signaling does not appear to be the only means by which RIP1-mediated necroptosis can be induced. FADD knock-out cells have been found to undergo RIP1-dependent necroptosis following treatment with either IFNα, IFNβ, or IFNγ. This death is dependent on JAK/STAT-mediated activation of PKR [83].

RIP1 is not necessary for all necroptotic pathways. TRIF, the adapter molecule for toll like receptors 3 and 4, also contains a RHIM domain that allows it to associate with RIP3. TLR stimulation via treatment with poly(I:C) or LPS has been shown to induce TRIF/RIP3 complexes that lead to the activation of the latter, which is then able to activate MLKL [84, 85]. In addition to its interferon-stimulatory functions, DAI also has a RHIM domain and has been shown to complex with and activate RIP3 during viral infections [22, 86, 87].

Besides caspases 3,7, and 9, active caspase 8 has been found to cleave and inactivate RIP1 and RIP3 [66, 88]. As all known necroptotic pathways necessitate RIP3-mediated activation of MLKL, necroptosis cannot occur when caspase 8 is active [89] In this manner, caspase 8 acts as an important molecular "switch" in determining

whether a cell undergoes apoptosis or necroptosis[90]. Because TNFα is known to lead to caspase 8 activation, caspase activity must be inhibited for TNFα-mediated necroptosis to occur.

Vaccinia virus inhibits apoptosis, necroptosis, and inflammation. Figure 7 summarizes the apoptosis, necroptosis, and inflammatory pathways. Vaccinia must navigate this complex network of interconnected sensors and effectors in order to have a productive infection. It does so by expressing numerous immune evasion genes that serve to obfuscate the virus's presence from the cellular antiviral sensors and inhibit the activation and activity of the antiviral effectors.

Several immune evasion genes contribution to the inhibition of apoptosis. An early member of this family to be described was the cowpox virus protein Cytokine response modifier A (CrmA), which confers resistance to TNFα[91, 92, 93]. CrmA is a serine proteinase inhibitor (serpin) that blocks the activation of several caspases, including 1, 8, and 9 [94, 95]. Homologs of this protein exist in VACV, including B13R and B24R. However, while B24R is well conserved among VACV strains, B13R is more diversely found; for example while B13 is conserved in the neruovirulent WR strain, but absent in the Copenhagen strain used as a vaccine against smallpox in some countries [96, 97, 98]. Another TNFα inhibitor found in some but not all VACV strains is CrmE, a soluble TNF receptor that competitively binds to TNFα to inhibit apoptosis [99]. Finally, F1L acts to inhibit the intracellular proteins that trigger the release of cytochrome c from the mitochondria, thereby abrogating intrinsic apoptosis [100].

VACV also suppresses inflammation. This is mediated by inhibitors of of NF-κB, including C4, N1, and K1. C4 inhibits it at or downstream of IκB [101]. N1 is able to

inhibit both NF-κB and apoptosis through distinct amino acid residues [102]. Finally, K1 acetylates one of the subunits of NF-κB, thereby preventing even activated protein from initiating transcription [103].

A46R produces an inhibitor of TRIF, which reduces the ability of TLR3 to initiate an interferon response after detection of endosomal dsRNA [104]. Although TRIF is also associated with necroptosis, there have not been any reports of A46R inhibiting TRIF-dependent necroptosis. However, one VACV protein has been identified that inhibits necroptosis: E3.

E3 was first identified as an IFN resistance gene in 1992 [105]. Initially this resistance was associated with the inhibition of PKR, which was dependent on the ability of E3 to bind dsRNA via a carboxyl-terminal dsRNA binding domain [106, 107, 108, 109]. Later it was found that the amino terminus is necessary for full pathogenesis in mice [110], contributes to the inhibition of PKR [111], and confers resistance to DAI-mediated necroptosis [87]. Sequence analysis revealed that the amino terminus of E3 contains a consensus Z-form nucleic acid binding domain.

Nucleic acids in the Z-form have zig-zagging left turning double-helices. The initial report on the structure of DNA described it as a right-handed double helix, resembling a spiral staircase [112]. However, in 1979 a novel DNA x-ray crystallography structure was published of poly [d(CG)] that described a left-turning, zig-zagging helix. This orientation of DNA was dubbed Z-form. Five years later, a similar structure was found for dsRNA [113, 114]. It is thought that the Z-form is energetically unfavorable under normal physiologic conditions, but nucleic acids can enter it under high salt conditions, when they are under torsional strain (such as by the unwinding of DNA to allow transcription), or in stretches of alternating purines and pyrimidines [115, 116].

To date, all observed ZNA has been double-stranded. However, it has been proposed that certain single-stranded DNA and RNA sequences may be capable of adopting "Z-like steps" with conformations similar to dsZNA [117]. Initially, it was uncertain whether ZNA had a biological function or was an artifact only seen under the specific conditions needed to crystallize it. The identification of proteins that can bind to ZNA indicated that it in fact serves a biologic purpose. The first of these proteins to be identified was Adenosine Deaminase, RNA Specific (ADAR1) [118].

ADAR1 is an enzyme that disrupts dsRNA by converting adenosine into inosine; as the latter does not base pair with uracil this destabilizes the dsRNA strand. ADAR1 consists of a Zα domain, a similar Zβ domain, three dsRNA binding domains, and a catalytic domain [119, 120, 121]. ADAR1 exists as two isoforms. The p110 isoform is expressed constitutively, is primarily nuclear, and lacks the Zα binding domain. The p150 isoform is expressed upon interferon stimulation, contains the Zα domain, and is cytoplasmic. In the context of a viral infection, ADAR1 has been observed to be both pro and antiviral. For some viruses, disruption of dsRNA inhibits their life cycle. For others, it eliminates a potent PAMP, thereby assisting in immune evasion. We have observed ADAR1 to be pro-viral in the case of vaccinia virus [122, 123] It is the Zα domain that can bind to Z-form nucleic acids [124, 125, 126]. Furthermore, ADAR1 has a higher affinity for dsRNA containing sequences prone to entering the Z form [127]. Finally it is worth noting that despite ADAR1 being associated with dsRNA, the Zα domain has been shown to be able to bind to both Z-form dsDNA and Z-form dsRNA [128].

A second protein with ZNA binding capability is found in zebrafish. PKZ is a homolog of PKR, in which the two dsRNA binding domains are replaced with two Zα

domains [129, 130]. PKZ+ fish are still able to express PKR, and it appears that the two proteins have non-redundant, synergistic effects [131]. The importance of PKZ in fish immunity was highlighted by the discovery that the fish pathogen cyprinid herpesvirus 3 encodes a protein, ORF112, with a ZNA binding domain that inhibits the activity of PKZ [132].

The third cellular protein with known ZNA-binding activity is DLM1. This protein was initially isolated from tumor-stimulated mouse macrophages [133] It was later found to have $Z\alpha$ and $Z\beta$ sites homologous to those in ADAR1, and gained the name Z-DNA Binding Protein 1 (ZBP1) [134]. Both domains are necessary for efficient ZNA binding [135]. Later, it was found that ZBP1 can bind to cytosolic dsDNA and induce type I interferons, and was given a third name: DNA-dependent Activator of IFN-regulatory factors, which has been previously described for its role in IFN signaling and RIP1-independent necroptosis [20, 21]. ZNA binding in DAI/ZBP1 is necessary for the induction of necroptosis during influenza A virus infection [136].

E3 contains a domain homologous to the $Z\alpha$ domains found in ADAR1 and DAI. Although $Z\alpha_{E3}$ has a lower affinity for ZNA than ADAR1 and DAI [137, 138], the ability to bind ZNA is nevertheless necessary for full pathogenesis in mice [110]. E3 inhibition of DAI-dependent necroptosis is also dependent on ZNA binding [87].

To date, all known host ZNA-binding proteins have been found to have anti-viral properties. Another interesting property shared by all, including VACV E3, is that they home to stress granules [139].

Stress granules are aggregations of stalled mRNA and RNA binding proteins. RNA translation requires a complex assembly of proteins and mRNA. If

translation becomes stalled, the mRNA and RNA binding proteins can aggregate into non-membrane bound organelles. These aggregations recruit and are stabilized by RNA binding proteins such as Ras GTPase-activating protein-binding protein 1 (G3PB1), T-cell intracellular antigen (TIA)-1 and TIA-1-related protein (TIAR). If the stall in translation is ameliorated, these complexes can disassemble as protein synthesis resumes. Otherwise, they will be removed via autophagy [140].

One of the most important causes of stalled translation is the phosphorlyation of eukaryotic translation initiation factor 2α (eIF2α). This phosphorylation causes the formation of an inactive eIF2-GDP and eIF2B complex, causing the cessation of the majority of protein translation [141, 142]. However, this inhibition does allow for the expression of the transcription factor ATF4, leading to an upregulation of stress-response associated genes [143].

Depending on the context, stress granules can be either pro or anti-viral [144]. Granules formed by reovirus have been reported to be proviral. While this effect can be partially explained by increased viral transcription mediated by eIF2α phosphorylation-induced ATF4, it may also be due to the sequestration of host mRNA, thereby eliminating competitors to viral transcripts [145]. Polio virus induces stress granules early in infection, but goes on to inhibit them as infection progresses; loss of viral proteins that inhibit stress granule formation attenuates the virus [146]. Finally, vaccinia virus mutants lacking the E3 protein induce stress granules; formation of granules correlated with reduced viral replication [147].

The phosphorylation of eIF2α is mediated by the eIF2α kinase family, whose members are activated by various forms of stress. Heme-regulated eIF2α kinase (HRI) responds to iron deficiency [148]. GCN2 is activated by amino acid starvation [149].

PERK is triggered by misfolded proteins in the endoplasmic reticulum [150]. Finally, eIF2α-phosphorylation is yet another activity of PKR [151]. A number of chemical stressors have been identified that are able to initiate eIF2α phosphorylation. One of these is sodium arsenite.

Sodium arsenite induces stress granule formation. Sodium arsenite has been used in biomedical research for over a century. An 1882 publication describes the toxicity of arsenite in frogs [152], while a 1900 article reported several case studies in which arsenite injections were used to treat tuberculosis enteritis [153]. In more recent times, arsenite has been used to probe the oxidative stress response.

Sodium arsenite treatment causes cellular stress that is detected by heat shock proteins [154]. These in turn activate the eIF2α kinase HRI, leading to a cessation of the majority of translation [155, 156]. This is associated with the accumulation of stress granules [157]. For this reason, arsenite is commonly used in experiments involving the cellular stress response.

Arsenite has diverse effects in the cell beyond HRI activation [158]. These include the induction of apoptosis [159] and sensitizing cells to TNFα[160]. Some of these effects have been observed to be dose dependent. Lower concentration exposure has been found to be stimulatory for the pro-survival and proliferation ERK MAP Kinase pathway, while higher doses trigger pro-death JNK-mediated signals [161, 162, 163].

The work described in this document. This dissertation details my work to better understand the ways in which cell death is triggered, and the means by which a virus might abrogate them. In Chapter 2, I explore a possible mechanism by which monkeypox virus could compensate for the partial loss of the amino terminus of its E3

homolog. In Chapter 3, I use mutants of VACV E3 to ask if ZNA binding is necessary for PKR inhibition and if PKR inhibition is necessary for the inhibition of necroptosis. Finally, in chapter 4 I use sodium arsenite to ask if a viral ligand is necessary for the induction of DAI/ZBP1-dependent necroptosis.
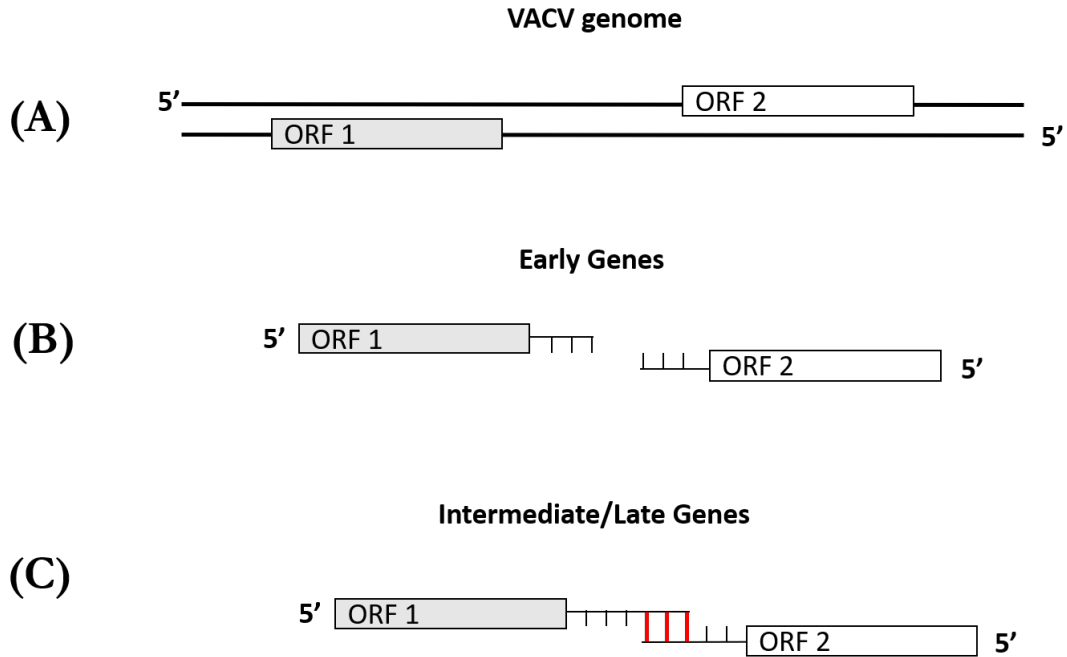
Figure 1: Model for how double-stranded RNA accumulates in VACV-infected cells. (A) The VACV genome has several instances of open reading frames present on opposite strands that face towards one another. (B) Genes that are expressed in the Early phase of the virus life cycle have precise transcription termination, and produce mRNA that does not overlap. (C) Following genome replication, the virus enters the Intermediate and eventually Late phases of its life cycle. Genes expressed in these phases lack transcription termination signals, and so can produce long mRNA transcripts. For opposing ORFs, this creates the possibility of overlapping mRNA that hybridizes into dsRNA.

	0 Hours	4 Hours	6 Hours
TNFα + ZVD			
TNFα + Cycloheximide			
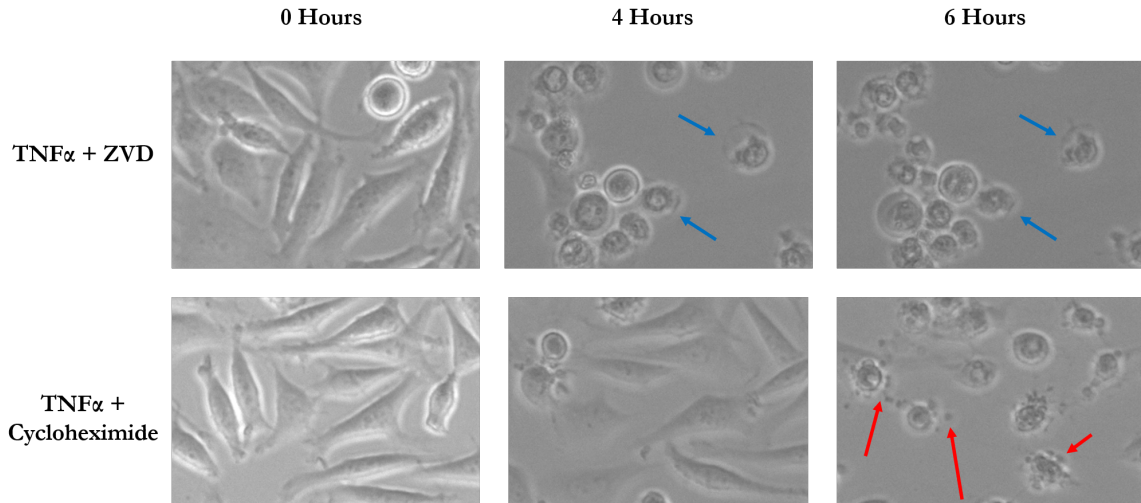
Figure 2: Timelapse images of cells treated to induce either necroptosis or apoptosis. L929 cells were treated with TNFα, and either the pan caspase inhibitor Z-VAD-FMK to induce necroptosis (top row) or the protein synthesis inhibitor Cycloheximide to induce apoptosis (bottom row). In necroptosis, cells round and burst; blue arrows point to representative cells. In apoptosis, cells shrink and bleb; red arrows point to blebs.
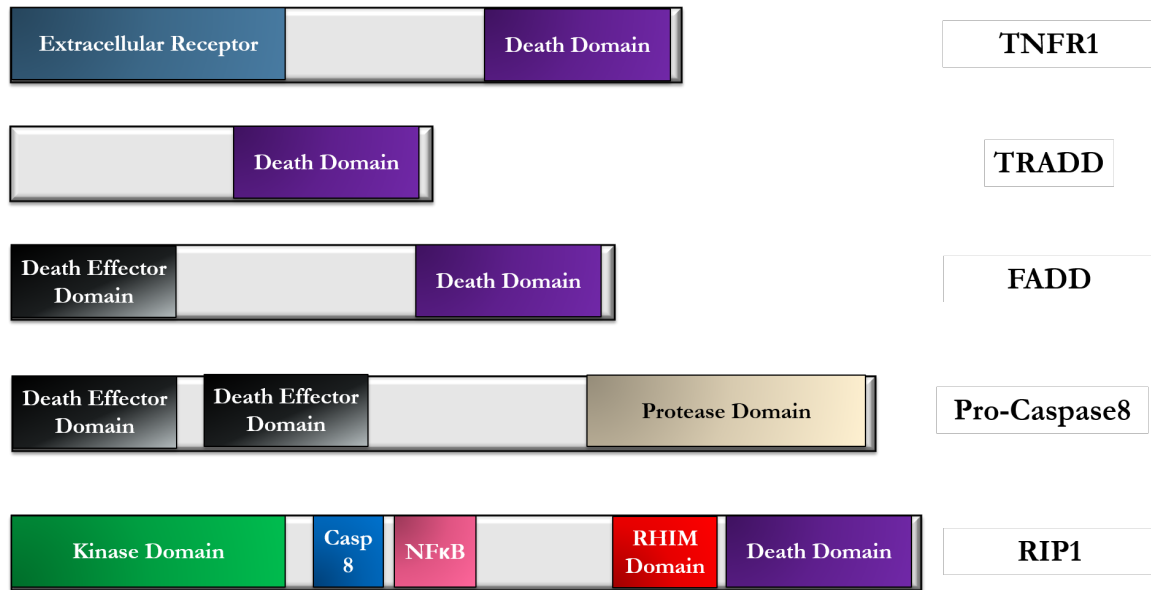
Figure 3: Shared motifs link members of the extrinsic apoptosis pathway. TNFR1 is a trans-membrane protein with an extracellular receptor that recognizes TNFα and an intracellular Death Domain. This Death Domain allows TRADD and RIP1 to associate with it, forming complex I. FADD has a Death Domain that allows it to associate with complex I and a Death Effector Domain that can recruit Pro-Caspase 8; if these proteins join complex I it becomes complex II.
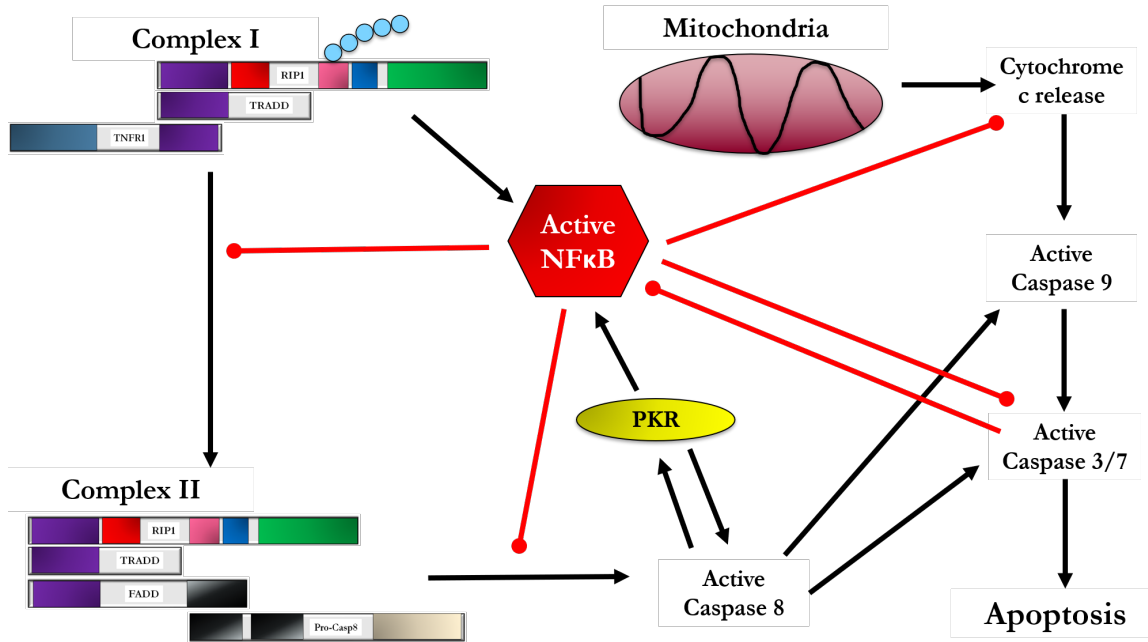
Figure 4: Overview of pathways leading to apoptosis. Complex I formation can be triggered by TNFα binding to its receptor. If RIP1 is ubiquitinated, NF-κB becomes activated and induces the expression of prosurvival proteins that inhibit apoptosis. If RIPI is not ubiquitinated, FADD and caspase 8 are recruited, forming Complex II. In this complex, caspase 8 can self-cleave and activate. Activated caspase 8 can cleave and activate caspases 3 and 7, the effectors of apoptosis. Alternatively, intracellular signals can trigger the release of cytochrome C from the mitochondria. This leads to the activation of caspase 9, which can also activate caspases 3 and 7. PKR can activate and be activated by caspase 8.
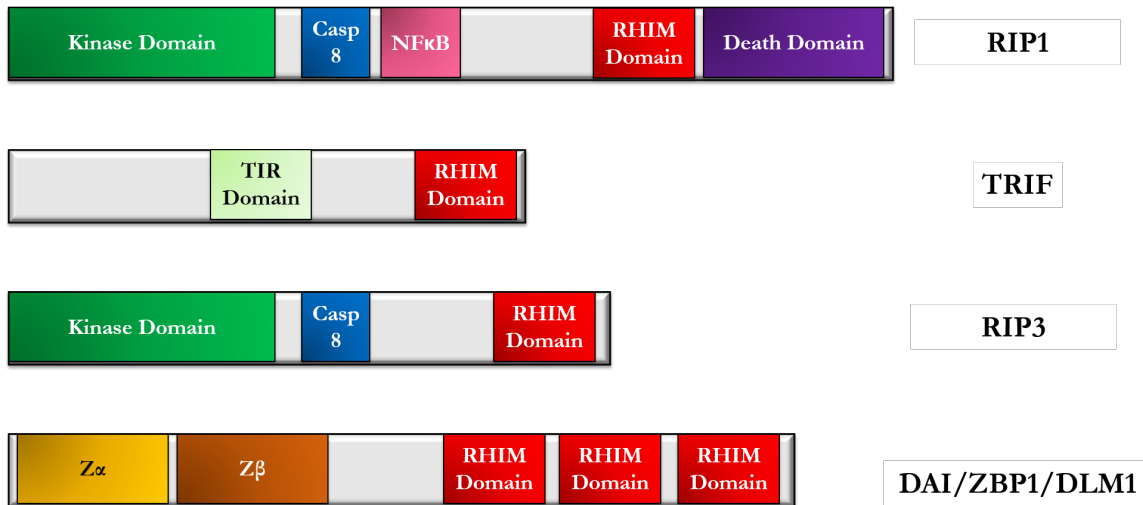
Figure 5: Shared RHIM domains link members of the necroptosis pathway. RIP1 is a member of TNF complexes I and II via its Death Domain. TRIF is a signal transducer for TLRs 3 and 4 via its TIR domain. DAI/ZBP1/DLM1 binds to Z-form nucleic acids via its Zα domain. These three proteins are able to associate with RIP3 via their RHIM domains. The association of any of these molecules with RIP3 leads to its phosphorylation. Phosphorylated RIP3 is able to phosphorylate MLKL, leading to necroptosis.
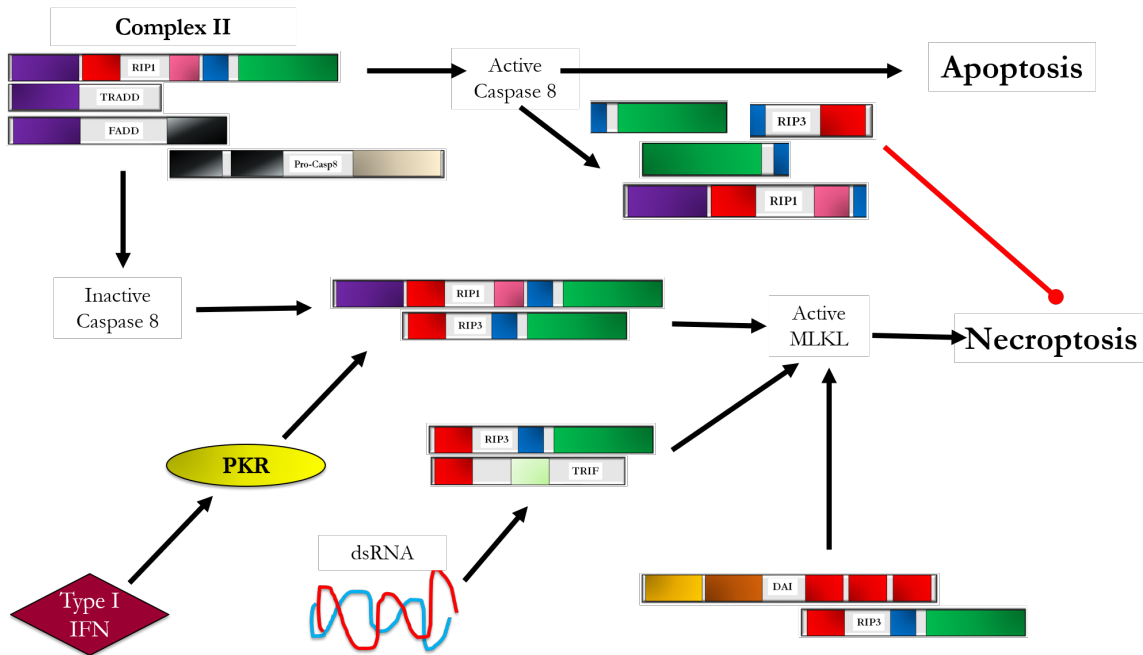
Figure 6: Overview of the extrinsic and intrinsic apoptosis pathways. The effector of necroptosis is MLKL; all known necroptotic pathways end with RIP3-mediated phosphorylation and activation of MLKL. In death receptor-mediated necroptosis, Complex II forms but the activation of caspase 8 is inhibited, allowing RIP1 to dissociate from the complex and instead interact with and activate RIP3. RIP3 can also be activated by the RHIM-domain-containing proteins TRIF and DAI/ZBP1. TRIF is an adapter for TLRs 3 and 4, while DAI can bind to cytosolic dsRNA and dsDNA.
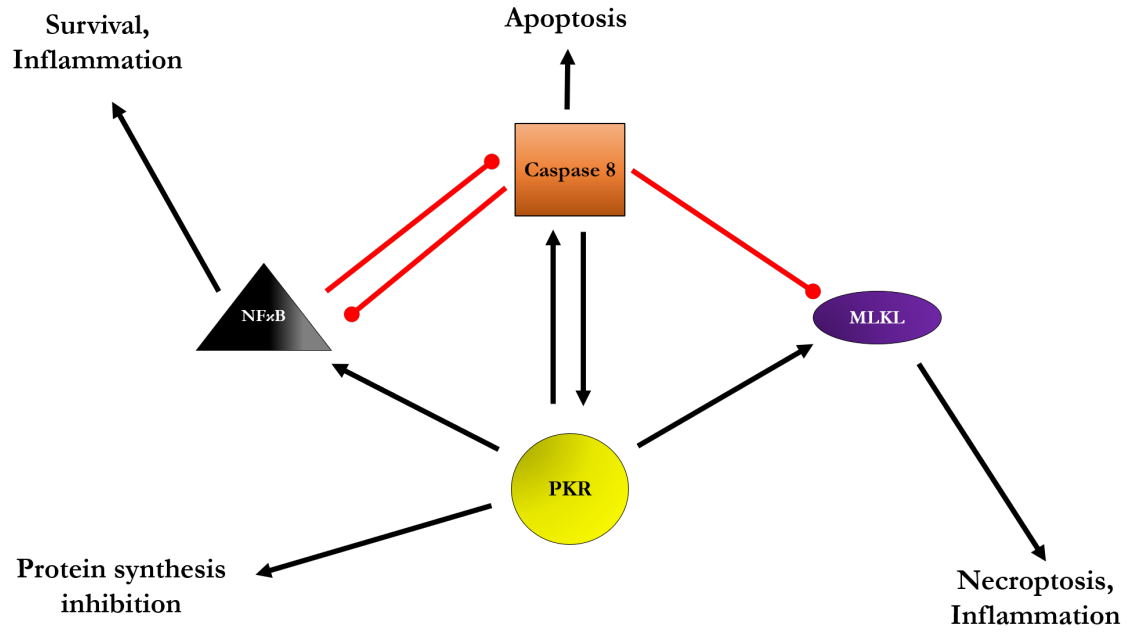
Figure 7: Simplified schematic of cell pathways leading to death or inflammation. The phosphorylation of MLKL leads to necroptosis. The activation of caspase 8 triggers a signal cascade that leads to apoptosis and inhibits necroptosis. NFϰB induces the expression of prosurvival and proinflammatory proteins that can inhibit apoptosis and necroptosis. PKR has been found to be able to induce all three pathways in certain contexts.

Chapter 2

MONKEYPOX VIRUS MAKES LESS DOUBLE-STRANDED RNA THAN VACCINIA VIRUS

2.1 Abstract

Monkeypox virus is a reemerging human pathogen. Despite the pathology MPXV can cause, it is known to have a partial truncation in the protein F3, the MPXV homolog of the vaccinia virus interferon-resistance protein E3. A similar mutation in E3 attenuates VACV and leads to the phosphorylation of PKR. However, we do not observe this in MPXV-infected cells.

Because PKR activation is associated with viral production of dsRNA, we decided to test whether or not MPXV synthesizes less double-stranded RNA than VACV. VACV mutants that are resistant to the antiviral drug isatin-β-thiosemicarbazone are known to have reduced accumulation of dsRNA in infected cells. We determined that MPXV is naturally resistant to IBT compared to wild-type VACV, suggesting that it as well synthesizes less dsRNA. For direct confirmation, we performed a slot blot on total RNA extracts from infected cells and probed with an antibody specific for dsRNA. We found that while wild-type VACV had a significant increase in detectable dsRNA as early as 9 hours post infection, neither MPXV clade produces dsRNA to comparable levels. These data suggest that reduced accumulation of dsRNA is a possible strategy that a virus can use to compensate for loss-of-function mutations that reduce its ability to inhibit PKR.

2.2 Introduction

Monkeypox virus is an emerging pathogen Monkeypox virus (MPXV) is a member of the genus Orthopoxvirus, which also includes variola virus and vaccinia virus (VACV). MPXV is split into two clades, West African and Central African. Although both clades have been found to infect humans, Central African MPXV has a worse prognosis, with mortality rates as high as 10% [164, 165]. Although the vast majority of MPXV infections occur in Africa, there was an outbreak in the United States in 2003 that was traced to the import of African rodents [166, 167].

During the global campaign to eradicate variola virus, MPXV cases were reduced as well due to cross protection between the smallpox vaccine and other members of Orthopoxvirus. However, following the eradication of smallpox vaccination against it has largely ceased, meaning that over time there has been an increase in the number of people vulnerable to other poxviruses, including monkeypox virus [168]. Therefore, there is considerable value in better understanding the virus and the risks it poses to human health.

Monkeypox virus has a deletion in the amino terminus of its homolog of the vaccinia virus IFN-resistance gene E3L The gene E3L is highly conserved among members of the chordopoxviridae family, with homologs found in all members with the exception of molluscum contagiosum virus and the avipoxvirus genus [169, 170]. For the remaining chordopoxviridae, E3L expresses a protein consisting of a dsRNA binding domain on the carboxyl terminus [171] and a Z-form nucleic acid binding domain on the amino terminus [110]. For vaccinia virus, both domains are necessary for pathogenesis in mice [172] and inhibiting PKR [105, 111] and inhibition

of necroptosis is dependent on the ZNA binding domain [87]. However, the amino terminus is not necessary for pathogenesis for all of chordopoxviridae. It has been found that the E3 homolog in the Leporipoxvirus family lacks an amino-terminal ZNA binding domain [173, 174]. Despite this, myxoma virus is fully pathogenic in European rabbits, a phenotype that is lost in the absence of the E3 homolog [175]. Another poxvirus lacking a complete E3 amino terminus is monkeypox virus.

Due to leaky AUG scanning, E3 is sometimes expressed in a truncated form lacking the first 37 amino acids, p20. As this truncation extends into the ZNA binding domain, p20 is not expected to be capable of binding to the molecule. Sequence analysis of the MPXV genome reveals that a series of mutations in F3L, the E3L homolog, cause it to only be capable of being expressed as the truncated p20 [176]. Based on observations that the amino-terminus is involved in PKR inhibition, we might expect the partial loss of it to sensitize virus to PKR activation [177, 111]. In fact, we observe that VACV with an equivalent mutation in E3 (E3Δ37N) or that has E3 replaced with MPXV F3 leads to eIF2α and PKR phosphorylation. However, MPXV fails to induce PKR phosphorylation under the same experimental conditions [178]. Therefore, MPXV must have evolved some alternative mechanism to inhibit PKR phosphorylation.

PKR activation is associated with the accumulation of dsRNA [179]. VACV produces this dsRNA due to imprecise transcription termination. This results in the synthesis of long mRNA molecules that can potentially overlap and hybridize into dsRNA. dsRNA accumulation can be further enhanced by treating infected cells with isatin-β-thiosemicarbazone (IBT), which increases the processivity of the VACV RNA polymerase. This increases dsRNA accumulation to the extent that E3 is no longer

able to fully obfuscate it, leading to the activation of PKR and RNase L and restriction of viral replication [6]. Several IBT-resistant mutants of VACV have been identified; this resistance appears to be mediated by reduced RNA polymerase processivity, resulting in reduced dsRNA accumulation both in the presence and absence of IBT [180, 181]. Figure 8 illustrates this process.

Based on these observations, we hypothesized that MPXV has evolved reduced transcript processivity to produce less dsRNA in order to compensate for the reduced ability of F3 to inhibit PKR.

2.3   Materials and Methods

Cells and viruses. L929 cells were maintained in minimum essential medium (MEM, Cellgro) supplemented with 5% fetal bovine serum (FBS) (HyClone). BSC40 cells were maintained in Dulbecco's Modified Eagle Medium (DMEM, Cellgro) supplemented with 5% FBS and 2 µM L-Glutamine. All vaccinia virus work was performed with the WR strain of virus. In addition to wild-type VACV we also used the previously generated VACV E3Δ37N [182]. Two strains of MPXV were studied, one from each clade. MPXV WRAIR 7-61 (7-61) was used as an example of a West African clade virus and Zaire V79-I-005 (Zaire) was the Central African clade member.

Slot Blot HeLa cells were mock-infected or infected with VACV, MPXV 7-61, or MPXV Zaire. Total RNA was extracted with the RNeasy Mini Kit, using QiaShredder homogenization and in-column DNase treatment as described by the manufacturer (Qiagen). An equal volume of total RNA (2 µL) was diluted in ddH20 (198 µL). Diluted RNA was applied through a VacuSlot VS manifold and transferred onto BrightStar-Plus Positively Charged Nylon Membrane (Ambion). The membrane was UV crosslinked with a Stratagene Stratalinker 1800 (Stratagene). dsRNA was detected using the J2 monoclonal anti-dsRNA antibody (Scicons). Goat anti-mouse HRP conjugate was used as the secondary antibody. Probe specificity was verified using dsRNA and ssRNA ladders (New England Biolabs) as positive and negative controls respectively. As additional controls, RNaseIII (NEB) and RnaseA (ThermoFisher) digestions were performed as described by the manufacturer; RNaseA digestion was performed with 0.5µg/mL enzyme in 2x SSC buffer (300 mM NaCl and 30 mM Sodium Citrate).

IBT-resistance assay BSC40 cells were infected with serial dilutions of virus. Following 30 minutes of rocking, media was added that included 0, 15, 30, 60, or 90 µM of IBT. After 48 hours, the cells were stained and plaques were counted. Each virus and IBT concentration was tested in triplicate and significance was determined using a two-tailed unpaired T-test.

Bioinformatics NCBI's BLAST algorithm [183] was used to compare the nucleotide and amino acid sequences of VACV genes known to have IBT-resistance alleles with their MPXV homologs. Strains used for analysis were VACV Western Reserve and MPXV WRAIR7-61. The specific genes and their Ref sequences follow. VACV genes are preceeded by YP; MPXV by AAU. A18R: YP233020.1 AAU01334.1, A24R: YP233026.1 AAU01340.1, G2R: YP232962.1 AAU01276.1, H5R: YP232985.1 AAU01299.1, J3R: YP232977.1 AAU01291.1, and J6R: YP232980.1, AAU01294.1.

This analysis determined that the gene H5R differed the most between VACV and MPXV. For further anlysis, we used ClustalW [184, 185] to compare the H5R homologs of vaccinia, monkeypox, horsepox, ectromelia, variola, taterapox, camelpox, cowpox, and myxoma virus.

2.4 Results

Monkeypox virus produces less double-stranded RNA than vaccinia virus To determine whether MPXV produces less dsRNA than vaccinia virus, we used a slot blot to detect dsRNA present in total RNA extract. To verify the specificity of the J2 antibody, we tested whether it would give signal in preparations that we would expect to have no dsRNA. First, it is known that treatment with cytosine arabinoside (araC) inhibits the synthesis of VACV dsRNA [186]. We found that extracts from araC-treated and VACV-infected cells had reduced dsRNA compared to untreated infected cells (Figure 9a). Next, we collected total RNA from VACV-infected cells and boiled it for 5 minutes at 95°C in order to denature any dsRNA present. We then either snap-froze the solution or left it at room temperature to reanneal in different concentrations of salt. We found that while the snap frozen and no salt preparations failed to give dsRNA signal, low and high salt did (Figure 9b). Finally, dsRNA ladder, ssRNA ladder (New England Biolabs), and VACV 12HPI extract were either mock treated or treated with RNAse III (dsRNA specific) or RnaseA (ssRNA specific). As seen in Figure 10b, signal was detected in mock and RNAseA-treated dsRNA ladder and VACV extract, while no signal was detected for ssRNA ladder or samples treated with RNAseIII. Taken together, these data demonstrate that the J2 antibody is dsRNA specific in the conditions we are using it.

To determine the amount of dsRNA produced by MPXV, HeLa cells were mock infected or infected with wild-type VACV, VACV E3Δ37N, MPXV 7-61, or MPXV Zaire at an MOI of 5. Total RNA was collected at 6, 9, and 12 hours post infection and then a slot blot was performed to detect dsRNA (Figure 10a). To verify that extracts were in the linear range, 2 fold serial dilutions of the 12 hour wild-type VACV

30

extract were also measured (Figure 10b). The slot blot was performed in triplicate, and the resulting bands were quantified using TotalLab Quant. As shown in Figure 10c, neither the West nor Central African strains of MPXV accumulated as much dsRNA as VACV, confirming our prediction.

Monkeypox virus is IBT-resistant Because resistance to the drug isatin-β-thiosemicarbazone (IBT) is associated with reduced accumulation of dsRNA [187, 181], we assayed the sensitivity of MPXV to IBT. BSC-40 cells were infected with serial dilutions of MPXV-761 and wild-type VACV. An IBT-resistant mutant of VACV, A24R-1R, was used as a resistance control [180]. Infected cells were treated with increasing concentrations of IBT and then stained with crystal violet 48 HPI. As seen in Figure 11, wild-type VACV was highly sensitive, with plaques almost completely eliminated at 15 µM IBT, the lowest concentration tested. MPXV 7-61 was resistant to IBT, though it's phenotype was intermediate compared to A24R-1R; A24R-1R never reached 50% reduction, even at the highest concentration tested (90 µM) while the IC50 of MPXV was reached at 60 µM (Figure 11).

MPXV has polymorphisms in known IBT-resistance genes, but none known to confer resistance. Several VACV genes have been identified to have IBT-resistance alleles. In an attempt to identify the gene responsible for MPXV's IBT resistance, we used BLAST to compare the nucleotide and amino acid sequences of the MPXV homologs of VACV genes known to have alleles that confer IBT resistance. The overall percentage match is shown in Figure 12. Although differences were found, none of the MPXV polymorphisms mapped to residues previously shown to confer IBT resistance.

As H5R had the most divergence between the two viruses, with 89% sequence

homology, we decided to further analyze it by aligning the h5R homologs of vaccinia, monkeypox, horsepox, ectromelia, variola, taterapox, camelpox, cowpox, and myxoma virus (data not shown). Unsurprisingly, myxoma virus differed the most from the others. We also noted that VACV had two unique deletions relative to the other orthopoxviruses, while MPXV had a unique amino acid addition and variola virus has a series of DN repeats inserted.

2.5 Discussion

Despite missing a portion of the F3 amino terminus, MPXV does not lead to PKR activation. The purpose of this project was to determine if monkeypox virus produces less double-stranded RNA than vaccinia virus as a possible mechanism for this lack of activation. Our results demonstrate that monkeypox virus produces less dsRNA than VACV and is naturally IBT-resistant. These results suggest that a decrease in dsRNA production is able to compensate for the partial loss of the amino terminus. If this is the case, then an IBT-resistant strain of VACV E3Δ37N should also fail to phosphorylate PKR.

Our findings lead to a number of new questions. First, the specific mechanism for MPXV's reduced transcript processivity is not known. While BLAST analysis indicated that MPXV does have some polymorphisms compared to VACV genes with IBT-resistance alleles, it is unclear which of these, if any, might be responsible for the reduced accumulation of dsRNA. It is entirely possible that IBT-resistance in MPXV is conferred by a gene previously unassociated with the phenotype. Mapping of the gene in MPXV will be needed to resolve this issue.

The amino terminal of E3 is not only involved in the inhibition of PKR but in inhibiting DAI/ZBP1-mediated necroptosis as well [87]. Because DAI has been shown to bind to viral RNA [188] one might predict that reduced dsRNA accumulation contributes to necroptosis inhibition as well. However, we have found that IBT resistance alone is not sufficient to rescue VACV amino-terminal mutants in necroptosis-competent cell lines (unpublished observations), suggesting that MPXV inhibits

necroptosis through an alternate mechanism. Identifying it would give considerable insight into the life cycle of the virus.

Another question is why PKR activation inhibits VACV in some cell lines but not others. Although VACV E3Δ83N is IFN-sensitive in MEF129 cells, this sensitivity is lost in PKR knockouts [111]. In contrast, E3Δ83N is IFN-resistant in L929 cells in which necroptosis is inhibited or deficient [87]. HeLa cells are also permissive to E3Δ83N despite the virus triggering phosphorylation of PKR and eIF2α. Interestingly, rather than blocking global translation, E3Δ83N-mediated phosphorylation of eIF2α instead was found to only restrict the expression of secreted cellular and viral proteins. In these same cells, ΔE3 infection lead to earlier phosphorlyation of PKR and eIF2α and the complete cessation of translation [189]. One possible explanation for this difference between the partial and total loss of E3 is that the carboxyl terminus has been found to associate with the interferon-inducible protein ISG15. ISG15 is a ubiqutin-like protein that can trigger antiviral activity when conjugated to protein. E3 inhibition of this protein is independent of the amino terminus and PKR activation [190]. therefore, it could be that in HeLa cells the difference between E3Δ83N and ΔE3 isn't the amount or timing of PKR activation but instead the loss of inhibition of ISG15.

Finally, it has been reported that despite having a full length E3 homolog, the orthopoxvirus Ectromelia virus also makes less dsRNA compared to VACV; it has been proposed that this is to compensate for the lack of a homolog of K3, another inhibitor of PKR-mediated eIF2α phosphorylation [191]. This raises the question of how representative the high dsRNA accumulation observed in vaccinia virus is for the rest of poxviridae; is it a result of the unique evolutionary pressures that come

from being primarily grown in tissue culture rather than whole organism over several decades? If this is the case, what is the advantage conferred (at least in cell culture) by increase polymerase processivity? Studies comparing pathogenicity to processivity might begin to elucidate these questions.
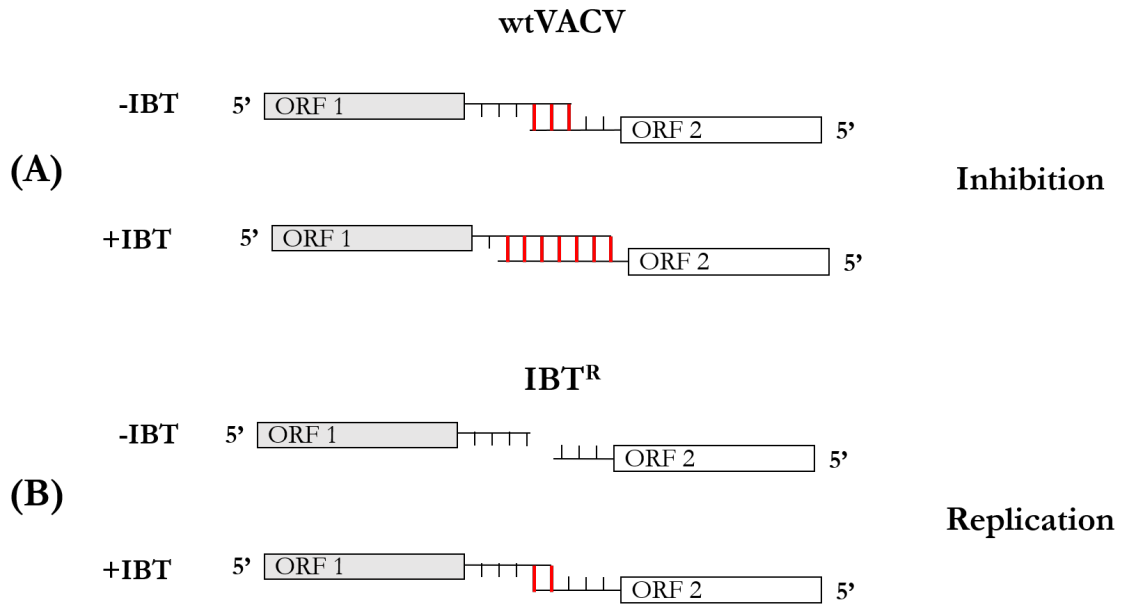
Figure 8: IBT-resistant vaccinia virus produces less dsRNA. (A)Wild-type vaccinia virus naturally produces extended mRNA transcripts at the intermediate and late stages of its life cycle, leading to hybridization into dsRNA. Treatment with IBT further increases transcript length, leading to an increase in dsRNA accumulation. In wild-type virus, this leads to replication inhibition. (B) VACV mutants that confer IBT-resistance decrease the processivity of viral RNA polymerase, leading to shorter mRNA transcripts and reduced accumulation of dsRNA. While treatment with IBT still increases transcript length, these mRNA molecules are still not as long as is observed in wild-type virus treated with IBT and so replication is not inhibited.
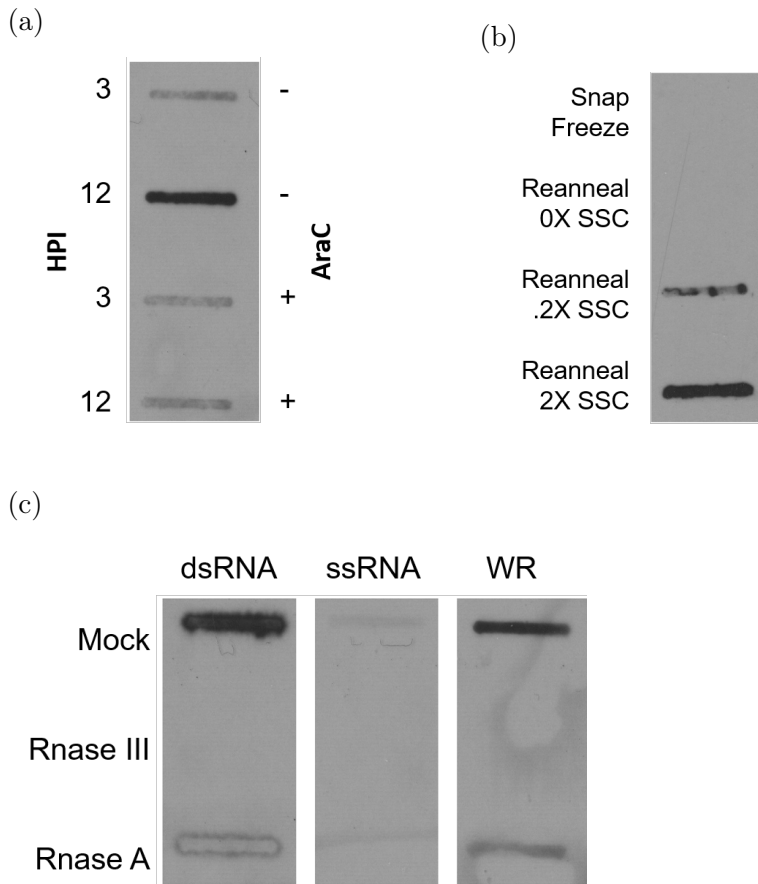
Figure 9: The J2 antibody can specifically bind to dsRNA in a slot blot. dsRNA was transferred onto BrightStar®-Plus Positively Charged Nylon Membrane (Ambion) using a vacuum slot apparatus. dsRNA was visualized on the blot by probing with J2 anti-dsRNA antibody and Goat anti-mouse HRP conjugate secondary antibody. (a) Hela cells were mock pretreated or pretreated with 40ug/mL AraC 1 hour prior to infection with VACV WR. Total RNA was extracted at 3 and 12 HPI. (b) BSC40 cells were infected with VACV and total RNA was extracted at 8HPI. RNA was denatured by boiling at 95°C for 5 minutes; samples where then either snap frozen or left at room temperature to reanneal in either no, low, or high salt conditions. (c) dsRNA ladder, ssRNA ladder, and VACV 12HPI extract were either mock treated or treated with RNAse III (dsRNA specific) or RnaseA (ssRNA specific).
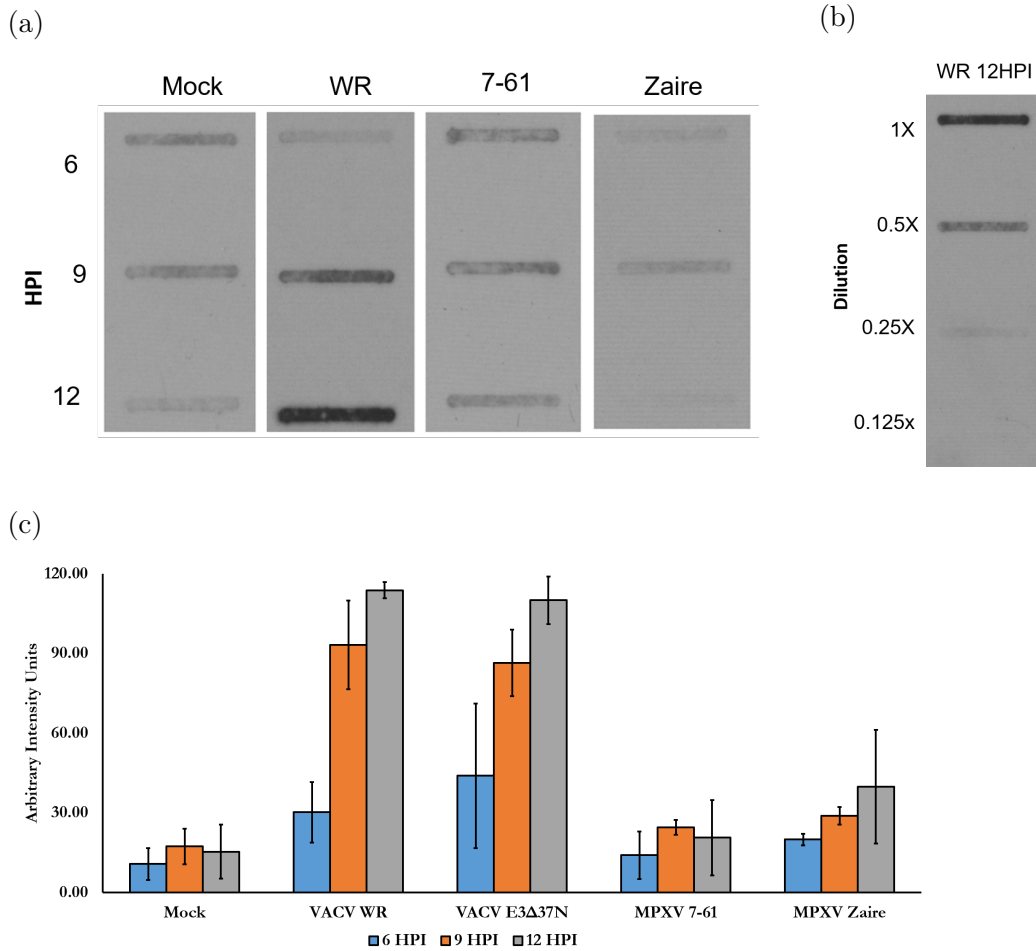
Figure 10: Monkeypox virus infection leads to less accumulation of dsRNA than infection with vaccinia virus. dsRNA was transferred onto BrightStar®-Plus Positively Charged Nylon Membrane (Ambion) using a vacuum slot apparatus. dsRNA was visualized on the blot by probing with J2 anti-dsRNA antibody and Goat-anti-mouse HRP conjugate secondary antibody. (a) HeLa cells were mock infected or infected with VACV WR, MPXV 7-61, or MPXV Zaire at an MOI of 5. Total RNA was collected at 6, 9, and 12 hours post infection. RNA extractions were performed in triplicate; figure shows representative results. (b) Serial 2-fold dilutions of the VACV WR 12HPI extract were included to verify the exposure was in the linear range. (c) Band intensity of slot blots was analyzed with TotalLab Quant. The intensity of the WR 12HPI extraction was calibrated to 100 arbitrary units. The triplicate extraction intensities were averaged; error bars show standard deviation. Significance was calculated with unpaired 2-tailed t-test. Asterisks indicate significance of difference from the 6HPI time point of the same treatment. *p $<.05$, ** p: $<.005$

38
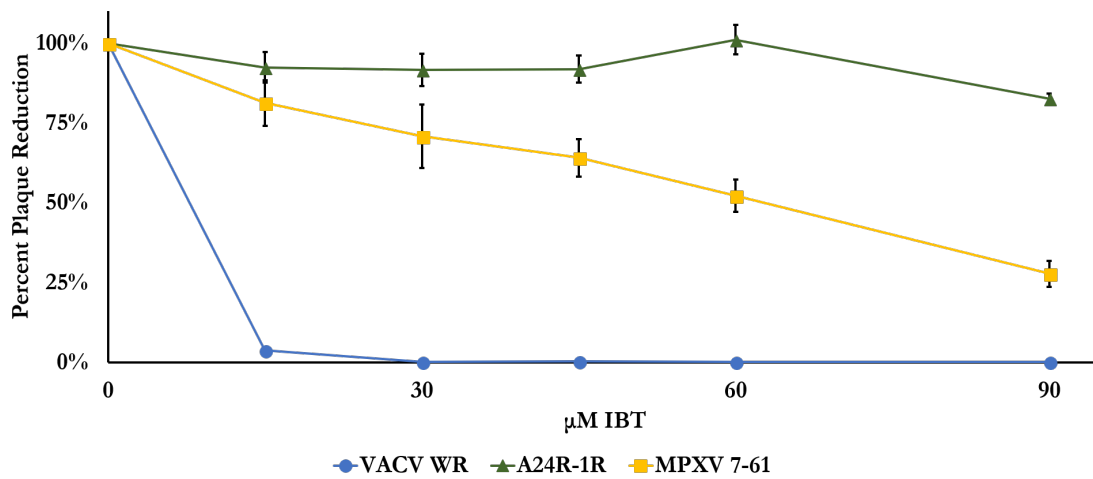
Figure 11: Monkeypox virus is IBT-resistant. BSC40 cells were infected with serial dilutions of wild-type VACV, VACV A24R-1R, or MPXV 7-61. Infected cells were treated with the indicated concentrations of IBT. After 48 hours, the cells were stained with crystal violet and plaques were counted. Presented data are the averages of three independent experiments.

VACV Gene	wtVACV vs MPXV Nucleotide Match	wtVACV vs MPXV Protein Match
G2R	646/663 (97%)	217/220 (99%)
J3R	986/1002 (98%)	330/333 (99%)
J6R	3791/3863 (98%)	1268/1286 (99%)
A24R	3426/3496 (98%)	1143/1164 (98%)
H5R	604/642 (94%)	176/199 (88%)
A18R	1429/1483 (96%)	472/493 (96%)

Figure 12: MPXV has polymorphisms in its homologs of VACV genes with known IBT-R alleles. BLAST and BLAST-P were used to compare the nucleotide and amino acid sequences of the MPXV homologs of VACV genes with known IBT-R alleles. Although differences were found, none of the MPXV polymorphisms mapped to residues previously shown to confer IBT resistance.

Chapter 3

Z-FORM NUCLEIC ACID BINDING IS NOT NECESSARY FOR VACCINIA E3-MEDIATED INHIBITION OF PKR, NOR IS THE INHIBITION OF PKR SUFFICIENT FOR THE INHIBITION OF NECROPTOSIS.

3.1 Abstract

Vaccinia E3L is a potent immune evasion gene, with a C-terminal dsRNA binding domain and an n-terminal Z-form nucleic acid binding domain. We have previously shown that the amino terminus contributes to the inhibition of PKR, and have recently found that N-terminus of E3L can also inhibit necroptosis, a rapid and explosive cell death. Necroptosis is observed in E3L mutants with total loss of the N-terminus as well as point mutants that lose the capacity to bind to Z-DNA in vitro. To determine the role of PKR and ZNA binding in cell death, we searched for viruses which can bind to ZNA but do not inhibit PKR and virus that inhibits PKR but does not bind ZNA, then tested these viruses for cell death. We have found that the VACV mutant $Z\alpha_{ADAR1}$-E3, which replaces the amino terminus of E3 with the $Z\alpha$ binding domain from ADAR1, binds to ZNA and causes PKR phosphorylation, but fails to induce necroptosis. Conversely, the mutant E3:Y48A inhibits PKR and does not bind ZNA, and induces necroptosis. These data suggest that the mechanism for the N-terminal mediated loss of PKR-inhibition is distinct from that for inhibition of necroptosis.

3.2 Introduction

Vaccinia virus infection leads to the production of double-stranded RNA, a potent Pathogen-Associated Molecular Pattern Vaccinia virus (VACV) is a large double-stranded DNA virus in the Orthopoxvirus genus, which also includes variola virus, the causative agent of smallpox, and monkeypox virus, an emerging human pathogen. The virus's entire life cycle is cytosolic, and it encodes its own transcription machinery in order to produce mRNA [192]. This transcription is split into three phases: Early genes are expressed immediately upon viral entry by proteins brought in with the virion core. Intermediate genes are produced following replication of the DNA genome, and include the transcription factors for the final, Late genes [3].

Starting at the Intermediate phase, VACV makes double-stranded RNA [5]. It is believed that this is due to the presence of opposing open reading frames in the VACV genome. Unlike Early genes, which have precise transcription termination signals [4], at the Intermediate and Late stages of the virus life cycle transcription is no longer terminated precisely. This results in the synthesis of long mRNA transcripts [6]. When these transcripts derive from opposing ORFs, it is possible for them to have overlapping complementary sequence, thereby allowing hybridization and the formation of double-stranded RNA.

Type-I Interferons induce expression of antiviral proteins Viral ligands such as dsRNA can lead to the expression of type I interferon (IFN). IFN exposure will cause a cell to enter an antiviral state, in which several antiviral sensor and effector genes are upregulated [11]. One important interferon-stimulated gene is Protein Kinase

R (PKR). PKR has a dsRNA binding domain, and if sufficient dsRNA is present to allow two PKR proteins bind in close proximity, they will auto-phosphorylate, thereby activating [179]. Activated PKR has numerous effects, including phosphorlyation of eukaryotic Translation Initiation Factor 2α (eIF2α), leading to the cessation of the majority of translation. It is also associated with signaling leading to apoptosis [64], necroptosis [83], and further stimulation of Type-I interferon expression [193]. Another protein induced by Type-I interferon is DAI/ZBP1/DLM1. This protein has been shown to be necessary for inducing necroptosis in cells infected with VACV [87], influenza A virus [86], or murine cytomegalovirus [22].

Vaccinia virus is resistant to Type I Interferons Despite the potency of the interferon-stimulated genes, vaccinia virus is resistant to type I interferon. This is largely due to the activity of the viral gene E3L, which encodes the 25 kDa protein E3 [105]. Figure 13 illustrates the domains of E3 and their functions. E3 has two major regions: a z-form nucleic acid (ZNA) binding domain located toward the amino terminus [110] and a dsRNA binding domain on the carboxyl terminus [171]. Both domains are necessary for pathogenesis in mice [172] and both are highly conserved in the Orthopoxvirus genus. A notable exception is monkeypox virus, which expresses a homolog lacking the first 37 amino acids; this loss extends into the ZNA binding domain [176, 178].

We have found that the ZNA binding domain is necessary for full pathogenesis in mice[110]. This attenuation correlates with both the activation of PKR [111] and of DAI-dependent necroptosis [87]. However, it is not currently known if the inhibition of these pathways is linked or if E3 does so through distinct mechanisms. To determine

if PKR inhibition is necessary for necroptosis inhibition, we screened for E3 mutant viruses that either inhibit PKR or bind to ZNA but not both.

For virus that binds ZNA but fails to inhibit PKR, we tested E3:L36R, E3:L50P, and $Z\alpha_{ADAR1}$-E3. In $Z\alpha_{ADAR1}$-E3, the ZNA binding domain of VACV was replaced with the equivalent $Z\alpha$domain from human ADAR1. Previous results indicated that it is able to bind ZNA but fails to suppress PKR [110, 177] but its ability to inhibit necroptosis has not been determined. The L36R and L50P mutations were initially identified by screening plasmid-expressed variola E3 mutants in yeast with inducible PKR; these mutants failed to rescue PKR-mediated death while still maintaining the ability to bind to ZNA [194]. They have not been characterized when expressed by VACV.

To determine if ZNA binding is necessary for PKR inhibition, we tested the virus E3:Y48A. This mutant was generated based on the known crystal structure of the $Z\alpha$ ZNA binding domain in ADAR1. Because the equivalent mutation in the the ADAR1 α domain has been shown to lose the ability to bind ZNA, we believe that E3:Y48A is unable to as well. Previous work has found it to be attenuated in inter-cranial injections [110]. However, its ability to inhibit PKR has not been determined.

Figure 14 summarizes the viruses used in the following experiments.

3.3 Materials and Methods

Cells and virus. HeLa cells were maintained in Dulbecco's Modified Eagle Medium (DMEM, Cellgro) supplemented with 5% FBS and 2 µM L-Glutamine. Wild-type, ΔPKR, and ΔDAI L929 cells were maintained in minimum essential medium (MEM, Cellgro) supplemented with 5% fetal bovine serum (FBS) (HyClone) and not allowed to exceed 7 passages.

Generation of ΔDAI and ΔPKR L929 cells. L929 ΔDAI/ZBP1 and ΔPKR were generated using CRISPR/Cas9 technology [195]. Cas9-expressing L929 cells were generated by Jackie Sicalo Williams using Edit-R Lentiviral Blast-Cas9 Nuclease Particles (Dharmacon) according to manufacturer instructions. In brief, a 24 well dish was seeded with L929 cells to 50% confluency. Individual wells were mock infected or infected with lentivirus containing a transformable cassette that contained genes for Cas9 and blasticidin resistance. After 24 hours, blasticidin was added to the media. After 48 hours, cell were trypsinized and serial diluted into 24 well palate in order to achieve single cell seeding. These were grown in the presence of Blasticidin. Blasticidin-resistant clonal lineages were stored in LN2 for future use.

Following the generation of Cas9-expressing cells, the cells were transformed to stably express guide RNA against the proteins of interest using Edit-R CRISPR Mouse Lentiviral sgRNA (Dharmacon). Cas9+ L929 cells were infected with lentivirus containing a transformable cassette that contained genes for puromycin resistance and express guide RNA specific for either PKR or DAI/ZBP1. Isolation of clonal lineages of puromycin-resistant cells was performed as described above. Successful

gene knockdown was verified via Western blot. DAI knockouts were generated by Jackie Sicalo Williams.

Treatments and Inhibitors The pan-caspase inhibitor Z-VAD-FMK (ZVD, ApexBio) was prepared in DMSO and used at a final concentration of 100 µM. The RIP3 inhibitor GSK872 and RIP1 inhibitor GSK963 (GlaxoSmithKline) were prepared in DMSO and used at a final concentration of 3 µM. Sodium arsenite (Sigma) was used at a final concentration of 500 µM. Mouse TNFα (Sigma) was used at a final concentration of 10 ng/mL. SYTOX Green (ThermoFisher) was used at a final concentration of 1.25 µM.

Cell viability assay L929 cells were pretreated for 18 hours with 500 units of mouse IFNα. When applicable, they were then treated for one hour with ZVD, GSK872, and/or GSK963. Following treatment with inhibitors, without changing the media either sodium arsenite or TNFα were added. Finally, all cells were treated with SYTOX Green. The cells were then placed in the heated incubator stage of an EVOS FL Auto microscope (ThermoFisher), which was calibrated to take Z-Stack images in the Phase and GFP channels at selected time-points. At each time-point the ratio of green to non-green cells was used to determine the number of viable cells. Each experimental condition was performed in triplicate.

Generation of virus E3 mutants. Vaccinia viruses expressing E3:L36R or E3:L50P were generated as described previously [107, 182]. Briefly, point mutants to generate E3:L36R or E3:L50P were generated via whole plasmid PCR of the plasmid PMP-E3L. Following plasmid purification and sequence validation, transfection reactions were prepared using X-tremeGENE 9 (Sigma) according to the manufacturer's instructions. BHK cells were infected at an MOI of 0.5 with VACV ΔE3:LacZ. After

rocking the dishes at 15 minute intervals for 30 minutes, the cells were overlaid with media containing the previously-prepared transfection reagent. Two days post infection, virus was harvested from the infected cells and plaque purified via blue-white screen. White plaques were selected as these presumably contained virus in which LacZ was replaced with the recombinant E3L. Several such plaques were collected and screened via Sanger sequencing of PCR product for the correct E3L sequence.

Treatments and Inhibitors The pan-caspase inhibitor Z-VAD-FMK (ZVD, ApexBio) was prepared in DMSO and used at a final concentration of 100 µM. The RIP3 inhibitor GSK872 (GlaxoSmithKline) was prepared in DMSO and used at a final concentration of 3 µM. Mouse TNFα (Sigma) was used at a final concentration of 10 ng/mL. SYTOX Green (ThermoFisher) was used at a final concentration of 1.25 µM

Cell viability assay. L929 cells were pretreated for 18 hours with 500 units of mouse IFNα. When applicable, they were then treated for one hour with GSK872. Following treatment with inhibitors, the cells were infected with virus. After 30 minutes of rocking, media containing 1.5 µM of SYTOX Green was added. The cells were then placed in the heated incubator stage of an EVOS FL Auto microscope (ThermoFisher), which was calibrated to take Z-Stack images in the Phase and GFP channels at selected time-points. At each time-point the ratio of green to non-green cells was used to determine the number of viable cells. Each experimental condition was performed in triplicate.

Protein extraction Cells were scrapped at the indicated times then spun at 1000G for 10 minutes at 4°C. The media was aspirated, then RIPA buffer containing Halt Protease and Phosphatase Inhibitor Cocktail (ThermoFisher) was added; the

pellet was disrupted via pipetting. Following a 10 minute incubation on ice, the lysate was spun at 16000G for 20 minutes at 4°C. The supernatant was collected and combined with 2X SDS buffer containing DTT and Halt Protease and Phosphatase Inhibitor Cocktail. This solution was then heated for 10 minutes at 95 °C.

Western Blot Protein samples were separated via SDS PAGE using a 7% loading gel and 10% stacking gel. Protein was transferred to nitrocellulose membrane that was then blocked at room temperature for 1 hour with TBS-Tween containing 3% BSA. Following blocking, membranes were incubated with antibodies in TBS-T 3% BSA overnight at 4°C. They were then washed with TBS-T and probed with secondary antibody in TBS-T 3% dry milk (Carnation) for 1 hour at room temperature. After a final 1 hour wash in TBS-T at room temperature, the membranes were treated with Pierce ECL Western Blotting Substrate (ThermoFisher) and exposed to X-ray film.

3.4   Results

VACV E3:L36R but not E3:L50P induces PKR phosphorlyation Vaccinia virus expressing E3:L36R and E3:L50P, and wild-type revertants of these viruses, were generated using IVR. HeLa cells were then mock infected or infected with wt-VACV, VACV ΔE3, E3:L36R, or E3:L50P. Total cell lysate was harvested 9HPI to probe for PKR phosphorlyation. As shown in Figure 15, E3:L36R showed high levels of PKR phosphorylation similar to ΔE3, while E3:L50P had low phosphorylation more similar to mock and wt infection. This data is in contrast to what was reported previously, in which both L36R and L50P were unable to inhibit PKR-mediated death in yeast

VACV E3:L36R and E3:L50P are interferon-sensitive and induce necroptosis in L929 cells The phenotypes of VACV E3:L36R and E3:L50P were further characterized by determining if they were IFN-sensitive and if said sensitivity was due to necroptosis. L929 cells were infected with these viruses and revertants and SYTOX Green was used to measure cell viability over time. In IFN-negative cells, there was no significant change in viability over 12 hours (Figure 17a). In IFNα-treated cells, infection with E3:L36R and E3:L50P but not the revertants lead to death, approaching 25% viability by 12HPI (Figure 17b). The timing and morphology of the death was consistent with previous observations of necroptotic cells [87]. Furthermore, treatment with the RIP3 kinase inhibitor GSK872 delayed and reduced death for E3:L36R and E3:L50P, with both viruses only reaching 75% viability by 12HPI (Figure 18). Taken together, these experiments suggest that VACV E3:L36R and E3:L50P are both able to induce necroptosis in L929 cells.

To determine if this death correlated with reduced viral yield, we performed a plaque reduction assay. L929 cells were infected with serial dilutions of VACV expressing either wild-type E3, E3Δ83N, E3:L36R, E3:L50P, or the wild-type revertants of the latter two viruses (Figure 16). All six viruses were able to form plaques in untreated L929 cells. However, pre-treatment with IFNα caused a reduction in plaques for virus that expressed E3Δ83N, E3:L36R, or E3:L50P. Treating IFN pre-treated cells with the RIP3 kinase inhibitor GSK872 rescued plaque formation for E3Δ83N, and E3:L50P, suggesting that IFN sensitivity in these viruses was due to necroptosis. However, GSK872 did not lead to a statistically significant change from IFN-treatment alone for E3:L36R. Given that the timelapse experiment showed that GSK872 treatment is able to inhibit E3:L36R-mediated rapid cell death, this suggested that additional factors to necroptosis contribute to the IFN-sensitivity of E3:L36R. One candidate for this is PKR, as unlike E3:L50P, E3:L36R causes PKR phosphorylation.

VACV E3:L36R and E3:L50P fail to accumulate E3 to wild-type levels
We had observed several discrepancies between the observed behaviors for VACV expressing E3:L36R and L50P and what was predicted based on the properties of these proteins when expressed via plasmid in yeast. One possible explanation for this is that these mutants lead to unstable proteins that do not persist and therefore cannot accumulate to wild-type levels in a virus infection. Plasmid expression generally gives higher protein yields which could have masked this effect. To test this hypothesis, we measured the accumulation of total E3 in HeLa cells at several times post-infection. We compared this to E3 accumulation in wild-type virus and to VACV E3Δ54N, which we have previously found to be an unstable protein [196].

As shown in Figure 19, we were able to observe E3 in total cell lysate by 3HPI in

wild-type VACV, which persisted to the final point checked, 9HPI. VACV E3Δ54N also produced observable E3 by 3HPI, but by 9HPI it was almost completely absent. In contrast to these, E3:L36R did not produce detectable E3 until 9HPI, and E3:L50P until 6HPI.

This delay in accumulation compared to wild-type virus may be responsible for the differences between our observations and what was reported previously. In earlier work, both E3 leucine mutants were expressed via a plasmid expression system rather than in whole virus, and were expressed at similar levels as wild-type E3 [194]. Because the virally-expressed mutants do not accumulate to detectable levels until much later in an infection, there may simply not be enough E3 present to inhibit necroptosis in cells with an intact pathway.

VACV Zα$_{ADAR1}$-E3 but not E3:Y48A induces PKR phosphorylation in HeLa cells Our original goal for this project was to identify one or more VACV E3 n-terminal mutants in which inhibition of PKR was separated from binding to Z-form nucleic acids. The altered accumulation of VACV E3:L36R and E3:L50P introduces additional variables to this characterization, making them unsuitable tools for this question. We moved on to another virus, VACV Zα$_{ADAR1}$-E3. In this virus, the ZNA-binding domain of E3 was replaced with the Zα ZNA binding domain from ADAR1. Although this E3 mutant maintains ZNA binding, it induces phosphorlyation of eIF2α and is attenuated in mice [177].

To determine if VACV E3:Y48A infection leads to PKR phosphorlyation, we infected HeLa cells with it or VACV expressing wild-type E3, E3Δ83N, or Zα$_{ADAR1}$-E3 (Figure 20). Cells were harvested 9HPI and the total cell lysate underwent a Western Blot probing for phosphorylated PKR. The membrane was then stripped and

probed for total PKR. As has been reported previously, we observed higher levels of phosphorlyation in E3Δ83N and Zα$_{ADAR1}$-E3 than cells that were either mock infected or infected with wild-type VACV [111] [177]. VACV E3:Y48A gave phosphorlyation similar to wild-type VACV, suggesting that loss of Z-form nucleic acid binding does not enhance activation of the PKR pathway.

VACV E3:Y48A but not VACV Zα$_{ADAR1}$-E3 induces DAI-dependent necroptosis and is interferon-sensitive in L929 cells With the identification of viruses that separately either bind ZNA or are able to inhibit PKR, we then tested whether or not they would undergo necroptosis. L929 cells were infected with wild-type virus, VACV E3Δ83N, E3:Y48A, or Zα$_{ADAR1}$-E3. SYTOX Green was used to measure cell viability over time. In IFN-negative cells, there was no significant change in viability over 12 hours (Figure 21a), while in IFNα pre-treated cells, viability was reduced by 50% by 9HPI for E3Δ83N and E3:48A while significant death was not observed for wild-type and Zα$_{ADAR1}$-E3 infection (Figure 21b). Treatment with GSK872 fully rescued death, further supporting the idea that the interferon sensitivity E3:Y48A is due to necroptosis. (Figure 22)

As an alternate method to show that VACV Zα$_{ADAR1}$-E3 does not undergo necroptosis, we used a western blot to determine if MLKL was being phosphorylated (Figure 23). IFNα-treated L929 cells were infected with the four viruses above with an additional mock infection. Total cell lysate was harvested via RIPA at 3HPI. We then analyzed the lysate using a Western Blot and probed for phosphorylated MLKL and total MLKL. Consistent with our cell viability data, we observed phosphorylated MLKL in virus expressing E3Δ83N and E3:Y48A but not wild-type E3 or Zα$_{ADAR1}$-E3.

To determine the interferon sensitivity of VACV Zα$_{ADAR1}$-E3 and E3:Y48A, we

infected L929 cells with serial dilutions of it and VACV expressing wild-type E3, E3Δ83N, and E3:Y48A (Figure 24). The cells were either mock treated, pretreated 18 hours with IFNα, or pretreated 18 hours with IFNα and 1 hour with the RIP3 kinase inhibitor GSK872. We found that while VACV expressing wild-type E3 and Zα$_{ADAR1}$-E3 did not show a statistically significant decrease in plaque numbers in interferon-treated cells, both E3Δ83N and E3:Y48A yielded fewer plaques in IFNα-treated cells. However, GSK872 treatment was able to fully restore plaque yields for these viruses, suggesting that IFN-sensitivity was dependent on necroptosis.

Finally, to determine if E3:Y48A-mediated necroptosis is DAI-dependent, we repeated the SYTOX Green viability assay using L929 cells in which CRISPR was used to knockout DAI. In these cells, while TNF-ZVD was still able to induce death, none of the viruses were able to (Figure 25). This suggests that like E3Δ83N, E3:Y48A induces necroptosis via the DAI pathway.

PKR is not necessary for VACV-induced necroptosis in L929 cells It has previously been reported that PKR activation can lead to necroptosis [83]. To determine if PKR plays a role in VACV-induced necroptosis, we used CRISPR-Cas9 to generate PKR-knockout L929 cells. The knockout was verified through a western blot (Figure 26). Using SYTOX Green, we then measured the viability of these cells when infected with VACV expressing wild-type E3, E3Δ83N, Zα$_{ADAR1}$-E3, and E3:Y48A. We found that as was the case with wild-type L929 cells, we did not observe significant death in untreated cells (Figure 27a). In IFNα-treated cells, E3Δ83N and E3:Y48A induced a rapid death morphologically consistent with necroptosis while wild-type E3 and Zα$_{ADAR1}$-E3 did not significantly reduce viability (Figure 27b). Finally, death was fully rescued with GSK872 treatment (Figure 28). These data suggest that although

PKR activity can be a potent inhibitor of VACV [105], it does not play a role in necroptotic inhibition of VACV.

Figure 29 shows an updated list of the phenotypes associated with the viruses used in the preceding experiments.

3.5   Discussion

The purpose of this project was to determine if PKR inhibition and ZNA binding were necessary for vaccinia virus E3 protein inhibition of DAI-dependent necroptosis. We initially believed that VACV E3:L36R and E3:L50P would bind ZNA but not inhibit PKR phosphorylation due to the variola virus homolog proteins' ability to bind to ZNA but not rescue PKR-mediated death in yeast. However, we found that when expressed in vaccinia virus, only E3:L36R induced phosphorylation of PKR. One possible explanation for this discrepancy is that these mutants accumulate less E3 protein than wild-type protein in the same time frame, and therefore some of the resulting phenotypes are due to the decreased levels of E3 rather than unique properties of the point mutants themselves.

Despite this, we were able to identify E3 mutants with the desired phenotypes. $Z\alpha_{ADAR1}$-E3 is able to bind to Z-form nucleic acids but leads to PKR phosphorylation. E3:Y48A does not bind ZNA but is able to inhibit PKR activation. We found that of the two viruses, only E3:Y48A induces DAI-depending necroptosis, suggesting that PKR activation is not necessary for this programmed death pathway.

It is known that PKR can act as a signal transducer in FADD-dependent necroptosis [83]. Because of this, it might have been expected that PKR plays some role in viral DAI-dependent necroptosis. Our data show that PKR is in fact dispensable for this necroptosis pathway, further supporting the idea that PKR and necroptosis inhibition are important, but separate functions of E3.

Taken together, these data indicate that in the context of a VACV infection, PKR activation and necroptosis constitute distinct antiviral systems that the virus

must overcome. This is especially significant when one considers that the reemerging pathogen monkeypox virus, another member of Orthopoxvirus, has a 37 amino acid truncation in the amino terminus of its E3 homolog F3. Based on our findings in VACV, we might predict such a mutation to induce PKR phosphorylation and necroptosis. Presumably, monkeypox virus has evolved alternative means to block these pathways. Identifying how it specifically accomplishes this could provide valuable insight into this human pathogen.

Several important questions remain. First, it is not clear how the amino terminus of wild-type E3 contributes to the inhibition of PKR. While VACV ΔE3 has detectable PKR phosphorylation as early as 6 hours post infection, we typically do not observe this activation in VACV E3Δ83N until 9 hours post infection, suggesting that the carboxy terminus contributes to but is not sufficient for total inhibition of PKR [189]. We have previously hypothesized that E3 inhibits PKR via competitive binding to dsRNA; the dsRNA binding domain on the carboxyl terminus associating with right-helical dsRNA and the ZNA-binding domain associating with left-helical dsRNA. However, the data presented here suggest that there is a mechanism of PKR inhibition independent of nucleic acid binding. This is consistent with the characterization of VACV E3:N123A, a c-terminal point mutant that is able to bind to dsRNA and pull down PKR in an affinity assay but does not inhibit PKR phosphorylation [197].

Another question this work raises is the role of the carboxyl terminus, especially the dsRNA binding domain, of E3 in inhibiting necroptosis. We have observed that VACV that expresses the ZNA and dsRNA binding domains as separate proteins rather than as a single linked protein induces PKR and eIF2α phosphorylation, suggesting that the two domains have a synergistic effect when bound together [198]. Is this

also true for inhibition of necroptosis? Answering these questions could provide further insight into the specific mechanisms by which E3 is able to inhibit PKR and necroptosis.

TRIF, an adapter for TLRs 3 and 4, has also been shown to be able to induce necroptosis in L929 cells following poly(IC) [85]. However, to date TRIF-mediated necroptosis has not been associated with any virus. VACV is known to produce an inhibitor of TRIF, A46 [104], which may be responsible for this. If this is the case, then knocking out this protein in VACV E3:Y48A should lead to necroptosis in DAI-deficient cells.

Finally, it has been reported that E3 has a lower affinity for ZNA than other $Z\alpha$ domain-containing proteins, including ADAR1 and E3 homologs in other poxviruses [199]. Is there an adaptive advantage to this, or is it a compromise brought about by the need to inhibit PKR? Identifying the specific residues responsible for PKR inhibition would help to answer this question. Although it is clear that VACV $Z\alpha_{ADAR1}$-E3 fails to inhibit PKR phosphorylation, it is not yet known what specific differences between the E3 ZNA binding domain and the ADAR1 $Z\alpha$ domain allow one but not the other to inhibit PKR. Due to the sequence variation between the two, predicting the specific residue(s) responsible may prove difficult. To date, the best candidates for these residues are Leu36 and Leu50. Although L36R and L50P viruses did not have the phenotypes we predict, this could be explained by the fairly significant amino acid substitutions that these mutants contain. There could be alternative amino acid substitutions that would result in stable proteins lacking PKR inhibition.
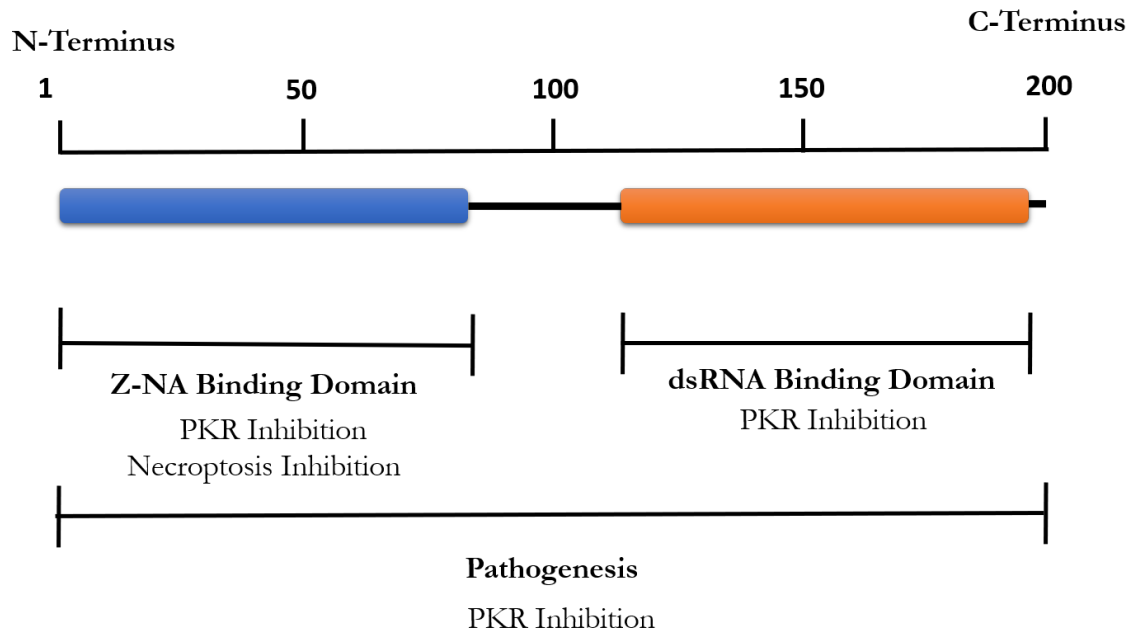
Figure 13: Schematic of the E3 protein, its domains, and their known functions. E3 consists of two major domains: a Z-form nucleic acid binding domain in the amino terminus and a dsRNA binding domain on the carboxyl terminus. These domains are joined by a linker region that is less well-conserved. Both ZNA and dsRNA binding domains have been shown to contribute to inhibition of PKR. Necroptosis inhibition is associated with the amino-terminal ZNA binding domain. Both domains must be present and linked for full pathogenesis in mice.

Protein	Domains	ZNA Binding	PKR Inhibition	Nec. Inhibition
E3	ZNA Binding / dsRNA Binding	+	+	+
E3Δ83N	dsRNA Binding	-	-	-
E3:L36R	ZNA Binding / dsRNA Binding	(+)	(-)	?
E3:L50P	ZNA Binding / dsRNA Binding	(+)	(-)	?
Zα$_{ADAR1}$E3	ADAR1 Zα / dsRNA Binding	+	-	?
E3:Y48A	ZNA Binding / dsRNA Binding	-	?	-

Figure 14: List of E3 mutants and their known and predicted phenotypes. Wild-type E3 has an amino-terminal ZNA binding domain and a carboxyl-terminal dsRNA binding domain. VACV that expresses this protein binds to ZNA, (indicated by "+"), inhibits PKR, and inhibits necroptosis. In E3Δ83N the amino-terminus, including the ZNA binding domain, has been deleted. This virus does not bind to ZNA (indicated by "-"), does not inhibit PKR 9-hours post infection, and does not inhibit necroptosis. E3:L36R and E3:L50P have point mutants in the ZNA binding domain. They are predicted to bind ZNA (indicated by "(+)") but are not predicted to inhibit PKR (indicated by "(-)"). Their ability to inhibit necroptosis is unknown, indicated by "?". ZαADAR1-E3 has the VACV ZNA binding domain replaced with the Zα ZNA binding domain from human ADAR1. It is able to bind to ZNA, and does not inhibit PKR 9 hours post infection; it's ability to inhibit necroptosis is unknown. Finally, E3:Y48A has a point mutation in the ZNA binding domain. This virus does not bind to ZNA and does not inhibit necroptosis; its ability to inhibit PKR is unknown.
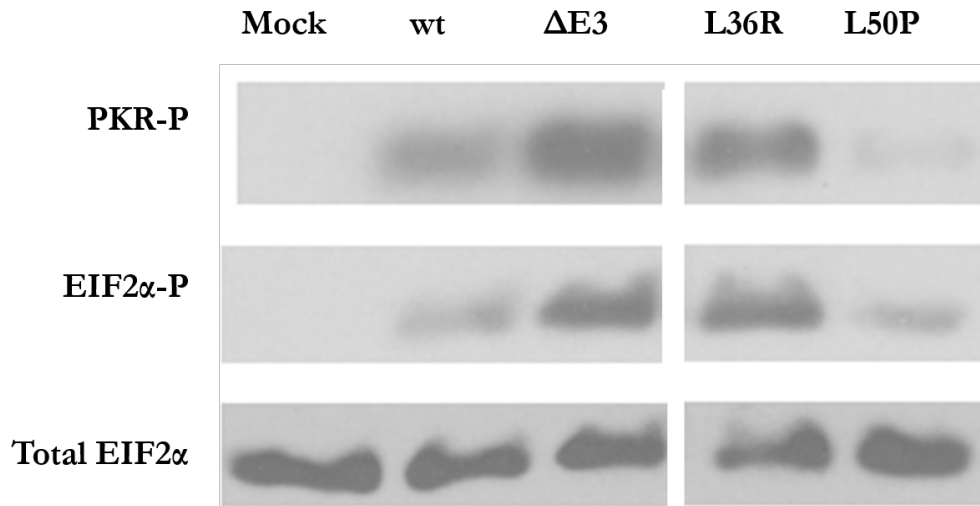
Figure 15: VACV E3:L36R but not E3:L50P infection leads to PKR phosphorlyation in HeLa cells. HeLa cells were infected with VACV, VACV E3Δ83N, E3:L36R or E3:L50P. At 9HPI total cell lysate was collected via RIPA extraction. The lysate was used in a Western blot probing for phosphorylated PKR, phosphorylated eIF2α, and total eIF2α.
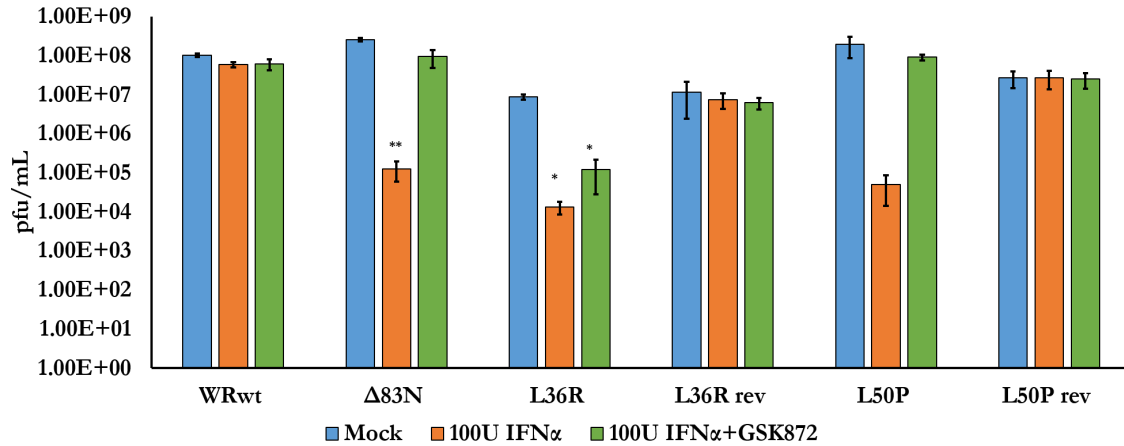
Figure 16: VACV E3:L36R and E3:L50P are interferon sensitive in L929 cells. L929 cells were either mock or treated with 100 U of IFNαfor 18 hours. Following IFN treatment, the cells were then mock treated or treated with 3 µM GSK872 for 1 hour. The cells were then infected with serial dilutions of VACV, VACV E3Δ83N, VACV E3:L36R, E3:L50P, or wild-type revertants of the point mutant viruses. After 4 days, the cells were stained with crystal violet and plaques were counted. The presented data are averages of thee independent experiments. Asterisks indicate a statistically-significant difference in plaque count from untreated cells. *p<.05 **p<0.005

(a)
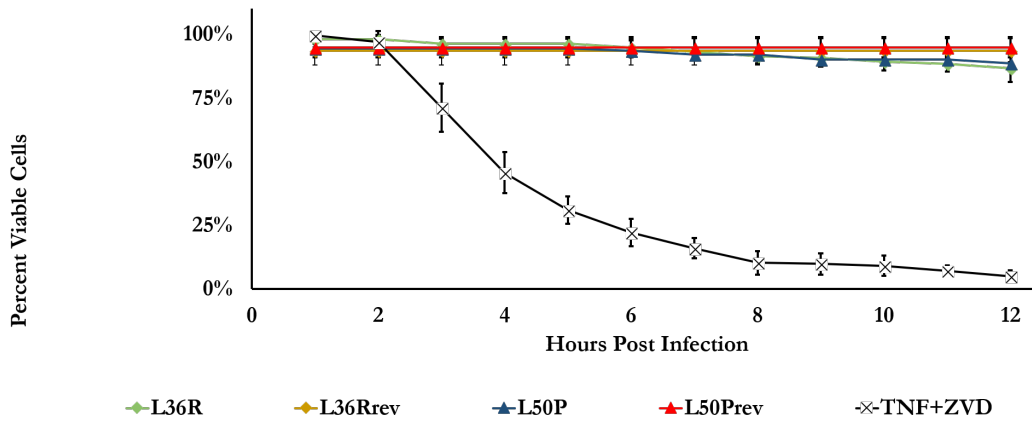
(b)
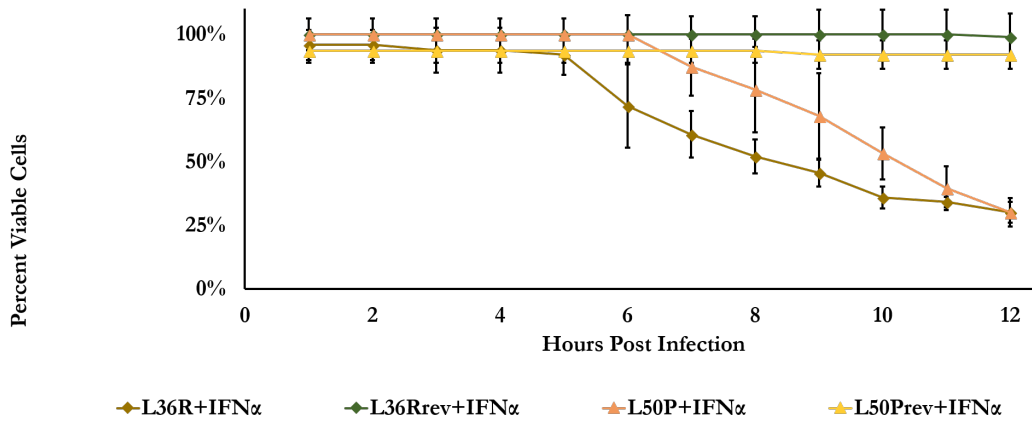
Figure 17: Interferon sensitizes L929 cells to rapid death when infected with VACV E3:L36R or E3:L50P. L929 cells were infected with VACV E3:L36R, E3:L50P, or wild-type revertants of these viruses. The cells were then treated with Sytox Green and loaded into an EVOS FL Auto heated incubator microscope. The microscope was programmed to take Z-Stack images in the Phase and GFP channels every hour for 12 hours. At teach time point the ratio of non-viable (green) cells to total cells was calculated. Presented data are averages of three independent experiments. (a) Untreated L929 cells (b) L929 cells pretreated 18 hours with 100 U of IFNα
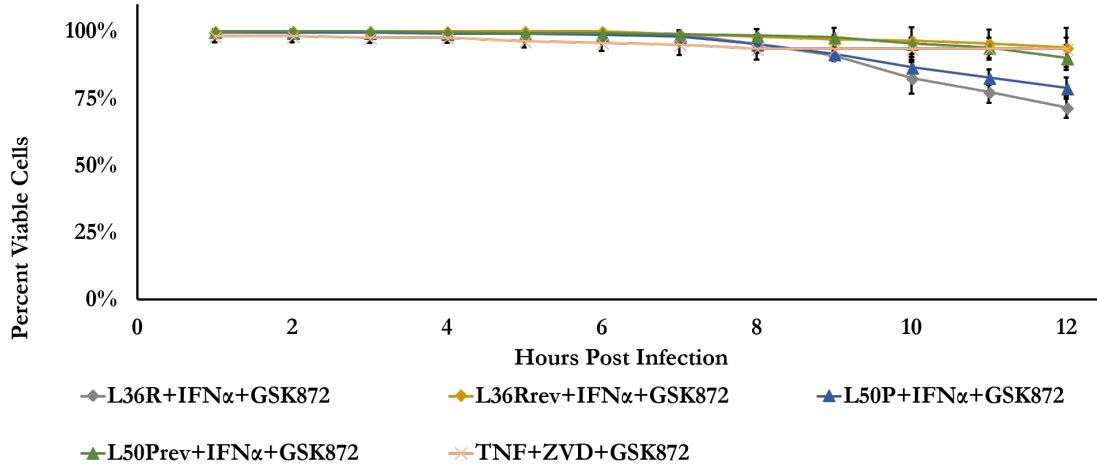
Figure 18: VACV E3:L36R and E3:L50P death in IFNα-treated L929 cells is inhibited by the RIP3 kinase inhibitor GSK872. L929 cells were treated 18 hours with 100 U of IFNα. Following IFN treatment, the cells were then treated for 1 hour with 3 μM GSK872. The cells were then infected with VACV E3:L36R, E3:L50P, or wild-type revertants of these viruses. The cells were then treated with Sytox Green and loaded into an EVOS FL Auto heated incubator microscope. The microscope was programmed to take Z-Stack images in the Phase and GFP channels every every hour for 12 hours. At teach time point the ratio of non-viable (green) cells to total cells was calculated. Presented data are averages of three independent experiments.

Figure 19: VACV E3:L36R and E3:L50P have delayed E3 accumulation in HeLa cells. HeLa cells were infected with VACV, VACV E3Δ54N, E3:L36R or E3:L50P. At 1, 3, 6, and 9 hours post infection total cell lysate was collected via RIPA extraction. The lysate was used in a Western blot probing for E3 and GAPDH.
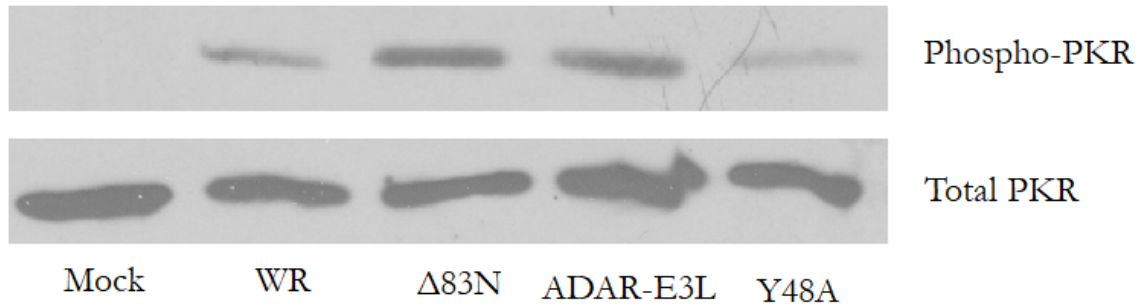
Figure 20: VACV Zα$_{ADAR1}$-E3 but not VACV E3:Y48A induces PKR phosphorlyation in HeLa cells. HeLa cells were infected with VACV, VACV E3Δ83N, VACV Zα$_{ADAR1}$-E3, or E3:Y48A. At 9HPI total cell lysate was collected via RIPA extraction. The lysate was used in a Western blot probing for phosphorylated PKR and total PKR.

(a)

(b)
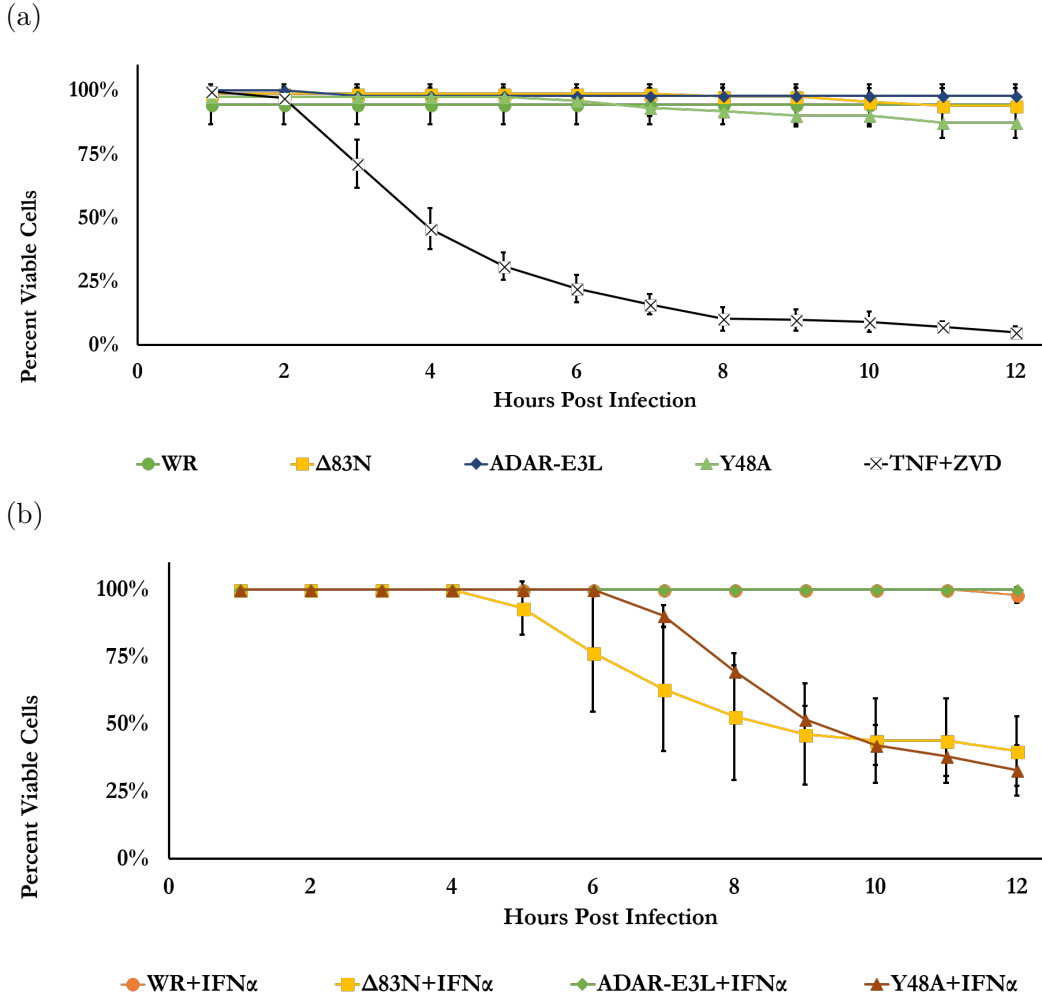
Figure 21: Interferon sensitizes L929 cells to rapid death when infected with VACV E3:Y48A but not $Z\alpha_{ADAR1}$-E3. L929 cells were infected with VACV, VACV E3Δ83N, VACV $Z\alpha_{ADAR1}$-E3, or E3:Y48A. The cells were then treated with Sytox Green and loaded into an EVOS FL Auto heated incubator microscope. The microscope was programmed to take Z-Stack images in the Phase and GFP channels every hour for 12 hours. At teach time point the ratio of non-viable (green) cells to total cells was calculated. Presented data are averages of three independent experiments. (a) Untreated L929 cells (b) L929 cells pretreated 18 hours with 100 U of IFNα

66
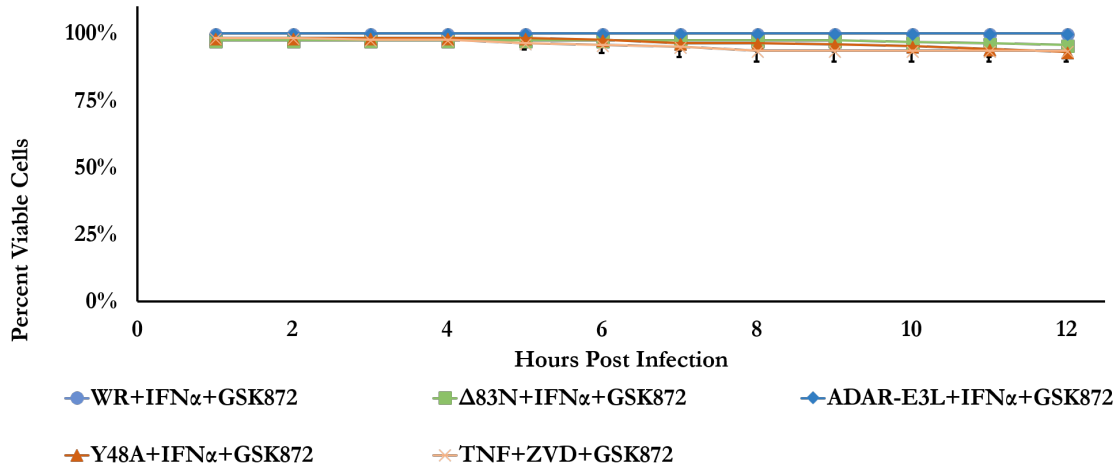
Figure 22: VACV E3:Y48A death in IFNα-treated L929 cells is inhibited by the RIP3 kinase inhibitor GSK872. L929 cells were treated 18 hours with 100 U of IFNα. Following IFN treatment, the cells were then treated for 1 hour with 3 µM GSK872. The cells were then infected with VACV, VACV E3Δ83N, VACV $Z\alpha_{ADAR1}$-E3, or E3:Y48A. The cells were then treated with Sytox Green and loaded into an EVOS FL Auto heated incubator microscope. The microscope was programmed to take Z-Stack images in the Phase and GFP channels every every hour for 12 hours. At teach time point the ratio of non-viable (green) cells to total cells was calculated. Presented data are averages of three independent experiments.

Figure 23: VACV Y48A but not $Z\alpha_{ADAR1}$-E3 induces MLKL phosphorlyation in L929 cells. L929 cells were infected with VACV, VACV E3Δ83N, VACV $Z\alpha_{ADAR1}$-E3, or E3:Y48A. At 3HPI total cell lysate was collected via RIPA extraction. The lysate was used in a Western blot probing for phosphorylated and total MLKL.
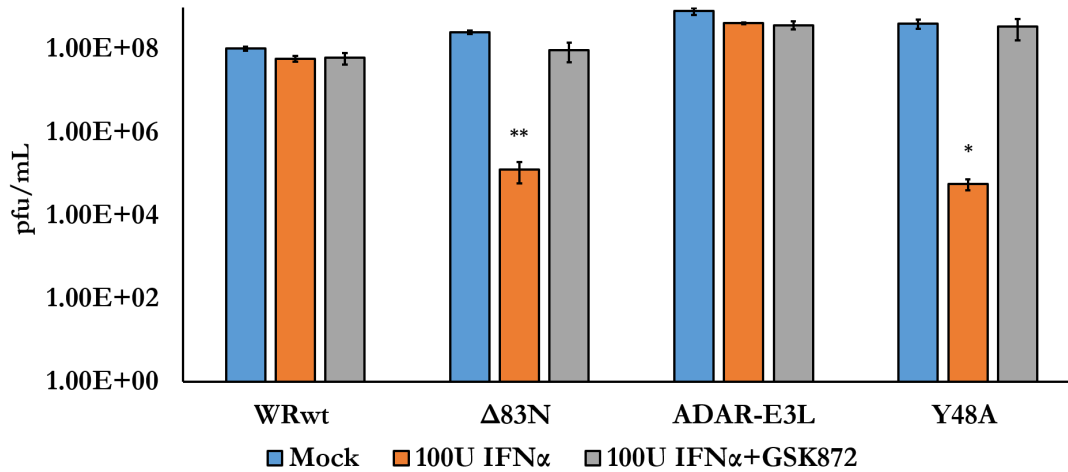
Figure 24: VACV E3:Y48A but not $Z\alpha_{ADAR1}$-E3 is interferon-sensitive in L929 cells. L929 cells were either mock or treated with 100 U of IFNαfor 18 hours. Following IFN treatment, the cells were then mock treated or treated with 3 µM GSK872 for 1 hour. The cells were then infected with serial dilutions of VACV, VACV E3Δ83N, VACV $Z\alpha_{ADAR1}$-E3, or E3:Y48A. After 4 days, the cells were stained with crystal violet and plaques were counted. The presented data are averages of thee independent experiments. Asterisks indicate a statistically-significant difference in plaque count from untreated cells. *p<.05 **p<0.005
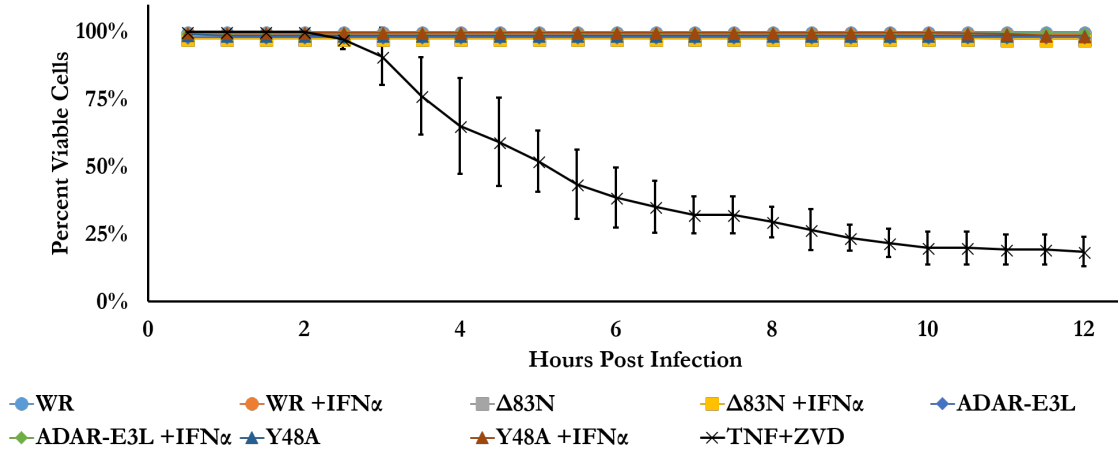
Figure 25: The interferon sensitivity of VACV E3:Y48A in L929 cells is DAI-dependent. DAI-knockout L929 cells were either mock treated or treated with 100 U of IFNα for 18 hours. The cells were then infected with VACV, VACV E3Δ83N, VACV Zα$_{ADAR1}$-E3, or E3:Y48A. The cells were then treated with Sytox Green and loaded into an EVOS FL Auto heated incubator microscope. The microscope was programmed to take Z-Stack images in the Phase and GFP channels every every hour for 12 hours. At teach time point the ratio of non-viable (green) cells to total cells was calculated. Presented data are averages of three independent experiments.
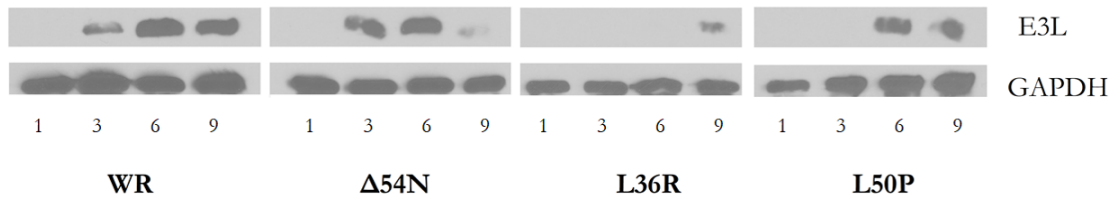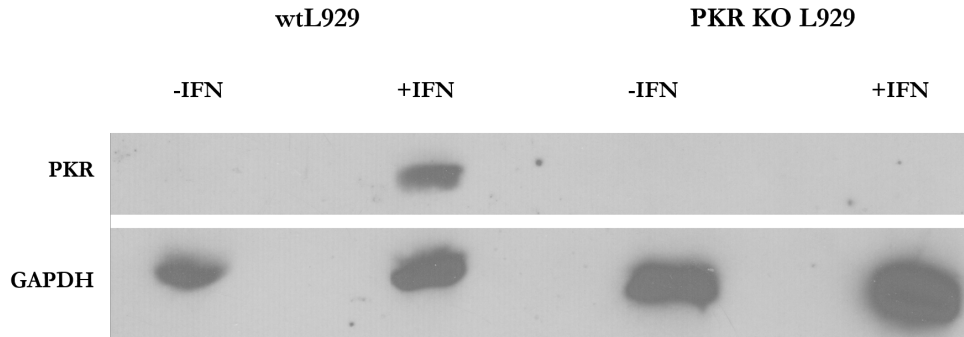
Figure 26: Verification of PKR knockout in L929 cells. Cas9-expressing L929 cells were infected with lentivirus containing a transformable cassette that encoded puromycin resistance and PKR guide RNA. Following puromycin selection, serial dilution was used to generate a clonal lineage derived from a single cell. These cells and wild-type L929 cells were then mock treated or treated for 18 hours with 100U IFNα. Total cell lysate was collected via RIPA extraction and used for a Western blot that probed for total GAPDH and total PKR.

(a)
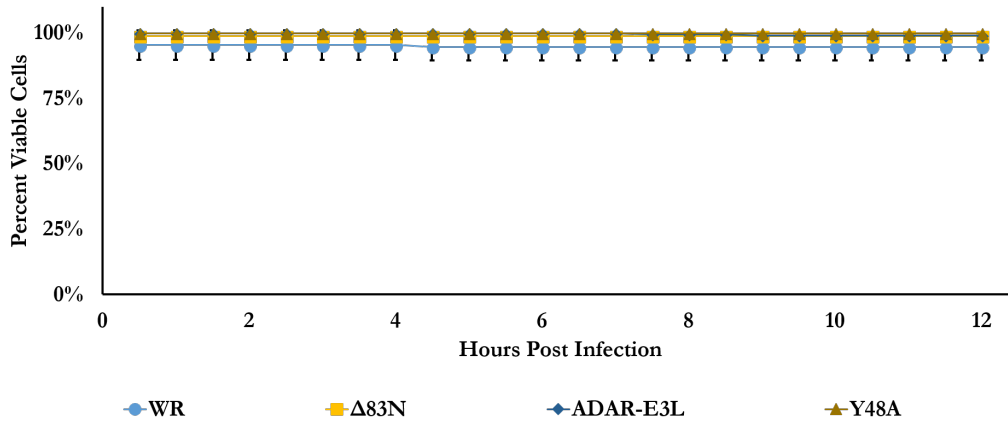
(b)
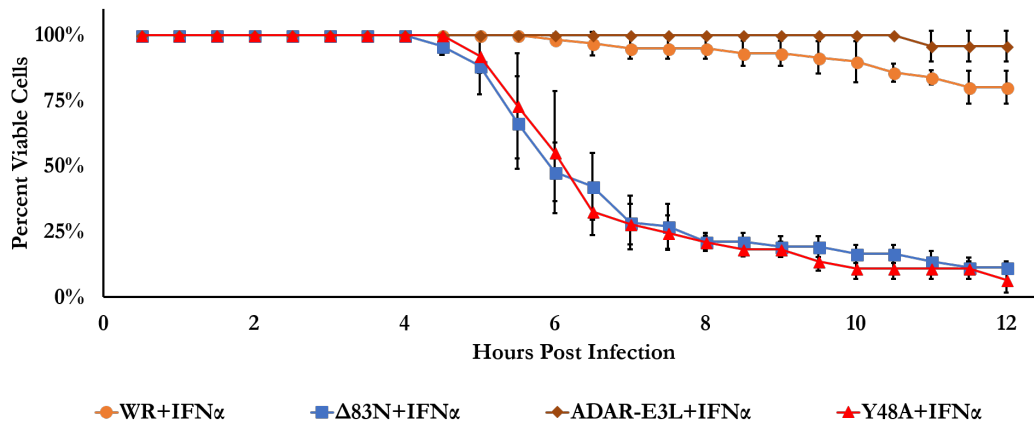
Figure 27: The interferon sensitivity of VACV E3Δ83N and E3:Y48A in L929 cells is not PKR-dependent. PKR-knockout L929 cells were infected with VACV, VACV E3Δ83N, VACV Zα$_{ADAR1}$-E3, or E3:Y48A. The cells were then treated with Sytox Green and loaded into an EVOS FL Auto heated incubator microscope. The microscope was programmed to take Z-Stack images in the Phase and GFP channels every hour for 12 hours. At teach time point the ratio of non-viable (green) cells to total cells was calculated. Presented data are averages of three independent experiments. (a) Untreated L929 cells (b) L929 cells pretreated 18 hours with 100 U of IFNα
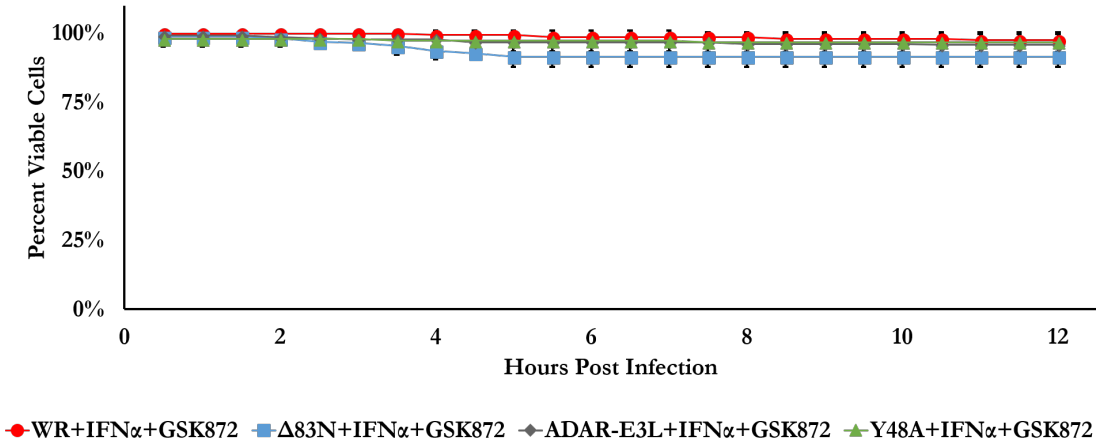
Figure 28: Loss of PKR does not affect GSK872 rescue of the interferon-sensitivity of VACV E3Δ83N and E3:Y48A. PKR-knockout L929 cells were treated 18 hours with 100 U of IFNα. Following IFN treatment, the cells were then treated for 1 hour with 3100 M GSK872. The cells were then infected with VACV, VACV E3Δ83N, VACV Zα$_{ADAR1}$-E3, or E3:Y48A. The cells were then treated with Sytox Green and loaded into an EVOS FL Auto heated incubator microscope. The microscope was programmed to take Z-Stack images in the Phase and GFP channels every every hour for 12 hours. At teach time point the ratio of non-viable (green) cells to total cells was calculated. Presented data are averages of three independent experiments.

Protein	Domains	ZNA Binding	PKR Inhibition	Nec. Inhibition
E3	ZNA Binding / dsRNA Binding	+	+	+
E3Δ83N	dsRNA Binding	-	-	-
E3:L36R	ZNA Binding / dsRNA Binding	(+)	-	-
E3:L50P	ZNA Binding / dsRNA Binding	(+)	+	-
Zα$_{ADAR1}$E3	ADAR1 Zα / dsRNA Binding	+	-	+
E3:Y48A	ZNA Binding / dsRNA Binding	-	+	-

Figure 29: Updated list of E3 mutant phenotypes using data from this study. Based on the results from these experiments, E3:L36R does not inhibit PKR as predicted, and does not inhibit necroptosis. E3:L50P does inhibit PKR, contrary to predictions, and does not inhibit necroptosis. ZαADAR1-E3 binds ZNA, does not inhibit PKR, and does inhibit necroptosis. Finally, E3:Y48A does not bind to ZNA, does inhibit PKR, and does not inhibit necroptosis.

Chapter 4

SODIUM ARSENITE INDUCES DAI/ZBP1-MEDIATED NECROPTOSIS INDEPENDENT OF VIRAL INFECTION

4.1   Abstract

Necroptosis is an anti-viral cell death pathway in which cells undergo a rapid and explosive death. One mechanism in which it can be induced is via the interferon-stimulated gene DAI/ZBP1. DAI has a Zα domain that confers the ability to interact with Z-form nucleic acids, and a RHIM domain allowing it to interact with and activate RIP3. This allows RIP3 to activate MLKL, the effector of necroptosis. This DAI-dependent pathway has been observed in herpes virus, influenza virus, and vaccinia virus infections. E3, the vaccinia virus interferon resistance protein, contains a Z-form nucleic acid binding domain. We have previously reported that loss-of-function mutations to this domain result in the virus inducing DAI/ZBP1-mediated necroptosis.

Since proteins that bind Z-form nucleic acid home to stress granules, we decided to ask if stress granule formation could lead to necroptosis. Stress granule formation was induced in L929 cells with the oxidative stressor sodium arsenite. While arsenite alone did not induce necroptosis, when DAI/ZBP1 was induced by IFN treatment MLKL phosphorylation and rapid cell death that was fully rescuable by a RIP3 inhibitor, was observed. We did not observe these hallmarks of necroptosis in L929 cells that did not express DAI/ZBP1, indicating that arsenite-mediated necroptosis is DAI/ZBP1

dependent. These data suggest that DAI/ZBP1 is not necessarily a sensor of viral ligands but perhaps is a sensor of stress signals brought about by viral infection.

4.2 Introduction

ZNA is an alternate form of double-stranded nucleic acid Z-form nucleic acids (ZNA) are DNA or dsRNA molecules that are in a left-handed helix as opposed to the more common right-handed helix. Although this form shares the same base-pair complementation as seen in right-handed helices, the overall shape of the resulting molecule tends to form a zig-zag pattern (hence Z-form) [113]. ZNA formation is associated with transcription and is thought to be caused when the nucleic acid is under torsional stress [200]. Several proteins have been identified with ZNA binding domains, including the mammalian proteins ADAR1 [125] and DAI/ZBP1/DLM1 [134], and the vaccinia virus protein E3 [110]. ZNA binding is necessary for complete functionality of these proteins.

ZNA-binding proteins home to stress granules Stress granules are complex mixtures of mRNA, translational machinery, and RNA binding proteins. They form when translation is inhibited, such as through lack of materials or cellular stress. Many stressors can induce stress granule formation, including the toxin sodium arsenite. Stress caused by exposure to arsenite is detected by heat shock proteins [154]; these proteins will then associate with and activate Heme-Regulated eIF2α kinase (HRI). Like Protein Kinase R (PKR), HRI phosphorylates eIF2α, leading to a cessation of the majority of translation [155, 156]. This leads to the aggregation of RNA-binding proteins such as G3BP1 and TIAR1 to stalled mRNA/ribosome complexes, forming stress granules [140].

It has been reported that proteins containing a function ZNA-binding domain, including the aforementioned E3 and DAI, will home to arsenite-induced stress granules

in HeLa cells [139]. Because of the role DAI plays in viral-associated necroptosis [22] and E3 plays in inhibiting necroptosis [87], this lead us to ask whether the colocalization of DAI with stress granules was necessary for the induction of necroptosis. If this is the case, we might expect that any cellular stressor that leads to stress granule formation in cells with an in-tact necroptosis pathway could induce DAI-dependent necroptosis.

4.3 Materials and Methods

Cells and treatments. HeLa cells were maintained in Dulbecco's Modified Eagle Medium (DMEM, Cellgro) supplemented with 5% FBS and 2 µM L-Glutamine.L929 cells were maintained in minimum essential medium (MEM, Cellgro) supplemented with 5% fetal bovine serum (FBS) (HyClone) and not allowed to exceed 7 passages.

Generation of ΔDAI and ΔPKR L929 cells. L929 ΔDAI/ZBP1 and ΔPKR were generated using CRISPR/Cas9 technology [195]. Cas9-expressing L929 cells were generated by Jackie Sicalo Williams using Edit-R Lentiviral Blast-Cas9 Nuclease Particles (Dharmacon) according to manufacturer instructions. In brief, a 24 well dish was seeded with L929 cells to 50% confluency. Individual wells were mock infected or infected with lentivirus containing a transformable cassette that contained genes for Cas9 and blasticidin resistance. After 24 hours, blasticidin was added to the media. After 48 hours, cell were trypsinized and serial diluted into 24 well palate in order to achieve single cell seeding. These were grown in the presence of Blasticidin. Blasticidin-resistant clonal lineages were stored in LN2 for future use.

Following the generation of Cas9-expressing cells, the cells were transformed to stably express guide RNA against the proteins of interest using Edit-R CRISPR Mouse Lentiviral sgRNA (Dharmacon). Cas9+ L929 cells were infected with lentivirus containing a transformable cassette that contained genes for puromycin resistance and express guide RNA specific for either PKR or DAI/ZBP1. Isolation of clonal lineages of puromycin-resistant cells was performed as described above. Successful gene knockdown was verified via Western blot. DAI knockouts were generated by Jackie Sicalo Williams.

79

Treatments and Inhibitors The pan-caspase inhibitor Z-VAD-FMK (ZVD, ApexBio) was prepared in DMSO and used at a final concentration of 100 µM. The RIP3 inhibitor GSK872 and RIP1 inhibitor GSK963 (GlaxoSmithKline) were prepared in DMSO and used at a final concentration of 3 µM. Sodium arsenite (Sigma) was used at a final concentration of 500 µM. Mouse TNFα (Sigma) was used at a final concentration of 10 ng/mL. SYTOX Green (ThermoFisher) was used at a final concentration of 1.25 µM.

Cell viability assay L929 cells were pretreated for 18 hours with 500 units of mouse IFNα. When applicable, they were then treated for one hour with ZVD, GSK872, and/or GSK963. Following treatment with inhibitors, without changing the media either sodium arsenite or TNFα were added. Finally, all cells were treated with SYTOX Green. The cells were then placed in the heated incubator stage of an EVOS FL Auto microscope (ThermoFisher), which was calibrated to take Z-Stack images in the Phase and GFP channels at selected time-points. At each time-point the ratio of green to non-green cells was used to determine the number of viable cells. Each experimental condition was performed in triplicate.

Protein extraction Cells were scrapped at the indicated times then spun at 1000 x g for 10 minutes at 4°C. The media was aspirated, then RIPA buffer containing Halt Protease and Phosphatase Inhibitor Cocktail (ThermoFisher) was added; the pellet was disrupted via pipetting. Following a 10 minute incubation on ice, the lysate was spun at 16000 x g for 20 minutes at 4°C. The supernatant was collected and combined with 2X SDS buffer containing DTT and Halt Protease and Phosphatase Inhibitor Cocktail. This solution was then heated for 10 minutes at 95 °C.

Western Blot Protein samples were separated via SDS PAGE using a 7% loading

gel and 10% stacking gel. Protein was transferred to nitrocellulose membrane that was then blocked at room temperature for 1 hour with Tris-buffered saline containing 0.1% Tween-20 (TBT-T) and 3% BSA. Following blocking, membranes were incubated with antibodies in TBS-T 3% BSA overnight at 4°C. They were then washed with TBS-T and probed with secondary antibody in TBS-T 3% dry milk (Carnation) for 1 hour at room temperature. After a final 1 hour wash in TBS-T at room temperature, the membranes were treated with Pierce ECL Western Blotting Substrate (ThermoFisher) and exposed to X-ray film.

4.4   Results

IFNα sensitizes L929 cells to sodium arsenite. Because DAI/ZBP1 is an interferon-stimulated gene, we began by determining if IFNα sensitizes sodium arsenite-treated L929 cells to cell death. L929 cells were mock treated or pretreated for 18 hours with 100 U of IFNα and then treated with increasing concentrations of sodium arsenite. At 6 hours post arsenite treatment, the percentage of nonviable cells was determined using SYTOX Green. Treatment with TNFα and the pan caspase inhibitor Z-VAD-FMK, which is known to induce RIP1-dependent necroptosis [79], was used a positive control. We found that while arsenite concentrations as high as 1000 µM failed to induce a significant amount of death in IFN-negative cells, concentrations as low as 250 µM of arsenite were sufficient to cause significant death (Figure 30a). Visually, we observed cell rounding and bursting without blebbing, which is morphologically consistent with a necroptotic death.

To further characterize the interferon sensitization, we pretreated L929 cells with 10 fold serial dilutions of IFNα for 18 hours and then treated them with 500 µM of arsenite. Cell viability was determined 6 hours post treatment with SYTOX Green. The lowest concentration to have significant death was 100 U of IFN (Figure 30b). Based on these results, in subsequent experiments we used 500 µM of sodium arsenite and 500U of IFNα.

Arsenite induces necroptosis in IFNα-treated L929 cells To determine if arsenite-mediated death was necroptosis, we administered necroptosis inhibitors to arsenite and IFN-treated cells and measured the percentage of viable cells over 12 hours using SYTOX Green. We found that the RIP3 kinase inhibitor GSK872 reduced

and delayed death for both arsenite+IFNα and TNFα+ZVD treated cells, suggesting that the death is in fact necroptosis. However, the RIP1 kinase inhibitor GSK963 rescued TNFα+ZVD but not arsenite+IFNα, suggesting that arsenite-mediated death is not RIP1 kinase dependent (Figure 31); this is consistent with our hypothesis that DAI/ZBP1 can act independently of viral ligands through stress granules as DAI-mediated necroptosis does not require RIP1 kinase activity.

For final confirmation that arsenite+IFNα induces necroptosis, we performed a western blot against total and phosphorylated MLKL on L929 lysate harvested 3 hours post treatment. As seen in Figure 32, phosphorylated MLKL was observed in cells treated with arsenite+IFNα and TNFα+ZVD. This phosphorylation was not observed in cells that were also treated with GSK872.

Arsenite-mediated necroptosis is DAI/ZBP1 dependent We next wanted to verify that arsenite-mediated necroptosis is DAI-dependent. To accomplish this, we used CRISPR/Cas9 to generate DAI/ZBP1-knockout L929 cells. We then assayed cell viability using the SYTOX Green assay. As seen in Figure 33a, TNFα+ZVD induced death, indicating that the cells were still capable of necroptosis despite the loss of DAI. However, neither arsenite alone nor arsenite+IFNα induced significant death by 12 hours post treatment. This indicated that arsenite-mediated necroptosis is DAI dependent. This was further supported by a western blot against MLKL in the DAI knockout cells, which showed phosphorylation of MLKL for TNFα+ZVD but much less in arsenite+IFNα-treated cells (Figure 33b).

Sodium arsenite-induced necroptosis does not require PKR. Although arsenite is known to induce eIF2 α phosphorylation via activation if HRI, it has also been observed that sodium arsenite treatment can induce activation of PKR through

PACT (PKR activating protein), which can heterodimerize with and activate PKR in the absence of dsRNA [201, 202]. PKR is also known to be recruited to stress granules via G3BP1 [203]. Because PKR has been shown to induce RIP1-dependent necroptosis [83], we asked whether it is necessary for arsenite-induced necroptosis.

Cell viability was determined using the SYTOX time lapse assay. We found that as was the case with wild-type L929 cells, IFNα-treated cells were sensitized to arsenite-mediated death, and this death was ameliorated by GSK872 (Figure 34a. Furthermore, arsenite + IFNα treatment led to the phosphorlyation of MLKL (Figure 34b). Together, these data indicate that arsenite is able to induce necroptosis in the absence of PKR.

4.5 Discussion

The purpose of this project was to determine if sodium arsenite can induce DAI/ZBP1-dependent necroptosis. Our results demonstrate that this is the case. We propose that the mechanism for this death is that the formation of stress granules allow DAI to aggregate and recruit RIP3, thereby initiating the signal cascade leading to necroptotic death; Figure 35 visualizes this model.

A key aspect of our findings is that it is possible to induce DAI-mediated death wholly independent of any viral ligands. This suggests that DAI/ZBP1 is not necessarily a sensor of viral ligands but perhaps is a sensor of stress signals brought about by viral infection. One important implication of this is that DAI-dependent necroptosis may play a far bigger part in the antiviral response than has previously been shown. One possible reason for the relative paucity of viruses shown to interact in some manner with the necroptotic pathway is that the pathway is not intact in many cell lines, especially those derived from cancers. For example, RIP3, a key signaling molecule for all known necroptosis pathways, has down-regulated expression in many cell lines including HeLa [204]. Therefore, it simply is not possible to detect necroptosis unless the correct cells are used. For example, although it has been known for some time that the ZNA-binding domain of E3 is necessary for full pathogenesis in mice [110], it was not until we used cells with intact necroptosis pathways that we were able to find that it inhibits necroptosis [87].

It has been reported that the flaviruses West Nile Virus, Dengue Virus, and Japanese Encephalitis Virus are able to inhibit arsenite-mediated stress granule formation. Interestingly, it was found that treating BHK cells in such a manner as to

prevent the inhibition of SG formation did not affect WNV replication in these cells [205]. Based on our results, we might expect that repeating this experiment in cells that are capable of DAI-dependent necroptosis would in fact lead to cell death and inhibition of viral replication. Further evidence for this prediction is the observation that MLKL necroptosis enhances the neuroinflammation associated with Japanese encephalitis virus, though it was not determined if this was DAI-dependent [206].

This work has implications for non-viral pathologies as well. Stress granule formation and necroptosis have separately been found to be linked to neurodegenerative disease [12, 207]. These findings suggest that a link exists between the two that is mediated by DAI/ZBP1. DAI-/- are viable, and could be useful tools by which to probe this relationship [208].

For future work, it would be valuable to generate a recombinant DAI/ZBP1 that replaces the Zα and/or RHIM domains with sites for chemically-induced dimerization, as has been done for PKR [209, 210]. This would allow for more precise analysis of the role of DAI without the use of treatments such as poly:IC and arsenite, which have diverse effects beyond those associated with DAI. In addition, while arsenite-mediated death is clearly DAI dependent, the specific pathway allowing this is only predicted and has not been verified experimentally. Colocalization assays and siRNA screens are necessary to gain a full understanding of this phenomenon.

(a)

(b)
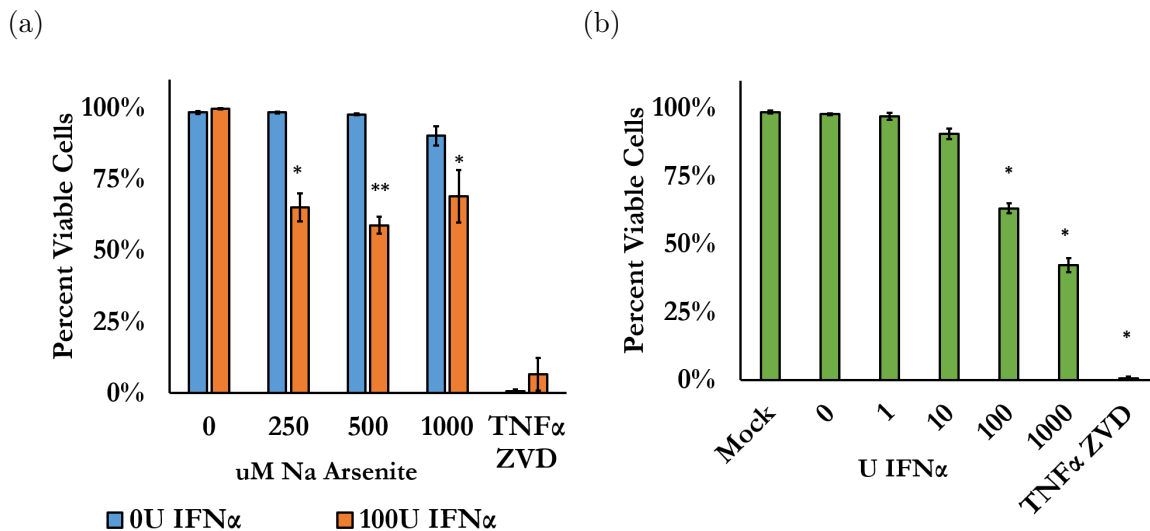
Figure 30: Interferon sensitizes L929 cells to sodium arsenite. L929 cells were mock or pretreated for 18 hours with mouse IFNα and then treated with sodium arsenite. The ratio of viable to total cells was determined at 6 hours post-treatment using SYTOX Green. TNFα+ZVD was used as a positive control. Graphed data are averages of 3 independent experiments. Significant was determined with unpaired two-tailed T-Test *p<.05 **p<0.005. (a) L929 cells were treated 500 µM of mouse IFNα and then varying concentrations of sodium arsenite. (b) L929 cells were pretreated with varying concentrations of mouse IFNα and then treated with 500 µM of sodium arsenite.
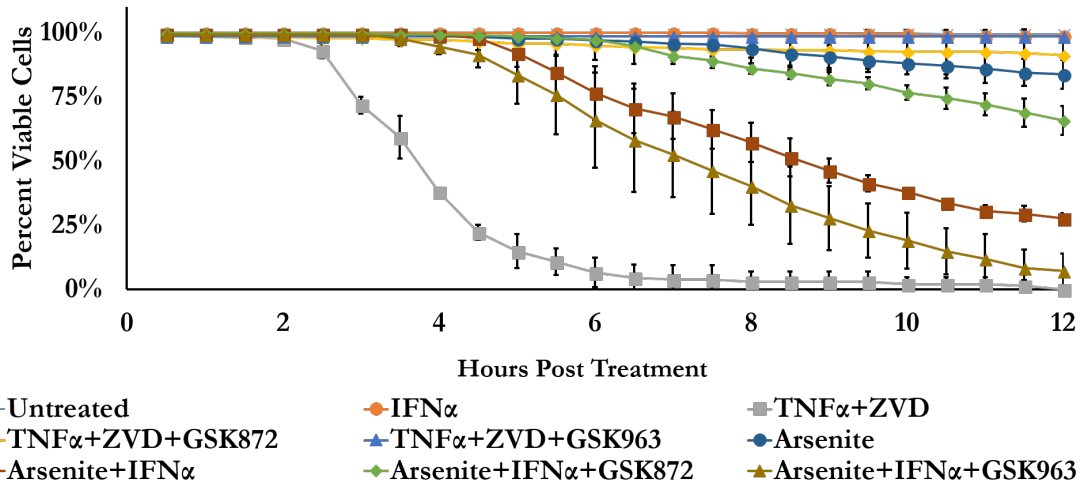
Figure 31: RIP3 but not RIP1 kinase activity is necessary for arsenite-mediated death. L929 cells were treated as indicated with arsenite and the RIP1 inhibitor GSK963 and the RIP3 inhibitor GSK872. TNFα+ZVD treatment was used as a positive control. Viability was measured over 12 hours using SYTOX Green. Graphed data is mean of three independent trials.
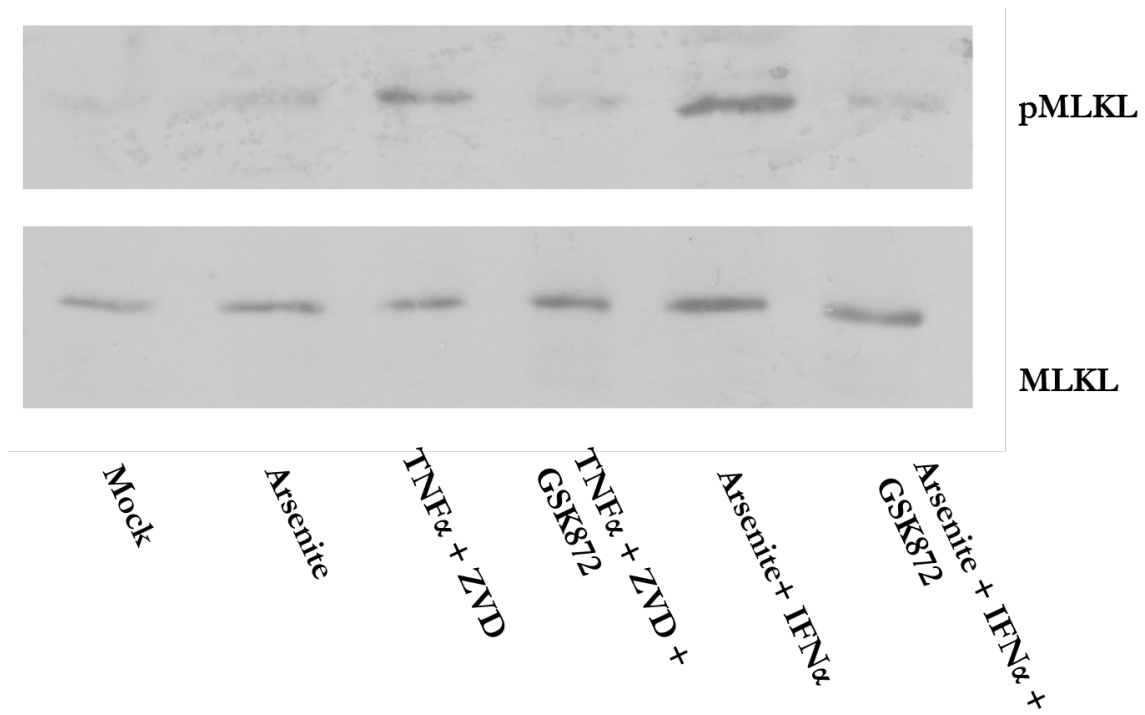
Figure 32: Sodium arsenite induces phosphorylation of MLKL in IFNα-treated L929 cells. L929 cells were treated as indicated. At 3 hours post-treatment, total cell lysate was collected via RIPA extraction. Lysate was then analyzed via Western Blot, probing for phosphorylated MLKL.
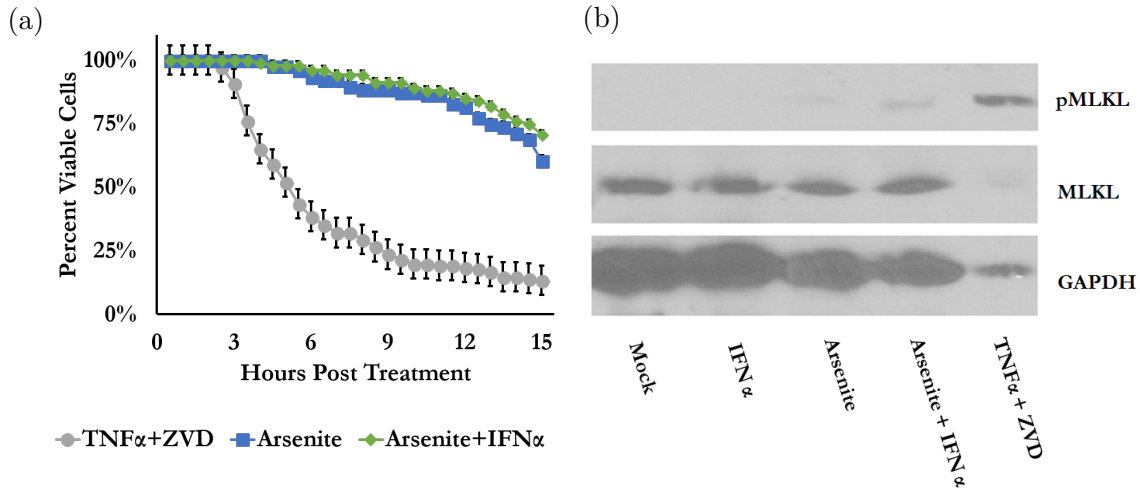
Figure 33: DAI/ZBP1 is necessary for arsenite-mediated necroptosis. ΔDAI L929 cells were mock treated or pre-treated with 100U of IFNα. 18 hours post-treatment, cells were either mock treated or treated with 100 µM ZVD or 3 µM GSK872. Following 1 hour, cells were were either mock treated or treated with 500 µsodium arsenite or 10 ng/mL TNFα. (a) Viability was measured over 12 hours using SYTOX Green. Graphed data is mean of three independent trials. (b)ΔDAI L929 cell total lysate was harvested 3 hours after the indicated treatments and probed via Western Blot for the indicated proteins.
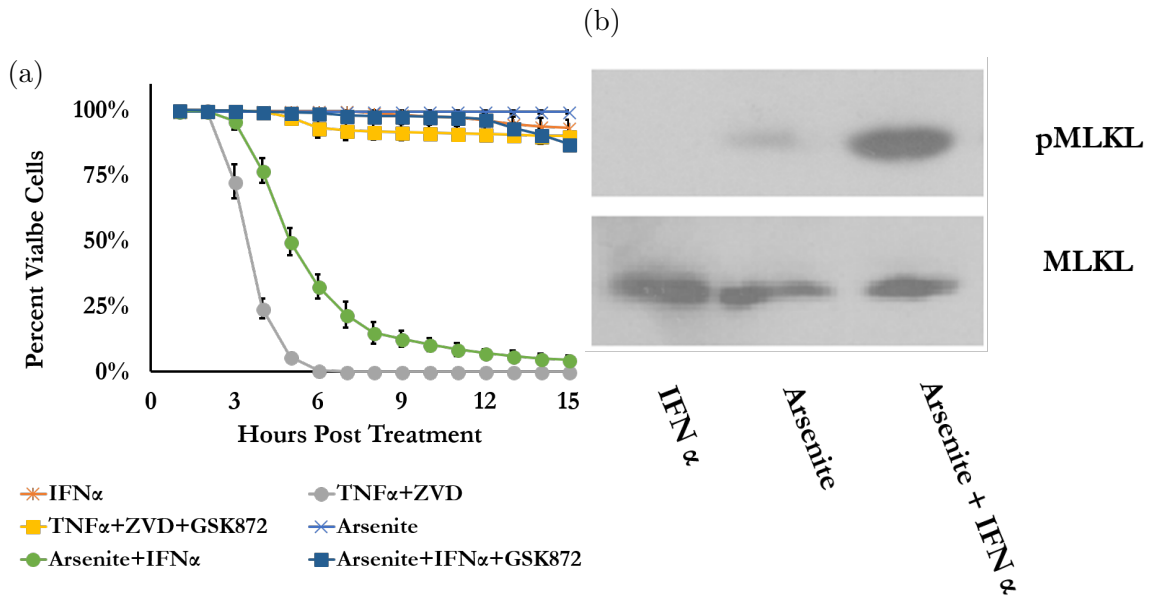
Figure 34: PKR is not necessary for arsenite-mediated necroptosis. ΔPKR L929 cells were mock treated or pre-treated with 100U of IFNα. 18 hours post-treatment, cells were either mock treated or treated with 100 µM ZVD or 3 µM GSK872. Following 1 hour, cells were were either mock treated or treated with 500 µsodium arsenite or 10 ng/mL TNFα. (a) Viability was measured over 12 hours using SYTOX Green. Graphed data is mean of three independent trials. Significance was determined using an unpaired two-tailed T-Test.(b)ΔPKR L929 cell total lysate was harvested 3 hours after the indicated treatments and probed via Western Blot for the indicated proteins.
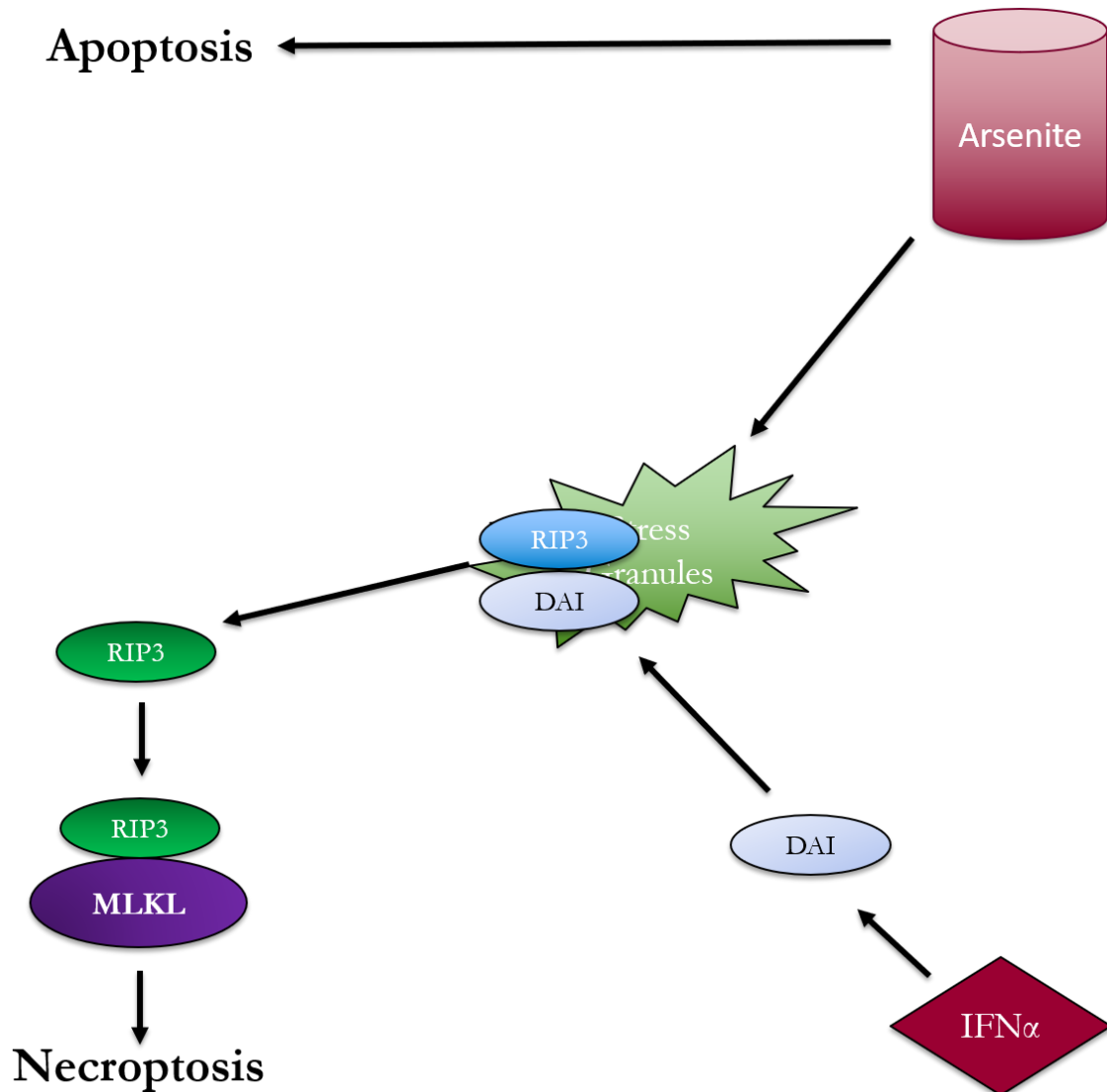
Figure 35: Proposed model for how sodium arsenite might induce DAI/ZBP1-dependent necroptosis. Treatment with arsenite triggers the formation of stress granules. Interferon-stimulation leads to the production of DAI/ZBP1, which homes to the stress granule, where it is able to recruit RIP3 due to their shared RHIM domains. RIP3 goes on to activate MLKL, leading to necroptosis.

Chapter 5

DISCUSSION

The overarching goal of the projects described in this document was to understand how PKR and necroptosis contribute to the attenuation of amino-terminal mutants of the vaccinia virus E3 protein. In Chapter 2, we report the finding that monkeypox virus produces less double-stranded RNA, and propose it as a means by which the virus can compensate for a partial deletion in its E3 homolog. In Chapter 3, we found that inhibition of PKR and of necroptosis are distinct activities of the vaccinia interferon-resistance gene E3, and that one is not necessary for the other. Finally, in Chapter 4, we found that DAI/ZBP1-dependent necroptosis is not necessarily dependent on the presence of viral ligands but instead might be activated via a more general stress response. Our proposed mechanism for this is that the stress response leads to the aggregation of DAI, which in turn allows RIP3 to become phosphorylated and propagate the necroptotic signal.

Based on these findings, we propose the following model for VACV inhibition of PKR activation and necroptosis, visualized in Figure 36. Vaccinia virus infection leads to the production of dsRNA. E3 inhibits the activation of PKR both by binding competitively to dsRNA and interacting with PKR directly. Separately, the stress brought about by virus infection can lead to the formation of stress granules. If DAI/ZBP1 is able to home to these granules, necroptosis will be induced. E3 is able to interfere with this, possibly via competitive binding to the stress granule ligand that recruits DAI. In this manner, E3 is able to block both PKR and necroptosis.

Why does vaccinia virus produce dsRNA? One fundamental question that remains unresolved is why VACV produces dsRNA in the first place. It is known that Early genes have precise transcription termination; it is only Intermediate and Late genes that lack the termination signal. Why is this the case? Imprecise transcription termination would seem to be a deleterious trait both from the metabolic cost of "inefficient" mRNA production as well as the production of dsRNA whose detection must be blocked in some manner. This is especially confounding when one considers that it is relatively easy for VACV to acquire low-dsRNA phenotypes. Multiple mutations in several genes have been found to confer IBT-resistance and by extension reduced RNA polymerase processivity and dsRNA accumulation [181]. Furthermore, the low-dsRNA phenotypes of pathogenic members of orthopoxvirus such as MPXV and ectromelia virus suggest that high dsRNA is not critical for virus success [211, 191].

One explanation for this phenomenon is that dsRNA is not desirable but is instead simply a byproduct of enhanced transcription. Unlike their eukaryotic homologs, some of the VACV elongation subunits are unable to dissociate from polymerase. It has been proposed that this increases the rate of transcription, leading to a faster accumulation of mRNA which allows for more rapid viral replication [212]. In this scenario, early transcription termination is precise because dsRNA is undesirable at the beginning of an infection as host sensors would detect and inhibt the infection. However, once immune modulators such as E3 are expressed, the virus is able to suppress the detection and response to dsRNA and so no longer has to compromise transcription speed for immune evasion. Precise studies on biochemical dynamics of IBT-resistant viruses are one means in which this could be explored. However, even if it is the case that dsRNA accumulation correlates with faster viral replication, this does not fully explain why

Intermediate and Late genes lack the transcription termination signals found in early genes.

An alternate explanation is that dsRNA is serving as a modulator of the innate immune response. It has previously been shown that PKR can activate the transcription factor NF-ϰB [67], and that VACV can activate NF-ϰB through PKR [68]. Furthermore, it has been demonstrated that PKR-mediated activation of NF-ϰB can enhance cell survival via induction of pro-survival signals such as c-IAPs [52, 213]. One interesting possibility is that the dsRNA produced by VACV exists in order to achieve low levels of PKR activation which in turn might lead to some pro-survival signals via NF-ϰB. However, it has also been shown that VACV produces several inhibitors of NF-ϰB, such as C4, K1, and N1 [101, 103, 102], so the full story is likely far more complicated. The ΔPKR L929 cell line would be a useful tool to test this hypothesis.

Can necroptosis be leveraged to make more effective oncolytic viruses? Oncolytic virus therapy entails the use of viruses in the clearance of cancer cells. T-VEC, a recombinant HSV-1 virus, was the first such therapy to be approved by the FDA in 2015 for use in melanoma patients [214]. A great many more are in clinical trials. In general, the underlying principle of onoclytic therapy is that the immune disregulation of tumor cells makes them more vulnerable to viral infection . As such, an attenuated virus that is inhibited in normal cells might be fully infective in a tumor line [215]. We have observed this with mutants of E3; E3Δ54N is apathogenic in SCID mice yet leads to the total loss of xenografted human cancer cells [216]. Another potential use of oncolytic viruses is to break tumor tolerance and recruit an immune response against it. Figure 37 illustrates these methods.

Necroptosis, or the lack thereof, may be a factor that contributes to tumor specificity. It has been found that many cancer cells transcriptionally repress the expression of RIP3, thereby preventing all known pathways leading to necroptosis [204]. Therefore, while a virus such as E3:Y48A would lead to rapid death and inhibition of virus spread in normal cells, it would not be blocked by necroptosis in the tumor cell and thus would be able to replicate and spread to adjacent tumor cells, potentially affecting the entire tumor bed.

Apoptosis and necroptosis can both lead to the release of tumor antigens. Although necroptosis is generally more inflammatory than apoptosis due to the release of intracellular cytokines such as HMGB1 [217], there have been conflicting reports as to the relative abilities of these programmed death pathways to induce tumor immunity. Some reports find that apoptosis but not necroptosis produces a potent antitumor response and stimulates dendridic cells [218, 219]. Others have found the opposite [220, 221]. This might be explained by the reported need for RIP1 and NF-κB activity in dying cells [222]. If true, a VACV with reduced ability to inhibit necroptosis and NF-κB might be a potent recruiter of anti tumor immunity. A further implication of this observation is that pyroptosis, which is not thought to involve NF-κB or RIP1 activity, may not be a suitable endpoint [223, 224]. Another possible explanation is that necroptosis has also been reported to be anti-inflammatory by the killing of inflammatory cytokine-releasing cells [225]. Whether the effects of necroptosis are net inflammatory or anti-inflammatory could be quite important for the ultimate fate of the tumor as the relative inflammatory environment of a tumor has huge impacts on clearance and spread. This highlights what I believe to be a critical problem facing any tumor intervention: the immense complexity of the death pathways.

PKR serves as an excellent example of this challenge. As has been reviewed in this document, besides inhibiting translation via the phosphorylation of eIF2α, PKR has been found to activate NF-ϰB and caspase 8 as well as RIP1-mediated necroptosis. In this regard it may be useful to consider the protein as as a more general signal amplifier rather than an activator of any specific pathway. Suppose VACV Zα$_{ADAR1}$-E3, which activates PKR but not necroptosis, were used as a virotherapy. The ultimate effects of such an infection would be dependent on the specific cellular environment. For example, it may skew towards apoptosis in cells with high expression of caspase 8, but be inflammatory when caspase 8 and RIP3 levels are low. Therefore, I would predict this virus to be anti-tumor in some situations and ineffective in others.

How might this uncertainty be navigated? While efforts to elucidate the different cellular pathways and their interactions, such as what has been described in this dissertation, are important steps, I do not believe that they alone will lead to a "silver bullet" drug. I propose that the next step needed is to determine the state of the transcriptome following various interventions, and what network effects correlate with the final state of the cell. With this information, it might be possible to predict the effects of a given intervention on a given cell based on its transcriptome [226, 227]. For pathologies where specific cell outcomes are known to be desirable a suite of personalized treatments could then be used that target the specific pathway. For example, if necroptosis is desirable but sequencing reveals that the tumors are RIP3 negative, RIP3-expressing virus could be introduced. This could also potentially surmount the challenge brought by tumor heterogeneity; while a particular cell might be resistant to effects of one virus, a cocktail of viruses each targeting distinct components of the desired death pathway would be more challenging to evade. Figure 38) illustrates this workflow.
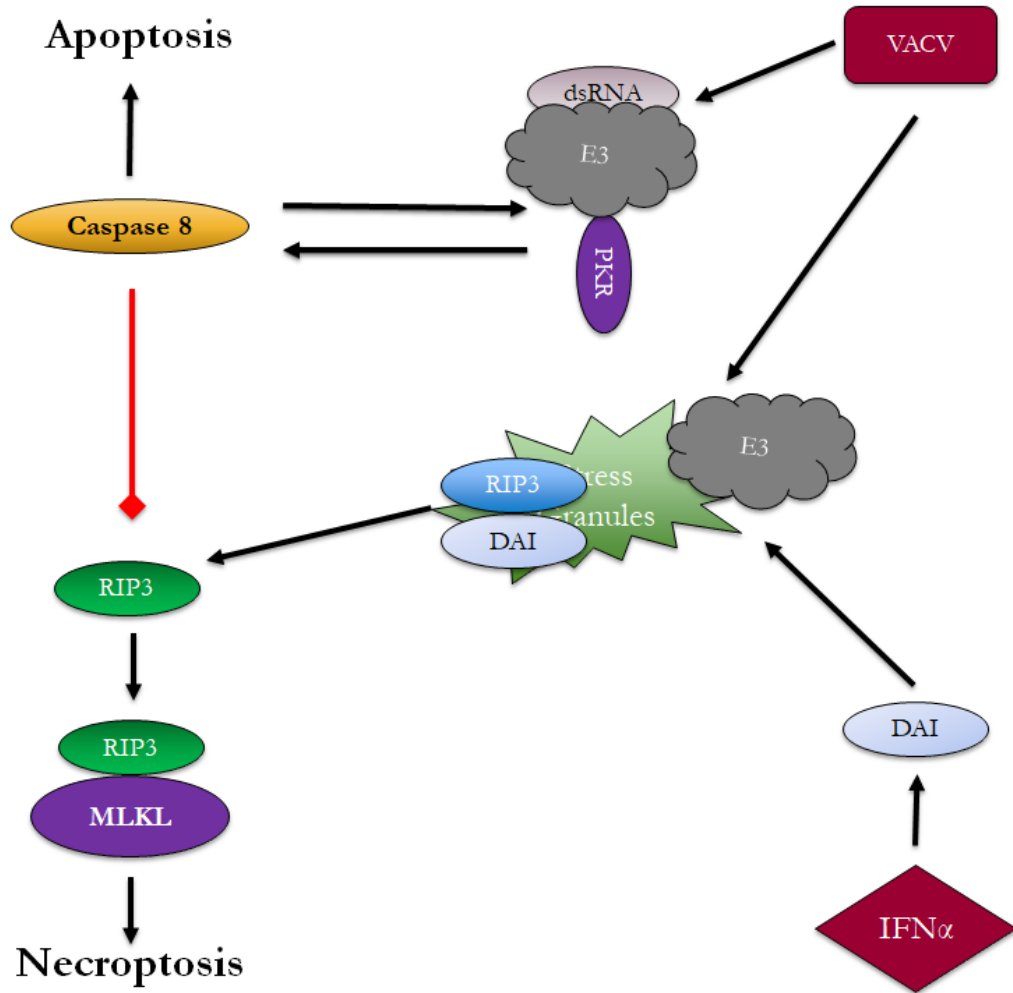
Figure 36: Proposed model for how VACV E3 separately inhibits PKR activation and necroptosis. VACV infection leads to the synthesis of dsRNA, which can be detected by PKR, leading to the activation of antiviral pathways such as apoptosis. E3 binds to dsRNA and interacts with PKR directly in order to prevent PKR activation. Separately, the stress caused by a viral infection can lead to the formation of stress granules, which recruit DAI/ZBP1 to activate RIP3 and lead to necroptosis. E3 inhibits this pathway, possibly by competing with the ligand target of DAI and preventing it from co-localizing to stress granules.
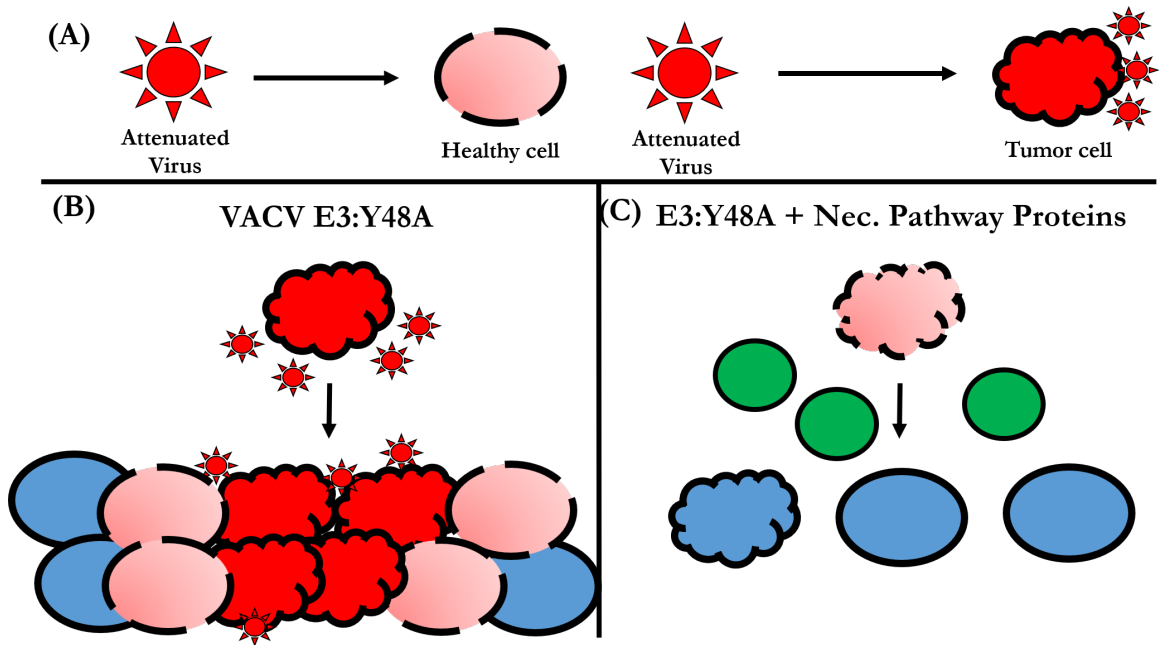
Figure 37: How necroptosis could be leveraged for oncolytic virotherapy. (A) Because many tumor cells have inhibited necroptosis, an attenuated virus that triggers necroptosis in a healthy cell might be fully replication competent in a given tumor cell. (B) Such a virus would be able to spread throughout the tumor bed, while being restricted by normal cells with intact death pathways. (C) Alternatively, a virus could be engineered to restore necroptosis in a tumor cell that lacks it. As necroptosis is inflammatory, triggering this death could potentially break tolerance and recruit an immune response against the tumor.
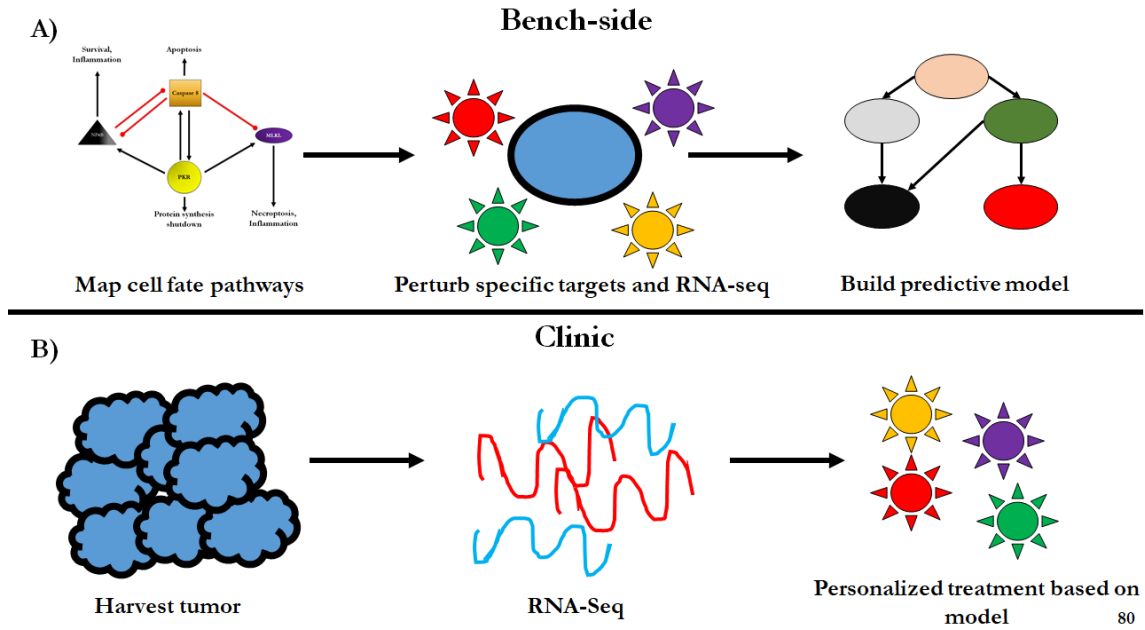
Figure 38: Possible workflow for personalized virotherapy. (A) In the laboratory setting, in vitro assays are used to identify the protein networks that contribute to cell fate. These networks would then be perturbed by targeting specific components, and the effects on the overall network, including the transcriptome, would be determined. This data would be used to build models to predict the effects of these specific stimuli on the network and the ultimate effect on cell fate. (B) In the clinic, tumor cells would be harvested and the status of their cell fate network determined by RNA-Seq. Using this information, personalized therapy would be delivered that is compatible with the specific status of the signaling pathways and the desired cell fate.

REFERENCES

1. Lamkanfi M, Dixit VM. 2010. Manipulation of Host Cell Death Pathways during Microbial Infections. *Cell Host & Microbe* 8:44–54. https://doi.org/10.1016/j.chom.2010.06.007.

2. Chou W, Ngo T, Gershon PD. 2012. An overview of the vaccinia virus infectome: a survey of the proteins of the poxvirus-infected cell. *Journal of virology* 86:1487–99. https://doi.org/10.1128/JVI.06084-11.

3. Broyles SS. 2003. Vaccinia virus transcription. *The Journal of general virology* 84:2293–303. https://doi.org/10.1099/vir.0.18942-0.

4. Yuen L, Moss B. 1987. Oligonucleotide sequence signaling transcriptional termination of vaccinia virus early genes. *Proceedings of the National Academy of Sciences of the United States of America* 84:6417–21. https://doi.org/10.1073/pnas.84.18.6417.

5. Duesberg PH, Colby C. 1969. On the biosynthesis and structure of doublestranded RNA in vaccinia virus-infected cells. *Proceedings of the National Academy of Sciences* 64:396–403. https://doi.org/10.1073/pnas.64.1.396.

6. Xiang Y, Simpson Da, Spiegel J, Zhou a, Silverman RH, Condit RC. 1998. The vaccinia virus A18R DNA helicase is a postreplicative negative transcription elongation factor. *Journal of virology* 72:7012–23.

7. Perdiguero B, Esteban M. 2009. The interferon system and vaccinia virus evasion mechanisms. *Journal of interferon & cytokine research : the official journal of the International Society for Interferon and Cytokine Research* 29:581–98. https://doi.org/10.1089/jir.2009.0073.

8. Henle W. 1950. Interference phenomena between animal viruses; a review. *Journal of immunology (Baltimore, Md. : 1950)* 64:203–36.

9. Isaacs A, Lindenmann J. 1957. Virus Interference. I. The Interferon. *Proceedings of the Royal Society B: Biological Sciences* 147:258–267. https://doi.org/10.1098/rspb.1957.0048.

10. Yan N, Chen ZJ. 2012. Intrinsic antiviral immunity. *Nature immunology* 13:214–22. https://doi.org/10.1038/ni.2229.

11. McNab F, Mayer-Barber K, Sher A, Wack A, O'Garra A. 2015. Type I interferons in infectious disease. *Nature Reviews Immunology* 15:87–103. https://doi.org/10.1038/nri3787.

12. Zhang B, Li M, Chen L, Yang K, Shan Y, Zhu L, Sun S, Li L, Wang C. 2009. The TAK1-JNK cascade is required for IRF3 function in the innate immune response. *Cell research* 19:412–28. https://doi.org/10.1038/cr.2009.8.

13. Honda K, Takaoka A, Taniguchi T. 2006. Type I interferon gene induction by the interferon regulatory factor family of transcription factors. *Immunity* 25:349–60. https://doi.org/10.1016/j.immuni.2006.08.009.

14. Alexopoulou L, Holt AC, Medzhitov R, Flavell RA. 2001. Recognition of double-stranded RNA and activation of NF-kappaB by Toll-like receptor 3. *Nature* 413:732–8. https://doi.org/10.1038/35099560.

15. Yamamoto M, Sato S, Mori K, Hoshino K, Takeuchi O, Takeda K, Akira S. 2002. Cutting edge: a novel Toll/IL-1 receptor domain-containing adapter that preferentially activates the IFN-beta promoter in the Toll-like receptor signaling. *Journal of immunology (Baltimore, Md. : 1950)* 169:6668–72.

16. Yamamoto M, Sato S, Hemmi H, Hoshino K, Kaisho T, Sanjo H, Takeuchi O, Sugiyama M, Okabe M, Takeda K, Akira S. 2003. Role of adaptor TRIF in the MyD88-independent toll-like receptor signaling pathway. *Science (New York, N.Y.)* 301:640–3. https://doi.org/10.1126/science.1087262.

17. Goubau D, Deddouche S, Reis e Sousa C. 2013. Cytosolic sensing of viruses. *Immunity* 38:855–69. https://doi.org/10.1016/j.immuni.2013.05.007.

18. McCartney SA, Colonna M. 2009. Viral sensors: diversity in pathogen recognition. *Immunological reviews* 227:87–94. https://doi.org/10.1111/j.1600-065X.2008.00726.x.

19. Silverman RH. 2007. A scientific journey through the 2-5A/RNase L system. *Cytokine & Growth Factor Reviews* 18:381–388. https://doi.org/10.1016/j.cytogfr.2007.06.012.

20. Takaoka A, Wang Z, Choi MK, Yanai H, Negishi H, Ban T, Lu Y, Miyagishi M, Kodama T, Honda K, Ohba Y, Taniguchi T. 2007. DAI (DLM-1/ZBP1) is a cytosolic DNA sensor and an activator of innate immune response. *Nature* 448:501–505. https://doi.org/10.1038/nature06013.

21. Wang Z, Choi MK, Ban T, Yanai H, Negishi H, Lu Y, Tamura T, Takaoka A, Nishikura K, Taniguchi T. 2008. Regulation of innate immune responses by DAI (DLM-1/ZBP1) and other DNA-sensing molecules. *Proceedings of the National Academy of Sciences of the United States of America* 105:5477–82. https://doi.org/10.1073/pnas.0801295105.

22. Upton JW, Kaiser WJ, Mocarski ES. 2012. DAI/ZBP1/DLM-1 Complexes with RIP3 to Mediate Virus-Induced Programmed Necrosis that Is Targeted by Murine Cytomegalovirus vIRA. *Cell Host & Microbe* 11:290–297. https://doi.org/10.1016/j.chom.2012.01.016.

23. Pindel A, Sadler A. 2011. The role of protein kinase R in the interferon response. *Journal of interferon & cytokine research : the official journal of the International Society for Interferon and Cytokine Research* 31:59–70. https://doi.org/10.1089/jir.2010.0099.

24. O'Malley WE, Achinstein B, Shear MJ. 1962. Action of bacterial polysaccharide on tumors. ii. damage of sarcoma 37 by serum of mice treated with serratia marcescens polysaccharide, and induced tolerance. *Journal of the National Cancer Institute* 29:1169–1175. https://doi.org/10.1093/jnci/29.6.1169.

25. Carswell EA, Old LJ, Kassel RL, Green S, Fiore N, Williamson B. 1975. An endotoxin-induced serum factor that causes necrosis of tumors. *Proceedings of the National Academy of Sciences* 72:3666–3670. https://doi.org/10.1073/pnas.72.9.3666.

26. Aggarwal BB, Kohr WJ, Hass PE, Moffat B, Spencer SA, Henzel WJ, Bringman TS, Nedwin GE, Goeddel DV, Harkins RN. 1985. Human tumor necrosis factor. Production, purification, and characterization. *The Journal of biological chemistry* 260:2345–54.

27. Aggarwal BB, Moffat B, Harkins RN. 1984. Human lymphotoxin. Production by a lymphoblastoid cell line, purification, and initial characterization. *The Journal of biological chemistry* 259:686–91.

28. Aggarwal BB, Gupta SC, Kim JH. 2012. Historical perspectives on tumor necrosis factor and its superfamily: 25 years later, a golden journey. *Blood* 119:651–65. https://doi.org/10.1182/blood-2011-04-325225.

29. Waring P, Müllbacher A. 1999. Cell death induced by the Fas/Fas ligand pathway and its role in pathology. *Immunology and cell biology* 77:312–7. https://doi.org/10.1046/j.1440-1711.1999.00837.x.

30. Thorburn A. 2007. Tumor necrosis factor-related apoptosis-inducing ligand (TRAIL) pathway signaling. *Journal of thoracic oncology : official publication of the International Association for the Study of Lung Cancer* 2:461–5. https://doi.org/10.1097/JTO.0b013e31805fea64.

31. Wong GHW, Goeddel DV. 1986. Tumour necrosis factors α and β inhibit virus replication and synergize with interferons. *Nature* 323:819–822. https://doi.org/10.1038/323819a0.

32. Mestan J, Digel W, Mittnacht S, Hillen H, Blohm D, Möller A, Jacobsen H, Kirchner H. 1986. Antiviral effects of recombinant tumour necrosis factor in vitro. *Nature* 323:816–819. https://doi.org/10.1038/323816a0.

33. Sträter J, Möller P. 2004. TRAIL and viral infection. *Vitamins and hormones* 67:257–74. https://doi.org/10.1016/S0083-6729(04)67014-2.

34. Bień K, Sokolowska J, Baska P, Nowak Z, Stankiewicz W, Krzyzowska M. 2015. Fas/FasL pathway participates in regulation of antiviral and inflammatory response during mousepox infection of lungs. *Mediators of inflammation* 2015:281613. https://doi.org/10.1155/2015/281613.

35. Zhou X, Jiang W, Liu Z, Liu S, Liang X. 2017. Virus Infection and Death Receptor-Mediated Apoptosis. *Viruses* 9:316. https://doi.org/10.3390/v9110316.

36. Veyer DL, Maluquer de Motes C, Sumner RP, Ludwig L, Johnson BF, Smith GL. 2014. Analysis of the anti-apoptotic activity of four vaccinia virus proteins demonstrates that B13 is the most potent inhibitor in isolation and during viral infection. *The Journal of general virology* 95:2757–68. https://doi.org/10.1099/vir.0.068833-0.

37. Sambhi SK, Kohonen-Corish MR, Ramshaw IA. 1991. Local production of tumor necrosis factor encoded by recombinant vaccinia virus is effective in controlling viral replication in vivo. *Proceedings of the National Academy of Sciences* 88:4025–4029. https://doi.org/10.1073/pnas.88.9.4025.

38. Taylor RC, Cullen SP, Martin SJ. 2008. Apoptosis: controlled demolition at the cellular level. *Nature Reviews Molecular Cell Biology* 9:231–241. https://doi.org/10.1038/nrm2312.

39. Henson PM, Bratton DL. 2013. Antiinflammatory effects of apoptotic cells. *Journal of Clinical Investigation* 123:2773–2774. https://doi.org/10.1172/JCI69344.

40. Elmore S. 2007. Apoptosis: a review of programmed cell death. *Toxicologic pathology* 35:495–516. https://doi.org/10.1080/01926230701320337.

41. O'Donnell MA, Legarda-Addison D, Skountzos P, Yeh WC, Ting AT. 2007. Ubiquitination of RIP1 Regulates an NF-κB-Independent Cell-Death Switch in TNF Signaling. *Current Biology* 17:418–424. https://doi.org/10.1016/j.cub.2007.01.027.

42. Kim YS, Schwabe RF, Qian T, Lemasters JJ, Brenner DA. 2002. TRAIL-mediated apoptosis requires NF-kappaB inhibition and the mitochondrial permeability transition in human hepatoma cells. *Hepatology (Baltimore, Md.)* 36:1498–508. https://doi.org/10.1053/jhep.2002.36942.

43. Imamura R, Konaka K, Matsumoto N, Hasegawa M, Fukui M, Mukaida N, Kinoshita T, Suda T. 2004. Fas Ligand Induces Cell-autonomous NF-κB Activation and Interleukin-8 Production by a Mechanism Distinct from That of Tumor Necrosis Factor-α. *Journal of Biological Chemistry* 279:46415–46423. https://doi.org/10.1074/jbc.M403226200.

44. Israël A. 2010. The IKK complex, a central regulator of NF-kappaB activation. *Cold Spring Harbor perspectives in biology* 2:a000158. https://doi.org/10.1101/cshperspect.a000158.

45. Luo JL, Kamata H, Karin M. 2005. IKK/NF-kappaB signaling: balancing life and death–a new approach to cancer therapy. *The Journal of clinical investigation* 115:2625–32. https://doi.org/10.1172/JCI26322.

46. Lawrence T. 2009. The nuclear factor NF-kappaB pathway in inflammation. *Cold Spring Harbor perspectives in biology* 1:a001651. https://doi.org/10.1101/cshperspect.a001651.

47. Wang CY, Guttridge DC, Mayo MW, Baldwin AS. 1999. NF-κB Induces Expression of the Bcl-2 Homologue A1/Bfl-1 To Preferentially Suppress Chemotherapy-Induced Apoptosis. *Molecular and Cellular Biology* 19:5923–5929. https://doi.org/10.1128/MCB.19.9.5923.

48. Kreuz S, Siegmund D, Scheurich P, Wajant H. 2001. NF- B Inducers Upregulate cFLIP, a Cycloheximide-Sensitive Inhibitor of Death Receptor Signaling. *Molecular and Cellular Biology* 21:3964–3973. https://doi.org/10.1128/MCB.21.12.3964-3973.2001.

49. Micheau O, Lens S, Gaide O, Alevizopoulos K, Tschopp J. 2001. NF- B Signals Induce the Expression of c-FLIP. *Molecular and Cellular Biology* 21:5299–5305. https://doi.org/10.1128/MCB.21.16.5299-5305.2001.

50. Listen P, Roy N, Tamai K, Lefebvre C, Baird S, Cherton-Horvat G, Farahani R, McLean M, Lkeda JE, Mackenzie A, Korneluk RG. 1996. Suppression of apoptosis in mammalian cells by NAIP and a related family of IAP genes. *Nature* 379:349–353. https://doi.org/10.1038/379349a0.

51. Stehlik C, Martin R de, Kumabashiri I, Schmid JA, Binder BR, Lipp J. 1998. Nuclear Factor (NF)-κB–regulated X-chromosome–linked iap Gene Expression Protects Endothelial Cells from Tumor Necrosis Factor α–induced Apoptosis. *The Journal of Experimental Medicine* 188:211–216. https://doi.org/10.1084/jem.188.1.211.

52. Wang CY, Mayo MW, Korneluk RG, Goeddel DV, Baldwin AS. 1998. NF-kappaB antiapoptosis: induction of TRAF1 and TRAF2 and c-IAP1 and c-IAP2 to suppress caspase-8 activation. *Science (New York, N.Y.)* 281:1680–3. https://doi.org/10.1126/science.281.5383.1680.

53. Mahul-Mellier AL, Pazarentzos E, Datler C, Iwasawa R, AbuAli G, Lin B, Grimm S. 2012. De-ubiquitinating protease USP2a targets RIP1 and TRAF2 to mediate cell death by TNF. *Cell death and differentiation* 19:891–9. https://doi.org/10.1038/cdd.2011.185.

54. Micheau O, Tschopp J. 2003. Induction of TNF Receptor I-Mediated Apoptosis via Two Sequential Signaling Complexes. *Cell* 114:181–190. https://doi.org/10.1016/S0092-8674(03)00521-X.

55. McIlwain DR, Berger T, Mak TW. 2013. Caspase functions in cell death and disease. *Cold Spring Harbor perspectives in biology* 5:a008656. https://doi.org/10.1101/cshperspect.a008656.

56. Walsh JG, Cullen SP, Sheridan C, Luthi AU, Gerner C, Martin SJ. 2008. Executioner caspase-3 and caspase-7 are functionally distinct proteases. *Proceedings of the National Academy of Sciences* 105:12815–12819. https://doi.org/10.1073/pnas.0707715105.

57. Liu X, Zou H, Slaughter C, Wang X. 1997. DFF, a heterodimeric protein that functions downstream of caspase-3 to trigger DNA fragmentation during apoptosis. *Cell* 89:175–84.

58. Halenbeck R, MacDonald H, Roulston A, Chen TT, Conroy L, Williams LT. 1998. CPAN, a human nuclease regulated by the caspase-sensitive inhibitor DFF45. *Current biology : CB* 8:537–40.

59. Hangen E, Blomgren K, Bénit P, Kroemer G, Modjtahedi N. 2010. Life with or without AIF. *Trends in biochemical sciences* 35:278–87. https://doi.org/10.1016/j.tibs.2009.12.008.

60. Rusch L, Zhou A, Silverman RH. 2000. Caspase-dependent apoptosis by 2',5'-oligoadenylate activation of RNase L is enhanced by IFN-beta. *Journal of interferon & cytokine research : the official journal of the International Society for Interferon and Cytokine Research* 20:1091–100. https://doi.org/10.1089/107999000750053762.

61. Zou H, Li Y, Liu X, Wang X. 1999. An APAF-1.cytochrome c multimeric complex is a functional apoptosome that activates procaspase-9. *The Journal of biological chemistry* 274:11549–56.

62. Der SD, Yang YL, Weissmann C, Williams BRG. 1997. A double-stranded RNA-activated protein kinase-dependent pathway mediating stress-induced apoptosis. *Proceedings of the National Academy of Sciences* 94:3279–3283. https://doi.org/10.1073/pnas.94.7.3279.

63. Srivastava SP, Kumar KU, Kaufman RJ. 1998. Phosphorylation of Eukaryotic Translation Initiation Factor 2 Mediates Apoptosis in Response to Activation of the Double-stranded RNA-dependent Protein Kinase. *Journal of Biological Chemistry* 273:2416–2423. https://doi.org/10.1074/jbc.273.4.2416.

64. Gil J, Esteban M. 2000. Induction of apoptosis by the dsRNA-dependent protein kinase (PKR): Mechanism of action. *APOPTOSIS* 5:107–114. https://doi.org/10.1023/A:1009664109241.

65. McDonnell MA, Wang D, Khan SM, Vander Heiden MG, Kelekar A. 2003. Caspase-9 is activated in a cytochrome c-independent manner early during TNFα-induced apoptosis in murine cells. *Cell Death & Differentiation* 10:1005–1015. https://doi.org/10.1038/sj.cdd.4401271.

66. Lin Y, Devin A, Rodriguez Y, Liu ZG. 1999. Cleavage of the death domain kinase RIP by caspase-8 prompts TNF-induced apoptosis. *Genes & development* 13:2514–26. https://doi.org/10521396.

67. Kumar A, Yang YL, Flati V, Der S, Kadereit S, Deb A, Haque J, Reis L, Weissmann C, Williams BR. 1997. Deficient cytokine signaling in mouse embryo

fibroblasts with a targeted deletion in the PKR gene: role of IRF-1 and NF-kappaB. *The EMBO journal* 16:406–16. https://doi.org/10.1093/emboj/16.2.406.

68. Gil J, Alcamí J, Esteban M. 2000. Activation of NF-κB by the dsRNA-dependent protein kinase, PKR involves the IκB kinase complex. *Oncogene* 19:1369–1378. https://doi.org/10.1038/sj.onc.1203448.

69. Bonnet MC, Weil R, Dam E, Hovanessian AG, Meurs EF. 2000. PKR stimulates NF-kappaB irrespective of its kinase function by interacting with the IkappaB kinase complex. *Molecular and cellular biology* 20:4532–42.

70. Chan FKM, Luz NF, Moriwaki K. 2015. Programmed necrosis in the cross talk of cell death and inflammation. *Annual review of immunology* 33:79–106. https://doi.org/10.1146/annurev-immunol-032414-112248.

71. Pasparakis M, Vandenabeele P. 2015. Necroptosis and its role in inflammation. *Nature* 517:311–20. https://doi.org/10.1038/nature14191.

72. Sawai H. 2016. Induction of Apoptosis in TNF-Treated L929 Cells in the Presence of Necrostatin-1. *International journal of molecular sciences* 17:1678. https://doi.org/10.3390/ijms17101678.

73. Sun L, Wang H, Wang Z, He S, Chen S, Liao D, Wang L, Yan J, Liu W, Lei X, Wang X. 2012. Mixed Lineage Kinase Domain-like Protein Mediates Necrosis Signaling Downstream of RIP3 Kinase. *Cell* 148:213–227. https://doi.org/10.1016/j.cell.2011.11.031.

74. Zhao J, Jitkaew S, Cai Z, Choksi S, Li Q, Luo J, Liu ZG. 2012. Mixed lineage kinase domain-like is a key receptor interacting protein 3 downstream component of TNF-induced necrosis. *Proceedings of the National Academy of Sciences* 109:5322–5327. https://doi.org/10.1073/pnas.1200012109.

75. Yoon S, Kovalenko A, Bogdanov K, Wallach D. 2017. MLKL, the Protein that Mediates Necroptosis, Also Regulates Endosomal Trafficking and Extracellular Vesicle Generation. *Immunity* 47:51–65.e7. https://doi.org/10.1016/j.immuni.2017.06.001.

76. Cai Z, Jitkaew S, Zhao J, Chiang HC, Choksi S, Liu J, Ward Y, Wu LG, Liu ZG. 2014. Plasma membrane translocation of trimerized MLKL protein is required for TNF-induced necroptosis. *Nature cell biology* 16:55–65. https://doi.org/10.1038/ncb2883.

77. Gong YN, Guy C, Olauson H, Becker JU, Yang M, Fitzgerald P, Linkermann A, Green DR. 2017. ESCRT-III Acts Downstream of MLKL to Regulate Necroptotic Cell Death and Its Consequences. *Cell* 169:286–300.e16. https://doi.org/10.1016/j.cell.2017.03.020.

78. Wang L, Du F, Wang X. 2008. TNF-α Induces Two Distinct Caspase-8 Activation Pathways. *Cell* 133:693–703. https://doi.org/10.1016/j.cell.2008.03.036.

79. Wu YT, Tan HL, Huang Q, Sun XJ, Zhu X, Shen HM. 2011. zVAD-induced necroptosis in L929 cells depends on autocrine production of TNFα mediated by the PKC–MAPKs–AP-1 pathway. *Cell Death and Differentiation* 1872:26–37. https://doi.org/10.1038/cdd.2010.72.

80. Zhang Y, Su SS, Zhao S, Yang Z, Zhong CQ, Chen X, Cai Q, Yang ZH, Huang D, Wu R, Han J. 2017. RIP1 autophosphorylation is promoted by mitochondrial ROS and is essential for RIP3 recruitment into necrosome. *Nature Communications* 8. https://doi.org/10.1038/ncomms14329.

81. He S, Wang L, Miao L, Wang T, Du F, Zhao L, Wang X. 2009. Receptor Interacting Protein Kinase-3 Determines Cellular Necrotic Response to TNF-α. *Cell* 137:1100–1111. https://doi.org/10.1016/j.cell.2009.05.021.

82. Zhang DW, Shao J, Lin J, Zhang N, Lu BJ, Lin SC, Dong MQ, Han J. 2009. RIP3, an energy metabolism regulator that switches TNF-induced cell death from apoptosis to necrosis. *Science (New York, N.Y.)* 325:332–6. https://doi.org/10.1126/science.1172308.

83. Thapa RJ, Nogusa S, Chen P, Maki JL, Lerro A, Andrake M, Rall GF, Degterev A, Balachandran S. 2013. Interferon-induced RIP1/RIP3-mediated necrosis requires PKR and is licensed by FADD and caspases. *Proceedings of the National Academy of Sciences* 110:E3109–E3118. https://doi.org/10.1073/pnas.1301218110.

84. He S, Liang Y, Shao F, Wang X. 2011. Toll-like receptors activate programmed necrosis in macrophages through a receptor-interacting kinase-3-mediated pathway. *Proceedings of the National Academy of Sciences of the United States of America* 108:20054–9. https://doi.org/10.1073/pnas.1116302108.

85. Kaiser WJ, Sridharan H, Huang C, Mandal P, Upton JW, Gough PJ, Sehon CA, Marquis RW, Bertin J, Mocarski ES. 2013. Toll-like Receptor 3-mediated Necrosis via TRIF, RIP3, and MLKL. *Journal of Biological Chemistry* 288:31268–31279. https://doi.org/10.1074/jbc.M113.462341.

86. Nogusa S, Thapa RJ, Dillon CP, Liedmann S, Oguin TH, Ingram JP, Rodriguez DA, Kosoff R, Sharma S, Sturm O, Verbist K, Gough PJ, Bertin J, Hartmann BM, Sealfon SC, Kaiser WJ, Mocarski ES, López CB, Thomas PG, Oberst A, Green DR, Balachandran S. 2016. RIPK3 Activates Parallel Pathways of MLKL-Driven Necroptosis and FADD-Mediated Apoptosis to Protect against Influenza A Virus. *Cell Host & Microbe* 20:13–24. https://doi.org/10.1016/j.chom.2016.05.011.

87. Koehler H, Cotsmire S, Langland J, Kibler KV, Kalman D, Upton JW, Mocarski ES, Jacobs BL. 2017. Inhibition of DAI-dependent necroptosis by the Z-DNA binding domain of the vaccinia virus innate immune evasion protein, E3. *Proceedings of the National Academy of Sciences* 114:11506–11511. https://doi.org/10.1073/pnas.1700999114.

88. Feng S, Yang Y, Mei Y, Ma L, Zhu De, Hoti N, Castanares M, Wu M. 2007. Cleavage of RIP3 inactivates its caspase-independent apoptosis pathway by removal of kinase domain. *Cellular Signalling* 19:2056–2067. https://doi.org/10.1016/j.cellsig.2007.05.016.

89. Nikoletopoulou V, Markaki M, Palikaras K, Tavernarakis N. 2013. Crosstalk between apoptosis, necrosis and autophagy. *Biochimica et Biophysica Acta (BBA) - Molecular Cell Research* 1833:3448–3459. https://doi.org/10.1016/j.bbamcr.2013.06.001.

90. Humphries F, Yang S, Wang B, Moynagh PN. 2015. RIP kinases: key decision makers in cell death and innate immunity. *Cell death and differentiation* 22:225–36. https://doi.org/10.1038/cdd.2014.126.

91. Tewari M, Dixit VM. 1995. Fas- and Tumor Necrosis Factor-induced Apoptosis Is Inhibited by the Poxvirus crmA Gene Product. *Journal of Biological Chemistry* 270:3255–3260. https://doi.org/10.1074/jbc.270.7.3255.

92. Enari M, Hug H, Nagata S. 1995. Involvement of an ICE-like protease in Fas-mediated apoptosis. *Nature* 375:78–81. https://doi.org/10.1038/375078a0.

93. Miura M, Friedlander RM, Yuan J. 1995. Tumor necrosis factor-induced apoptosis is mediated by a CrmA-sensitive cell death pathway. *Proceedings of the National Academy of Sciences* 92:8318–8322. https://doi.org/10.1073/pnas.92.18.8318.

94. Zhou Q, Snipas S, Orth K, Muzio M, Dixit VM, Salvesen GS. 1997. Target Protease Specificity of the Viral Serpin CrmA. *Journal of Biological Chemistry* 272:7797–7800. https://doi.org/10.1074/jbc.272.12.7797.

95. Garcia-Calvo M, Peterson EP, Leiting B, Ruel R, Nicholson DW, Thornberry NA. 1998. Inhibition of Human Caspases by Peptide-based and Macromolecular Inhibitors. *Journal of Biological Chemistry* 273:32608–32613. https://doi.org/10.1074/jbc.273.49.32608.

96. Smith GL, Howard ST, Chan YS. 1989. Vaccinia virus encodes a family of genes with homology to serine proteinase inhibitors. *The Journal of general virology* 70 (Pt 9):2333–43. https://doi.org/10.1099/0022-1317-70-9-2333.

97. Kettle S, Blake NW, Law KM, Smith GL. 1995. Vaccinia virus serpins B13R (SPI-2) and B22R (SPI-1) encode Mr 38.5 and 40K, intracellular polypeptides that do not affect virus virulence in a murine intranasal model. *Virology* 206:136–147. https://doi.org/10.1016/S0042-6822(95)80028-X.

98. Dobbelstein M, Shenk T. 1996. Protection against apoptosis by the vaccinia virus SPI-2 (B13R) gene product. *Journal of virology* 70:6479–85.

99. Reading PC, Khanna A, Smith GL. 2002. Vaccinia Virus CrmE Encodes a Soluble and Cell Surface Tumor Necrosis Factor Receptor That Contributes to Virus Virulence. *Virology* 292:285–298. https://doi.org/10.1006/viro.2001.1236.

100. Taylor JM, Quilty D, Banadyga L, Barry M. 2006. The vaccinia virus protein F1L interacts with Bim and inhibits activation of the pro-apoptotic protein Bax. *The Journal of biological chemistry* 281:39728–39. https://doi.org/10.1074/jbc.M607465200.

101. Ember SWJ, Ren H, Ferguson BJ, Smith GL. 2012. Vaccinia virus protein C4 inhibits NF-κB activation and promotes virus virulence. *The Journal of general virology* 93:2098–108. https://doi.org/10.1099/vir.0.045070-0.

102. Maluquer de Motes C, Cooray S, Ren H, Almeida GMF, McGourty K, Bahar MW, Stuart DI, Grimes JM, Graham SC, Smith GL. 2011. Inhibition of apoptosis and NF-κB activation by vaccinia protein N1 occur via distinct binding surfaces and make different contributions to virulence. *PLoS pathogens* 7:e1002430. https://doi.org/10.1371/journal.ppat.1002430.

103. Bravo Cruz AG, Shisler JL. 2016. Vaccinia virus K1 ankyrin repeat protein inhibits NF-κB activation by preventing RelA acetylation. *The Journal of general virology* 97:2691–2702. https://doi.org/10.1099/jgv.0.000576.

104. Stack J, Haga IR, Schröder M, Bartlett NW, Maloney G, Reading PC, Fitzgerald Ka, Smith GL, Bowie AG. 2005. Vaccinia virus protein A46R targets multiple Toll-like-interleukin-1 receptor adaptors and contributes to virulence.

The Journal of experimental medicine 201:1007–18. https://doi.org/10.1084/jem.20041442.

105. Chang HW, Watson JC, Jacobs BL. 1992. The E3L gene of vaccinia virus encodes an inhibitor of the interferon-induced, double-stranded RNA-dependent protein kinase. *Proceedings of the National Academy of Sciences* 89:4825–4829. https://doi.org/10.1073/pnas.89.11.4825.

106. Chang HW, Jacobs BL. 1993. *Identification of a conserved motif that is necessary for binding of the vaccinia virus E3L gene products to double-stranded RNA.* https://doi.org/10.1006/viro.1993.1292.

107. Chang HW, Uribe LH, Jacobs BL. 1995. Rescue of vaccinia virus lacking the E3L gene by mutants of E3L. *Journal of virology* 69:6605–8.

108. Kibler KV, Shors T, Perkins KB, Zeman CC, Banaszak MP, Biesterfeldt J, Langland JO, Jacobs BL. 1997. Double-stranded RNA is a trigger for apoptosis in vaccinia virus-infected cells. *Journal of virology* 71:1992–2003.

109. Veyer DL, Carrara G, Maluquer de Motes C, Smith GL. 2017. Vaccinia virus evasion of regulated cell death. *Immunology Letters* 186:68–80. https://doi.org/10.1016/j.imlet.2017.03.015.

110. Kim YG, Muralinath M, Brandt T, Pearcy M, Hauns K, Lowenhaupt K, Jacobs BL, Rich A. 2003. A role for Z-DNA binding in vaccinia virus pathogenesis. *Proceedings of the National Academy of Sciences* 100:6974–6979. https://doi.org/10.1073/pnas.0431131100.

111. White SD, Jacobs BL. 2012. The amino terminus of the vaccinia virus E3 protein is necessary to inhibit the interferon response. *Journal of virology* 86:5895–904. https://doi.org/10.1128/JVI.06889-11.

112. Watson JD, Crick FHC. 1953. Molecular Structure of Nucleic Acids: A Structure for Deoxyribose Nucleic Acid. *Nature* 171:737–738. https://doi.org/10.1038/171737a0.

113. Wang AHJ, Quigley GJ, Kolpak FJ, Crawford JL, Boom JH van, Marel G van der, Rich A. 1979. Molecular structure of a left-handed double helical DNA fragment at atomic resolution. *Nature* 282:680–6. https://doi.org/10.1038/282680a0.

114. Hall K, Cruz P, Tinoco I, Jovin TM, Sande JH van de. 1984. 'Z-RNA'—a left-handed RNA double helix. *Nature* 311:584–586. https://doi.org/10.1038/311584a0.

115. Pohl FM, Jovin TM. 1972. Salt-induced co-operative conformational change of a synthetic DNA: Equilibrium and kinetic studies with poly(dG-dC). *Journal of Molecular Biology* 67:375–396. https://doi.org/10.1016/0022-2836(72)90457-3.

116. Wittig B, Dorbic T, Rich A. 1989. The level of Z-DNA in metabolically active, permeabilized mammalian cell nuclei is regulated by torsional strain. *The Journal of cell biology* 108:755–64. https://doi.org/2921282.

117. D'Ascenzo L, Leonarski F, Vicens Q, Auffinger P. 2016. 'Z-DNA like' fragments in RNA: a recurring structural motif with implications for folding, RNA/protein recognition and immune response. *Nucleic Acids Research* 44:5944–5956. https://doi.org/10.1093/nar/gkw388.

118. Rich A, Zhang S. 2003. Timeline: Z-DNA: the long road to biological function. *Nature reviews. Genetics* 4:566–72. https://doi.org/10.1038/nrg1115.

119. Bass BL, Weintraub H. 1987. A developmentally regulated activity that unwinds RNA duplexes. *Cell* 48:607–13. https://doi.org/10.1016/0092-8674(87)90239-X.

120. Rebagliati MR, Melton DA. 1987. Antisense RNA injections in fertilized frog eggs reveal an RNA duplex unwinding activity. *Cell* 48:599–605. https://doi.org/10.1016/0092-8674(87)90238-8.

121. Wagner RW, Smith JE, Cooperman BS, Nishikura K. 1989. A double-stranded RNA unwinding activity introduces structural alterations by means of adenosine to inosine conversions in mammalian cells and Xenopus eggs. *Proceedings of the National Academy of Sciences of the United States of America* 86:2647–51. https://doi.org/2704740.

122. Samuel CE. 2011. Adenosine deaminases acting on RNA (ADARs) are both antiviral and proviral. *Virology* 411:180–93. https://doi.org/10.1016/j.virol.2010.12.004.

123. Huynh TP. 2013. Characterization of Host Responses to Vaccinia Virus Infection. Doctoral Dissertation. Arizona State University.

124. Herbert A, Lowenhaupt K, Spitzner J, Rich A. 1995. Chicken double-stranded RNA adenosine deaminase has apparent specificity for Z-DNA. *Proceedings of*

the National Academy of Sciences 92:7550–7554. https://doi.org/10.1073/pnas.92.16.7550.

125. Herbert A, Alfken J, Kim YG, Mian IS, Nishikura K, Rich A. 1997. A Z-DNA binding domain present in the human editing enzyme, double-stranded RNA adenosine deaminase. *Proceedings of the National Academy of Sciences* 94:8421–8426. https://doi.org/10.1073/pnas.94.16.8421.

126. Placido D, Brown BA, Lowenhaupt K, Rich A, Athanasiadis A. 2007. A Left-Handed RNA Double Helix Bound by the Zα Domain of the RNA-Editing Enzyme ADAR1. *Structure* 15:395–404. https://doi.org/10.1016/j.str.2007.03.001.

127. Koeris M, Funke L, Shrestha J, Rich A, Maas S. 2005. Modulation of ADAR1 editing activity by Z-RNA in vitro. *Nucleic acids research* 33:5362–70. https://doi.org/10.1093/nar/gki849.

128. Brown BA, Lowenhaupt K, Wilbert CM, Hanlon EB, Rich A. 2000. The zalpha domain of the editing enzyme dsRNA adenosine deaminase binds left-handed Z-RNA as well as Z-DNA. *Proceedings of the National Academy of Sciences of the United States of America* 97:13532–6. https://doi.org/10.1073/pnas.240464097.

129. Rothenburg S, Deigendesch N, Dittmar K, Koch-Nolte F, Haag F, Lowenhaupt K, Rich A. 2005. A PKR-like eukaryotic initiation factor 2 kinase from zebrafish contains Z-DNA binding domains instead of dsRNA binding domains. *Proceedings of the National Academy of Sciences* 102:1602–1607. https://doi.org/10.1073/pnas.0408714102.

130. Rosa M de, Zacarias S, Athanasiadis A. 2013. Structural basis for Z-DNA binding and stabilization by the zebrafish Z-DNA dependent protein kinase PKZ. *Nucleic Acids Research* 41:9924–9933. https://doi.org/10.1093/nar/gkt743.

131. Liu TK, Zhang YB, Liu Y, Sun F, Gui JF. 2011. Cooperative roles of fish protein kinase containing Z-DNA binding domains and double-stranded RNA-dependent protein kinase in interferon-mediated antiviral response. *Journal of virology* 85:12769–80. https://doi.org/10.1128/JVI.05849-11.

132. Tomé AR, Kuś K, Correia S, Paulo LM, Zacarias S, Rosa M de, Figueiredo D, Parkhouse RME, Athanasiadis A. 2013. Crystal structure of a poxvirus-like zalpha domain from cyprinid herpesvirus 3. *Journal of virology* 87:3998–4004. https://doi.org/10.1128/JVI.03116-12.

133. Fu Y, Comella N, Tognazzi K, Brown LF, Dvorak HF, Kocher O. 1999. Cloning of DLM-1, a novel gene that is up-regulated in activated macrophages, using RNA differential display. *Gene* 240:157–163. https://doi.org/10.1016/S0378-1119(99)00419-9.

134. Schwartz T, Behlke J, Lowenhaupt K, Heinemann U, Rich A. 2001. Structure of the DLM-1–Z-DNA complex reveals a conserved family of Z-DNA-binding proteins. *Nature Structural Biology* 8:761–765. https://doi.org/10.1038/nsb0901-761.

135. Ha SC, Kim D, Hwang HY, Rich A, Kim YG, Kim KK. 2008. The crystal structure of the second Z-DNA binding domain of human DAI (ZBP1) in complex with Z-DNA reveals an unusual binding mode to Z-DNA. *Proceedings of the National Academy of Sciences of the United States of America* 105:20671–6. https://doi.org/10.1073/pnas.0810463106.

136. Thapa RJ, Ingram JP, Ragan KB, Nogusa S, Boyd DF, Benitez AA, Sridharan H, Kosoff R, Shubina M, Landsteiner VJ, Andrake M, Vogel P, Sigal LJ, TenOever BR, Thomas PG, Upton JW, Balachandran S. 2016. DAI Senses Influenza A Virus Genomic RNA and Activates RIPK3-Dependent Cell Death. *Cell host & microbe* 20:674–681. https://doi.org/10.1016/j.chom.2016.09.014.

137. Kahmann JD, Wecking DA, Putter V, Lowenhaupt K, Kim YG, Schmieder P, Oschkinat H, Rich A, Schade M. 2004. The solution structure of the N-terminal domain of E3L shows a tyrosine conformation that may explain its reduced affinity to Z-DNA in vitro. *Proceedings of the National Academy of Sciences of the United States of America* 101:2712–7. https://doi.org/10.1073/pnas.0308612100.

138. Kim YG, Lowenhaupt K, Oh DB, Kim KK, Rich A. 2004. Evidence that vaccinia virulence factor E3L binds to Z-DNA in vivo: Implications for development of a therapy for poxvirus infection. *Proceedings of the National Academy of Sciences of the United States of America* 101:1514–8. https://doi.org/10.1073/pnas.0308260100.

139. Ng SK, Weissbach R, Ronson GE, Scadden ADJ. 2013. Proteins that contain a functional Z-DNA-binding domain localize to cytoplasmic stress granules. *Nucleic Acids Research* 41:9786–9799. https://doi.org/10.1093/nar/gkt750.

140. Protter DS, Parker R. 2016. Principles and Properties of Stress Granules. *Trends in Cell Biology* 26:668–679. https://doi.org/10.1016/j.tcb.2016.05.004.

141. Hershey JW. 1989. Protein phosphorylation controls translation rates. *The Journal of biological chemistry* 264:20823–6.

142. Kimball SR. 1999. Eukaryotic initiation factor eIF2. *The international journal of biochemistry & cell biology* 31:25–9.

143. Vattem KM, Wek RC. 2004. Reinitiation involving upstream ORFs regulates ATF4 mRNA translation in mammalian cells. *Proceedings of the National Academy of Sciences of the United States of America* 101:11269–74. https://doi.org/10.1073/pnas.0400541101.

144. McCormick C, Khaperskyy DA. 2017. Translation inhibition and stress granules in the antiviral immune response. *Nature reviews. Immunology* 17:647–660. https://doi.org/10.1038/nri.2017.63.

145. Smith JA, Schmechel SC, Raghavan A, Abelson M, Reilly C, Katze MG, Kaufman RJ, Bohjanen PR, Schiff LA. 2006. Reovirus induces and benefits from an integrated cellular stress response. *Journal of virology* 80:2019–33. https://doi.org/10.1128/JVI.80.4.2019-2033.2006.

146. Dougherty JD, Tsai WC, Lloyd RE. 2015. Multiple Poliovirus Proteins Repress Cytoplasmic RNA Granules. *Viruses* 7:6127–40. https://doi.org/10.3390/v7122922.

147. Simpson-Holley M, Kedersha N, Dower K, Rubins KH, Anderson P, Hensley LE, Connor JH. 2011. Formation of antiviral cytoplasmic granules during orthopoxvirus infection. *Journal of virology* 85:1581–93. https://doi.org/10.1128/JVI.02247-10.

148. Han AP, Yu C, Lu L, Fujiwara Y, Browne C, Chin G, Fleming M, Leboulch P, Orkin SH, Chen JJ. 2001. Heme-regulated eIF2alpha kinase (HRI) is required for translational regulation and survival of erythroid precursors in iron deficiency. *The EMBO journal* 20:6909–18. https://doi.org/10.1093/emboj/20.23.6909.

149. Dever TE, Feng L, Wek RC, Cigan AM, Donahue TF, Hinnebusch AG. 1992. Phosphorylation of initiation factor 2 alpha by protein kinase GCN2 mediates gene-specific translational control of GCN4 in yeast. *Cell* 68:585–96.

150. Harding HP, Zhang Y, Bertolotti A, Zeng H, Ron D. 2000. Perk is essential for translational regulation and cell survival during the unfolded protein response. *Molecular cell* 5:897–904. https://doi.org/10882126.

151. Okonski KM, Samuel CE. 2013. Stress granule formation induced by measles virus is protein kinase PKR dependent and impaired by RNA adenosine deaminase ADAR1. *Journal of virology* 87:756–66. https://doi.org/10.1128/JVI.02270-12.

152. Ringer S, Sainsbury H. 1882. Observations on the Physiological and Therapeutic Action of the Element Arsenic in the Form of Arsenite and Arseniate. *British medical journal* 2:1193–5. https://doi.org/20750413.

153. Kolipinski L. 1900. Chronic enteritis and tuberculosis enteritis treated with hypodermic injections of arsenic. *Medical News* Volume 77:202–206.

154. Levinson W, Oppermann H, Jackson J. 1980. Transition series metals and sulfhydryl reagents induce the synthesis of four proteins in eukaryotic cells. *Biochimica et Biophysica Acta (BBA) - Nucleic Acids and Protein Synthesis* 606:170–180. https://doi.org/10.1016/0005-2787(80)90108-2.

155. Brostrom CO, Prostko CR, Kaufman RJ, Brostrom MA. 1996. Inhibition of Translational Initiation by Activators of the Glucose-regulated Stress Protein and Heat Shock Protein Stress Response Systems. *Journal of Biological Chemistry* 271:24995–25002. https://doi.org/10.1074/jbc.271.40.24995.

156. Lu L, Han AP, Chen JJ. 2001. Translation initiation control by heme-regulated eukaryotic initiation factor 2alpha kinase in erythroid cells under cytoplasmic stresses. *Molecular and cellular biology* 21:7971–80. https://doi.org/10.1128/MCB.21.23.7971-7980.2001.

157. McEwen E, Kedersha N, Song B, Scheuner D, Gilks N, Han A, Chen JJ, Anderson P, Kaufman RJ. 2005. Heme-regulated inhibitor kinase-mediated phosphorylation of eukaryotic translation initiation factor 2 inhibits translation, induces stress granule formation, and mediates survival upon arsenite exposure. *The Journal of biological chemistry* 280:16925–33. https://doi.org/10.1074/jbc.M412882200.

158. Bode AM, Dong Z. 2002. The paradox of arsenic: molecular mechanisms of cell transformation and chemotherapeutic effects. *Critical reviews in oncology/hematology* 42:5–24. https://doi.org/10.1016/S1040-8428(01)00215-3.

159. William R, Watson G, Redmond HP, Wang JH, Bouchier-Hayes D. 1996. Mechanisms involved in sodium arsenite-induced apoptosis of human neutrophils. *Journal of Leukocyte Biology* 60:625–632. https://doi.org/10.1002/jlb.60.5.625.

160. Ivanov VN, Hei TK. 2004. Arsenite Sensitizes Human Melanomas to Apoptosis via Tumor Necrosis Factor α-mediated Pathway. *Journal of Biological Chemistry* 279:22747–22758. https://doi.org/10.1074/jbc.M314131200.

161. Ludwig S, Hoffmeyer A, Goebeler M, Kilian K, Häfner H, Neufeld B, Han J, Rapp UR. 1998. The Stress Inducer Arsenite Activates Mitogen-activated Protein Kinases Extracellular Signal-regulated Kinases 1 and 2 via a MAPK Kinase 6/p38-dependent Pathway. *Journal of Biological Chemistry* 273:1917–1922. https://doi.org/10.1074/jbc.273.4.1917.

162. Namgung U, Xia Z. 2000. Arsenite-Induced Apoptosis in Cortical Neurons Is Mediated by c-Jun N-Terminal Protein Kinase 3 and p38 Mitogen-Activated Protein Kinase. *The Journal of Neuroscience* 20:6442–6451. https://doi.org/10.1523/JNEUROSCI.20-17-06442.2000.

163. Lau ATY, Li M, Xie R, He QY, Chiu JF. 2004. Opposed arsenite-induced signaling pathways promote cell proliferation or apoptosis in cultured lung cells. *Carcinogenesis* 25:21–8. https://doi.org/10.1093/carcin/bgg179.

164. Likos AM, Sammons SA, Olson VA, Frace AM, Li Y, Olsen-Rasmussen M, Davidson W, Galloway R, Khristova ML, Reynolds MG, Zhao H, Carroll DS, Curns A, Formenty P, Esposito JJ, Regnery RL, Damon IK. 2005. A tale of two clades: monkeypox viruses. *The Journal of general virology* 86:2661–72. https://doi.org/10.1099/vir.0.81215-0.

165. Damon IK. 2011. Status of human monkeypox: clinical disease, epidemiology and research. *Vaccine* 29 Suppl 4:D54–9. https://doi.org/10.1016/j.vaccine.2011.04.014.

166. Di Giulio DB, Eckburg PB. 2004. Human monkeypox: an emerging zoonosis. *The Lancet Infectious Diseases* 4:15–25. https://doi.org/10.1016/S1473-3099(03)00856-9.

167. Reed KD, Melski JW, Graham MB, Regnery RL, Sotir MJ, Wegner MV, Kazmierczak JJ, Stratman EJ, Li Y, Fairley JA, Swain GR, Olson VA, Sargent EK, Kehl SC, Frace MA, Kline R, Foldy SL, Davis JP, Damon IK. 2004. The Detection of Monkeypox in Humans in the Western Hemisphere. *New England Journal of Medicine* 350:342–350. https://doi.org/10.1056/NEJMoa032299.

168. Rimoin AW, Mulembakani PM, Johnston SC, Lloyd Smith JO, Kisalu NK, Kinkela TL, Blumberg S, Thomassen HA, Pike BL, Fair JN, Wolfe ND, Shongo RL, Graham BS, Formenty P, Okitolonda E, Hensley LE, Meyer H, Wright LL, Muyembe JJ. 2010. Major increase in human monkeypox incidence 30

years after smallpox vaccination campaigns cease in the Democratic Republic of Congo. *Proceedings of the National Academy of Sciences* 107:16262–16267. https://doi.org/10.1073/pnas.1005769107.

169. Senkevich TG, Koonin EV, Bugert JJ, Darai G, Moss B. 1997. The genome of molluscum contagiosum virus: analysis and comparison with other poxviruses. *Virology* 233:19–42. https://doi.org/10.1006/viro.1997.8607.

170. Tulman ER, Afonso CL, Lu Z, Zsak L, Kutish GF, Rock DL. 2004. The genome of canarypox virus. *Journal of virology* 78:353–66.

171. Ho CK, Shuman S. 1996. Physical and functional characterization of the double-stranded RNA binding protein encoded by the vaccinia virus E3 gene. *Virology* 217:272–84. https://doi.org/10.1006/viro.1996.0114.

172. Brandt TA, Jacobs BL. 2001. Both carboxy- and amino-terminal domains of the vaccinia virus interferon resistance gene, E3L, are required for pathogenesis in a mouse model. *Journal of virology* 75:850–6. https://doi.org/10.1128/JVI.75.2.850-856.2001.

173. Cameron C, Hota-Mitchell S, Chen L, Barrett J, Cao JX, Macaulay C, Willer D, Evans D, McFadden G. 1999. The complete DNA sequence of myxoma virus. *Virology* 264:298–318. https://doi.org/10.1006/viro.1999.0001.

174. Willer DO, McFadden G, Evans DH. 1999. The complete genome sequence of shope (rabbit) fibroma virus. *Virology* 264:319–43. https://doi.org/10.1006/viro.1999.0002.

175. Rahman MM, Liu J, Chan WM, Rothenburg S, McFadden G. 2013. Myxoma virus protein M029 is a dual function immunomodulator that inhibits PKR and also conscripts RHA/DHX9 to promote expanded host tropism and viral replication. *PLoS pathogens* 9:e1003465. https://doi.org/10.1371/journal.ppat.1003465.

176. Shchelkunov SN, Totmenin aV, Babkin IV, Safronov PF, Ryazankina OI, Petrov Na, Gutorov VV, Uvarova Ea, Mikheev MV, Sisler JR, Esposito JJ, Jahrling PB, Moss B, Sandakhchiev LS. 2001. Human monkeypox and smallpox viruses: genomic comparison. *FEBS letters* 509:66–70.

177. Muralinath M. 2003. The role of the amino terminus of E3L in vaccinia virus pathogenesis. Doctoral Dissertation. Arizona State University.

178. Arndt WD, Cotsmire S, Trainor K, Harrington H, Hauns K, Kibler KV, Huynh TP, Jacobs BL. 2015. Evasion of the Innate Immune Type I Interferon System by Monkeypox Virus. *Journal of Virology* 89:10489–10499. https://doi.org/10.1128/JVI.00304-15.

179. Lemaire PA, Anderson E, Lary J, Cole JL. 2008. Mechanism of PKR Activation by dsRNA. *Journal of Molecular Biology* 381:351–360. https://doi.org/10.1016/j.jmb.2008.05.056.

180. Cresawn SG, Prins C, Latner DR, Condit RC. 2007. Mapping and phenotypic analysis of spontaneous isatin-β-thiosemicarbazone resistant mutants of vaccinia virus. *Virology* 363:319–332. https://doi.org/10.1016/j.virol.2007.02.005.

181. Cresawn SG, Condit RC. 2007. A targeted approach to identification of vaccinia virus postreplicative transcription elongation factors: genetic evidence for a role of the H5R gene in vaccinia transcription. *Virology* 363:333–41. https://doi.org/10.1016/j.virol.2007.02.016.

182. Shors T, Kibler KV, Perkins KB, Seidler-Wulff R, Banaszak MP, Jacobs BL. 1997. Complementation of vaccinia virus deleted of the E3L gene by mutants of E3L. *Virology* 239:269–76. https://doi.org/10.1006/viro.1997.8881.

183. Altschul SF, Madden TL, Schäffer AA, Zhang J, Zhang Z, Miller W, Lipman DJ. 1997. Gapped BLAST and PSI-BLAST: a new generation of protein database search programs. *Nucleic acids research* 25:3389–402.

184. Larkin MA, Blackshields G, Brown NP, Chenna R, McGettigan PA, McWilliam H, Valentin F, Wallace IM, Wilm A, Lopez R, Thompson JD, Gibson TJ, Higgins DG. 2007. Clustal W and Clustal X version 2.0. *Bioinformatics (Oxford, England)* 23:2947–8. https://doi.org/10.1093/bioinformatics/btm404.

185. Goujon M, McWilliam H, Li W, Valentin F, Squizzato S, Paern J, Lopez R. 2010. A new bioinformatics analysis tools framework at EMBL-EBI. *Nucleic acids research* 38:W695–9. https://doi.org/10.1093/nar/gkq313.

186. Colby C, Jurale C, Kates JR. 1971. Mechanism of synthesis of vaccinia virus double-stranded ribonucleic acid in vivo and in vitro. *Journal of virology* 7:71–6.

187. Prins C, Cresawn SG, Condit RC. 2004. An Isatin-β-thiosemicarbazone-resistant Vaccinia Virus Containing a Mutation in the Second Largest Subunit of the Viral RNA Polymerase Is Defective in Transcription Elongation. *Journal of Biological Chemistry* 279:44858–44871. https://doi.org/10.1074/jbc.M408167200.

188. Maelfait J, Liverpool L, Bridgeman A, Ragan KB, Upton JW, Rehwinkel J. 2017. Sensing of viral and endogenous RNA by ZBP1/DAI induces necroptosis. *The EMBO journal* 36:2529–2543. https://doi.org/10.15252/embj.201796476.

189. Langland JO, Jacobs BL. 2004. Inhibition of PKR by vaccinia virus: role of the N- and C-terminal domains of E3L. *Virology* 324:419–29. https://doi.org/10.1016/j.virol.2004.03.012.

190. Guerra S, Cáceres A, Knobeloch KP, Horak I, Esteban M. 2008. Vaccinia virus E3 protein prevents the antiviral action of ISG15. *PLoS pathogens* 4:e1000096. https://doi.org/10.1371/journal.ppat.1000096.

191. Frey TR, Lehmann MH, Ryan CM, Pizzorno MC, Sutter G, Hersperger AR. 2017. Ectromelia virus accumulates less double-stranded RNA compared to vaccinia virus in BS-C-1 cells. *Virology* 509:98–111. https://doi.org/10.1016/j.virol.2017.06.010.

192. Smith GL, Benfield CTO, Maluquer de Motes C, Mazzon M, Ember SWJ, Ferguson BJ, Sumner RP. 2013. Vaccinia virus immune evasion: mechanisms, virulence and immunogenicity. *Journal of General Virology* 94:2367–2392. https://doi.org/10.1099/vir.0.055921-0.

193. Pham AM, Santa Maria FG, Lahiri T, Friedman E, Marié IJ, Levy DE. 2016. PKR Transduces MDA5-Dependent Signals for Type I IFN Induction. *PLOS Pathogens* 12:e1005489. https://doi.org/10.1371/journal.ppat.1005489.

194. Thakur M, Seo EJ, Dever TE. 2014. Variola virus E3L $Z\alpha$ domain, but not its Z-DNA binding activity, is required for PKR inhibition. *RNA (New York, N.Y.)* 20:214–27. https://doi.org/10.1261/rna.042341.113.

195. Hsu PD, Lander ES, Zhang F. 2014. Development and Applications of CRISPR-Cas9 for Genome Engineering. *Cell* 157:1262–1278. https://doi.org/10.1016/j.cell.2014.05.010.

196. Brandt T, Heck MC, Vijaysri S, Jentarra GM, Cameron JM, Jacobs BL. 2005. The N-terminal domain of the vaccinia virus E3L-protein is required for neurovirulence, but not induction of a protective immune response. *Virology* 333:263–70. https://doi.org/10.1016/j.virol.2005.01.006.

197. Dueck KJ, Hu Y(, Chen P, Deschambault Y, Lee J, Varga J, Cao J. 2015. Mutational Analysis of Vaccinia Virus E3 Protein: the Biological Functions Do Not Correlate with Its Biochemical Capacity To Bind Double-Stranded RNA. *Journal of Virology* 89:5382–5394. https://doi.org/10.1128/JVI.03288-14.

198. Holechek S. 2011. Lessons from Vaccinia Virus Post-Exposure Prophylaxis: Insights into Control of Diseases and Epidemics. Doctoral Dissertation. Arizona State University.

199. Quyen DV, Ha SC, Lowenhaupt K, Rich A, Kim KK, Kim YG. 2007. Characterization of DNA-binding activity of Z alpha domains from poxviruses and the importance of the beta-wing regions in converting B-DNA to Z-DNA. *Nucleic acids research* 35:7714–20. https://doi.org/10.1093/nar/gkm748.

200. Wittig B, Dorbic T, Rich A. 1991. Transcription is associated with Z-DNA formation in metabolically active permeabilized mammalian cell nuclei. *Proceedings of the National Academy of Sciences* 88:2259–2263. https://doi.org/10.1073/pnas.88.6.2259.

201. Dabo S, Maillard P, Collados Rodriguez M, Hansen MD, Mazouz S, Bigot DJ, Tible M, Janvier G, Helynck O, Cassonnet P, Jacob Y, Bellalou J, Gatignol A, Patel RC, Hugon J, Munier-Lehmann H, Meurs EF. 2017. Inhibition of the inflammatory response to stress by targeting interaction between PKR and its cellular activator PACT. *Scientific reports* 7:16129. https://doi.org/10.1038/s41598-017-16089-8.

202. Patel RC, Sen GC. 1998. PACT, a protein activator of the interferon-induced protein kinase, PKR. *The EMBO journal* 17:4379–90. https://doi.org/10.1093/emboj/17.15.4379.

203. Reineke LC, Lloyd RE. 2015. The Stress Granule Protein G3BP1 Recruits Protein Kinase R To Promote Multiple Innate Immune Antiviral Responses. *Journal of Virology* 89:2575–2589. https://doi.org/10.1128/JVI.02791-14.

204. Koo GB, Morgan MJ, Lee DG, Kim WJ, Yoon JH, Koo JS, Kim SI, Kim SJ, Son MK, Hong SS, Levy JMM, Pollyea DA, Jordan CT, Yan P, Frankhouser D, Nicolet D, Maharry K, Marcucci G, Choi KS, Cho H, Thorburn A, Kim YS. 2015. Methylation-dependent loss of RIP3 expression in cancer represses programmed necrosis in response to chemotherapeutics. *Cell Research* 25:707–725. https://doi.org/10.1038/cr.2015.56.

205. Basu M, Courtney SC, Brinton MA. 2017. Arsenite-induced stress granule formation is inhibited by elevated levels of reduced glutathione in West Nile virus-infected cells. *PLOS Pathogens* 13:e1006240. https://doi.org/10.1371/journal.ppat.1006240.

206. Bian P, Zheng X, Wei L, Ye C, Fan H, Cai Y, Zhang Y, Zhang F, Jia Z, Lei Y. 2017. MLKL Mediated Necroptosis Accelerates JEV-Induced Neuroinflammation in Mice. *Frontiers in Microbiology* 8. https://doi.org/10.3389/fmicb.2017.00303.

207. Bentmann E, Haass C, Dormann D. 2013. Stress granules in neurodegeneration-lessons learnt from TAR DNA binding protein of 43 kDa and fused in sarcoma. *The FEBS journal* 280:4348–70. https://doi.org/10.1111/febs.12287.

208. Ishii KJ, Kawagoe T, Koyama S, Matsui K, Kumar H, Kawai T, Uematsu S, Takeuchi O, Takeshita F, Coban C, Akira S. 2008. TANK-binding kinase-1 delineates innate and adaptive immune responses to DNA vaccines. *Nature* 451:725–9. https://doi.org/10.1038/nature06537.

209. Ung TL, Cao C, Lu J, Ozato K, Dever TE. 2001. Heterologous dimerization domains functionally substitute for the double-stranded RNA binding domains of the kinase PKR. *The EMBO journal* 20:3728–37. https://doi.org/10.1093/emboj/20.14.3728.

210. Fegan A, White B, Carlson JCT, Wagner CR. 2010. Chemically controlled protein assembly: techniques and applications. *Chemical reviews* 110:3315–36. https://doi.org/10.1021/cr8002888.

211. Arndt W, White S, Johnson B, Huynh T, Liao J, Harrington H, Cotsmire S, Kibler K, Langland J, Jacobs B. 2016. Monkeypox virus induces the synthesis of less dsRNA than vaccinia virus, and is more resistant to the anti-poxvirus drug, IBT, than vaccinia virus. *Virology* 497. https://doi.org/10.1016/j.virol.2016.07.016.

212. Mirzakhanyan Y, Gershon PD. 2017. Multisubunit DNA-Dependent RNA Polymerases from Vaccinia Virus and Other Nucleocytoplasmic Large-DNA Viruses: Impressions from the Age of Structure. *Microbiology and molecular biology reviews : MMBR* 81. https://doi.org/10.1128/MMBR.00010-17.

213. Donzé O, Deng J, Curran J, Sladek R, Picard D, Sonenberg N. 2004. The protein kinase PKR: a molecular clock that sequentially activates survival and death programs. *The EMBO Journal* 23:564–571. https://doi.org/10.1038/sj.emboj.7600078.

214. Pol J, Kroemer G, Galluzzi L. 2016. First oncolytic virus approved for melanoma immunotherapy. *OncoImmunology* 5:e1115641. https://doi.org/10.1080/2162402X.2015.1115641.

215. Fukuhara H, Ino Y, Todo T. 2016. Oncolytic virus therapy: A new era of cancer treatment at dawn. *Cancer science* 107:1373–1379. https://doi.org/10.1111/cas.13027.

216. Arndt W. 2010. Characterization of the E3L Amino-Terminus in Poxvirus Replication and Tumor Regression. Thesis Dissertation. Arizona State University.

217. Scaffidi P, Misteli T, Bianchi ME. 2002. Release of chromatin protein HMGB1 by necrotic cells triggers inflammation. *Nature* 418:191–195. https://doi.org/10.1038/nature00858.

218. Albert ML, Sauter B, Bhardwaj N. 1998. Dendritic cells acquire antigen from apoptotic cells and induce class I-restricted CTLs. *Nature* 392:86–9. https://doi.org/10.1038/32183.

219. Scheffer SR, Nave H, Korangy F, Schlote K, Pabst R, Jaffee EM, Manns MP, Greten TF. 2003. Apoptotic, but not necrotic, tumor cell vaccines induce a potent immune response in vivo. *International journal of cancer* 103:205–11. https://doi.org/10.1002/ijc.10777.

220. Sauter B, Albert ML, Francisco L, Larsson M, Somersan S, Bhardwaj N. 2000. Consequences of cell death: exposure to necrotic tumor cells, but not primary tissue cells or apoptotic cells, induces the maturation of immunostimulatory dendritic cells. *The Journal of experimental medicine* 191:423–34. https://doi.org/10662788.

221. Aaes TL, Kaczmarek A, Delvaeye T, De Craene B, De Koker S, Heyndrickx L, Delrue I, Taminau J, Wiernicki B, De Groote P, Garg AD, Leybaert L, Grooten J, Bertrand MJM, Agostinis P, Berx G, Declercq W, Vandenabeele P, Krysko DV. 2016. Vaccination with Necroptotic Cancer Cells Induces Efficient Anti-tumor Immunity. *Cell reports* 15:274–87. https://doi.org/10.1016/j.celrep.2016.03.037.

222. Yatim N, Jusforgues-Saklani H, Orozco S, Schulz O, Barreira da Silva R, Reis e Sousa C, Green DR, Oberst A, Albert ML. 2015. RIPK1 and NF-κB signaling in dying cells determines cross-priming of CD8+ T cells. *Science (New York, N.Y.)* 350:328–34. https://doi.org/10.1126/science.aad0395.

223. Hornung V, Ablasser A, Charrel-Dennis M, Bauernfeind F, Horvath G, Caffrey DR, Latz E, Fitzgerald KA. 2009. AIM2 recognizes cytosolic dsDNA and forms a caspase-1-activating inflammasome with ASC. *Nature* 458:514–8. https://doi.org/10.1038/nature07725.

224. Man SM, Karki R, Kanneganti TD. 2017. Molecular mechanisms and functions of pyroptosis, inflammatory caspases and inflammasomes in infectious diseases. *Immunological reviews* 277:61–75. https://doi.org/10.1111/imr.12534.

225. Kearney CJ, Cullen SP, Tynan GA, Henry CM, Clancy D, Lavelle EC, Martin SJ. 2015. Necroptosis suppresses inflammation via termination of TNF- or LPS-induced cytokine and chemokine production. *Cell death and differentiation* 22:1313–27. https://doi.org/10.1038/cdd.2014.222.

226. Perez-Rathke A, Li H, Lussier YA. 2013. Interpreting personal transcriptomes: personalized mechanism-scale profiling of RNA-seq data. *Pacific Symposium on Biocomputing. Pacific Symposium on Biocomputing*:159–70.

227. Wang L, Acharya L, Bai C, Zhu D. 2017. Transcriptome assembly strategies for precision medicine. *Quantitative Biology* 5:280–290. https://doi.org/10.1007/s40484-017-0109-2.